
Assessment of the XSOR Codes

Final Report

Prepared by P. Cybulskis

Battelle Columbus Division

Prepared for
U.S. Nuclear Regulatory Commission

AVAILABILITY NOTICE

Availability of Reference Materials Cited in NRC Publications

Most documents cited in NRC publications will be available from one of the following sources:

1. The NRC Public Document Room, 2120 L Street, NW, Lower Level, Washington, DC 20555
2. The Superintendent of Documents, U.S. Government Printing Office, P.O. Box 37082, Washington, DC 20013-7082
3. The National Technical Information Service, Springfield, VA 22161

Although the listing that follows represents the majority of documents cited in NRC publications, it is not intended to be exhaustive.

Referenced documents available for inspection and copying for a fee from the NRC Public Document Room include NRC correspondence and internal NRC memoranda; NRC Office of Inspection and Enforcement bulletins, circulars, information notices, inspection and investigation notices; Licensee Event Reports; vendor reports and correspondence; Commission papers; and applicant and licensee documents and correspondence.

The following documents in the NUREG series are available for purchase from the GPO Sales Program: formal NRC staff and contractor reports, NRC-sponsored conference proceedings, and NRC booklets and brochures. Also available are Regulatory Guides, NRC regulations in the *Code of Federal Regulations*, and *Nuclear Regulatory Commission Issuances*.

Documents available from the National Technical Information Service include NUREG series reports and technical reports prepared by other federal agencies and reports prepared by the Atomic Energy Commission, former agency to the Nuclear Regulatory Commission.

Documents available from public and special technical libraries include all open literature items, such as books, journal and periodical articles, and transactions. *Federal Register* notices, federal and state legislation, and congressional reports can usually be obtained from these libraries.

Documents such as theses, dissertations, foreign reports and translations, and non-NRC conference proceedings are available for purchase from the organization sponsoring the publication cited.

Single copies of NRC draft reports are available free, to the extent of supply, upon written request to the Office of Information Resources Management, Distribution Section, U.S. Nuclear Regulatory Commission, Washington, DC 20555.

Copies of industry codes and standards used in a substantive manner in the NRC regulatory process are maintained at the NRC Library, 7920 Norfolk Avenue, Bethesda, Maryland, and are available there for reference use by the public. Codes and standards are usually copyrighted and may be purchased from the originating organization or, if they are American National Standards, from the American National Standards Institute, 1430 Broadway, New York, NY 10018.

DISCLAIMER NOTICE

This report was prepared as an account of work sponsored by an agency of the United States Government. Neither the United States Government nor any agency thereof, or any of their employees, makes any warranty, expressed or implied, or assumes any legal liability of responsibility for any third party's use, or the results of such use, of any information, apparatus, product or process disclosed in this report, or represents that its use by such third party would not infringe privately owned rights.

Assessment of the XSOR Codes

Final Report

Manuscript Completed: August 1989
Date Published: November 1989

Prepared by
P. Cybulskis

Battelle Columbus Division
505 King Avenue
Columbus, OH 43201

Prepared for
Division of Systems Research
Office of Nuclear Regulatory Research
U.S. Nuclear Regulatory Commission
Washington, DC 20555
NRC FIN D1595

ABSTRACT

A major feature of the NUREG-1150 analyses is the quantification of the uncertainties associated with the assessment of reactor accident risks, including the assessment of the uncertainties in the prediction of environmental source terms. The quantification of uncertainties was accomplished by the use of stratified sampling techniques over the ranges of uncertainties of the major variables. Since a separate source term is associated with each combination of variables in the statistical analysis, an extremely large number of source term estimates must be developed. For this purpose simplified methods of analysis, based on a limited number of detailed STCP calculations, were developed by Sandia National Laboratories. These source term estimation algorithms are known as the XSOR codes. These simplified source term methods were used not only as surrogates for the detailed calculations, but also to explore areas not currently addressed by the STCP. This report presents the results of an independent assessment of the ability of the XSOR codes to reproduce the results that would be obtained with the STCP, as well as to evaluate the reasonableness of the results when extended beyond the scope of the available STCP analyses.

TABLE OF CONTENTS

	<u>Page</u>
INTRODUCTION	1
PURPOSE OF THE XSOR CODES	2
APPROACH TO THE ASSESSMENT	4
SUMMARY DESCRIPTION OF THE XSOR CODES	5
COMPARISON OF XSOR AND STCP RESULTS	8
Comparison of SURSOR Central Estimates with STCP Results	8
SURSOR Source Term Distributions	21
Results of Final Version of SURSOR	47
Results of SURSOR-STCP Comparison	69
CONCLUSIONS	71
APPENDIX A: COMPARISON OF SEQSOR AND STCP RESULTS	A- 1
APPENDIX B: COMPARISON OF PBSOR AND STCP RESULTS	B- 1
APPENDIX C: COMPARISON OF GRSOR AND STCP RESULTS	C- 1
APPENDIX D: COMPARISON OF ZISOR AND STCP RESULTS	D- 1

LIST OF FIGURES

	<u>Page</u>
FIGURE 1. COMPARISON OF SURSOR WITH STCP RESULTS FOR TMLB-delta AND S3B-delta	11
FIGURE 2. COMPARISON OF SURSOR WITH STCP RESULTS FOR TMLB-beta	12
FIGURE 3. COMPARISON OF SURSOR WITH STCP RESULTS FOR TMLB-epsilon	13
FIGURE 4. COMPARISON OF SURSOR WITH STCP RESULTS FOR TMLB-leak-before-break	14
FIGURE 5. COMPARISON OF SURSOR WITH STCP RESULTS FOR S2D-gamma W/SPRAY FAILURE	15
FIGURE 6. COMPARISON OF SURSOR WITH STCP RESULTS FOR S2D-gamma	16
FIGURE 7. COMPARISON OF SURSOR WITH STCP RESULTS FOR S2D-beta	17
FIGURE 8. COMPARISON OF SURSOR WITH STCP RESULTS FOR AG-delta	18
FIGURE 9. COMPARISON OF SURSOR WITH STCP RESULTS FOR V-wet	19
FIGURE 10. COMPARISON OF SURSOR WITH STCP RESULTS FOR V-dry	20
FIGURE 11. LLH SAMPLE SOURCE TERM DISTRIBUTIONS SURRY BIN 1	27
FIGURE 12. LLH SAMPLE SOURCE TERM DISTRIBUTIONS SURRY BIN 2	28
FIGURE 13. LLH SAMPLE SOURCE TERM DISTRIBUTIONS SURRY BIN 3	29
FIGURE 14. LLH SAMPLE SOURCE TERM DISTRIBUTIONS SURRY BIN 4	30
FIGURE 15. LLH SAMPLE SOURCE TERM DISTRIBUTIONS SURRY BIN 5	31
FIGURE 16. LLH SAMPLE SOURCE TERM DISTRIBUTIONS SURRY BIN 6	32
FIGURE 17. LLH SAMPLE SOURCE TERM DISTRIBUTIONS SURRY BIN 7	33
FIGURE 18. LLH SAMPLE SOURCE TERM DISTRIBUTIONS SURRY BIN 8	34
FIGURE 19. LLH SAMPLE SOURCE TERM DISTRIBUTIONS SURRY BIN 9	35
FIGURE 20. LLH SAMPLE SOURCE TERM DISTRIBUTIONS SURRY BIN 10	36

LIST OF FIGURES
(Continued)

	<u>Page</u>
FIGURE 21. LLH SAMPLE SOURCE TERM DISTRIBUTIONS SURRY BIN 11	37
FIGURE 22. LLH SAMPLE SOURCE TERM DISTRIBUTIONS SURRY BIN 12	38
FIGURE 23. LLH SAMPLE SOURCE TERM DISTRIBUTIONS SURRY BIN 13	39
FIGURE 24. LLH SAMPLE SOURCE TERM DISTRIBUTIONS SURRY BIN 14	40
FIGURE 25. LLH SAMPLE SOURCE TERM DISTRIBUTIONS SURRY BIN 15	41
FIGURE 26. LLH SAMPLE SOURCE TERM DISTRIBUTIONS SURRY BIN 16	42
FIGURE 27. LLH SAMPLE SOURCE TERM DISTRIBUTIONS SURRY BIN 17	43
FIGURE 28. LLH SAMPLE SOURCE TERM DISTRIBUTIONS SURRY BIN 18	44
FIGURE 29. LLH SAMPLE SOURCE TERM DISTRIBUTIONS SURRY BIN 19	45
FIGURE 30. LLH SAMPLE SOURCE TERM DISTRIBUTIONS SURRY BIN 20	46
FIGURE 31. COMPARISON OF SURSOR WITH STCP RESULTS FOR TMLB-delta AND S3B-delta	51
FIGURE 32. COMPARISON OF SURSOR WITH STCP RESULTS FOR TMLB-beta	52
FIGURE 33. COMPARISON OF SURSOR WITH STCP RESULTS FOR TMLB-epsilon	53
FIGURE 34. COMPARISON OF SURSOR WITH STCP RESULTS FOR TMLB-leak-before-break	54
FIGURE 35. COMPARISON OF SURSOR WITH STCP RESULTS FOR TMLB-gamma	55
FIGURE 36. COMPARISON OF SURSOR WITH STCP RESULTS FOR S2D-gamma (w/spray fail)	56
FIGURE 37. COMPARISON OF SURSOR WITH STCP RESULTS FOR S2D-gamma (w/spray on)	57
FIGURE 38. COMPARISON OF SURSOR WITH STCP RESULTS FOR S2D-beta	58
FIGURE 39. COMPARISON OF SURSOR WITH STCP RESULTS FOR S2D-epsilon	59
FIGURE 40. COMPARISON OF SURSOR WITH STCP RESULTS FOR AG-delta	60

LIST OF FIGURES
(Continued)

	<u>Page</u>
FIGURE 41. COMPARISON OF SURSOR WITH STCP RESULTS FOR V-wet	61
FIGURE 42. COMPARISON OF SURSOR WITH STCP RESULTS FOR V-dry	62
FIGURE 43. COMPARISON OF SURSOR WITH STCP RESULTS FOR AB-epsilon	63
FIGURE 44. COMPARISON OF SURSOR WITH STCP RESULTS FOR AB-gamma	64
FIGURE 45. COMPARISON OF SURSOR WITH STCP RESULTS FOR AB-beta	65
FIGURE 46. COMPARISON OF SURSOR WITH STCP RESULTS FOR SGTR1	66
FIGURE 47. COMPARISON OF SURSOR WITH STCP RESULTS FOR SGTR2	67
FIGURE 48. COMPARISON OF SURSOR WITH STCP RESULTS FOR SGTR3	68
FIGURE A-1. COMPARISON OF SEQSOR WITH STCP RESULTS FOR TMLB-gamma	A- 5
FIGURE A-2. COMPARISON OF SEQSOR WITH STCP RESULTS FOR TMLB-delta	A- 6
FIGURE A-3. COMPARISON OF SEQSOR WITH STCP RESULTS FOR TMLB-beta	A- 7
FIGURE A-4. COMPARISON OF SEQSOR WITH STCP RESULTS FOR TML-gamma	A- 8
FIGURE A-5. COMPARISON OF SEQSOR WITH STCP RESULTS FOR TML-delta	A- 9
FIGURE A-6. COMPARISON OF SEQSOR WITH STCP RESULTS S2HF-gamma	A-10
FIGURE A-7. COMPARISON OF SEQSOR WITH STCP RESULTS FOR S3HF1	A-11
FIGURE A-8. COMPARISON OF SEQSOR WITH STCP RESULTS FOR S3HF3	A-12
FIGURE A-9. COMPARISON OF SEQSOR WITH STCP RESULTS FOR TMLU-SGTR	A-13
FIGURE A-10. COMPARISON OF SEQSOR WITH STCP RESULTS FOR TBA	A-14
FIGURE A-11. COMPARISON OF SEQSOR WITH STCP RESULTS FOR TBA1	A-15
FIGURE A-12. COMPARISON OF SEQSOR WITH STCP RESULTS FOR S3B-gamma	A-16
FIGURE A-13. COMPARISON OF SEQSOR WITH STCP RESULTS FOR S3HF-delta	A-17
FIGURE A-14. COMPARISON OF SEQSOR WITH STCP RESULTS FOR ACD	A-18
FIGURE A-15. COMPARISON OF SEQSOR WITH STCP RESULTS FOR TB-gamma	A-19
FIGURE B-1. COMPARISON OF PBSOR WITH STCP RESULTS FOR TC1	B- 4
FIGURE B-2. COMPARISON OF PBSOR WITH STCP RESULTS FOR TC2	B- 5

LIST OF FIGURES
(Continued)

	<u>Page</u>
FIGURE B-3. COMPARISON OF PBSOR WITH STCP RESULTS FOR TC3	B- 6
FIGURE B-4. COMPARISON OF PBSOR WITH STCP RESULTS FOR TB1	B- 7
FIGURE B-5. COMPARISON OF PBSOR WITH STCP RESULTS FOR TB1'	B- 8
FIGURE B-6. COMPARISON OF PBSOR WITH STCP RESULTS FOR TB2	B- 9
FIGURE B-7. COMPARISON OF PBSOR WITH STCP RESULTS FOR TBUX	B-10
FIGURE B-8. COMPARISON OF PBSOR WITH STCP RESULTS FOR S2E	B-11
FIGURE B-9. COMPARISON OF PBSOR WITH STCP RESULTS FOR S2E'	B-12
FIGURE B-10. COMPARISON OF PBSOR WITH STCP RESULTS FOR AE	B-13
FIGURE C-1. COMPARISON OF GGSOR WITH STCP RESULTS FOR TB1	C- 4
FIGURE C-2. COMPARISON OF GGSOR WITH STCP RESULTS FOR TB2	C- 5
FIGURE C-3. COMPARISON OF GGSOR WITH STCP RESULTS FOR TBS	C- 6
FIGURE C-4. COMPARISON OF GGSOR WITH STCP RESULTS FOR TBR	C- 7
FIGURE C-5. COMPARISON OF GGSOR WITH STCP RESULTS FOR TC	C- 8
FIGURE C-6. COMPARISON OF GGSOR WITH STCP RESULTS FOR TC1	C- 9
FIGURE C-7. COMPARISON OF GGSOR WITH STCP RESULTS FOR TP1	C-10
FIGURE C-8. COMPARISON OF GGSOR WITH STCP RESULTS FOR TQUV	C-11
FIGURE D-1. COMPARISON OF ZISOR WITH STCP RESULTS FOR S2DCR-delta . . .	D- 4
FIGURE D-2. COMPARISON OF ZISOR WITH STCP RESULTS FOR S2DCF-gamma . . .	D- 5
FIGURE D-3. COMPARISON OF ZISOR WITH STCP RESULTS FOR S2DCF-delta . . .	D- 6
FIGURE D-4. COMPARISON OF ZISOR WITH STCP RESULTS FOR TMLU-gamma . . .	D- 7
FIGURE D-5. COMPARISON OF ZISOR WITH STCP RESULTS FOR TMLB-epsilon . .	D- 8
FIGURE D-6. COMPARISON OF ZISOR WITH STCP RESULTS FOR TMLB-leak-before-break	D- 9
FIGURE D-7. COMPARISON OF ZISOR WITH STCP RESULTS FOR TMLB-beta	D-10
FIGURE D-8. COMPARISON OF ZISOR WITH STCP RESULTS FOR S2D-epsilon . . .	D-11

ASSESSMENT OF THE XSOR CODES

INTRODUCTION

A major feature of the NUREG-1150 analyses is the quantification of the uncertainties that are associated with the assessment of reactor accident risks. This requires the assessment of the uncertainties in the prediction of environmental source terms. The latter was accomplished by the use of stratified sampling techniques over the ranges of uncertainties of the major variables. Since a separate source term result is required for each different combination of the variables in the statistical sampling analysis, an extremely large number of source term estimates must be developed. For the Surry analyses in DRAFT NUREG-1150, for example, two thousand separate source terms were developed. It was obviously not practical to generate this large number of source terms by means of detailed calculations with the Source Term Code Package (STCP). Other more advanced tools for calculating severe accident source terms are more limited than the STCP in terms of their ability to generate large numbers of source term results. For this purpose simplified methods of analysis, based on a limited number of STCP results, have been developed by Sandia National Laboratories. These source term estimation algorithms are known collectively as the "XSOR" codes. In addition to economically providing source term estimates for situations in which detailed calculations are not available, these simplified methods include parametric representations of a number of source term issues that are not at present modeled by the STCP. Thus, the simplified source term methods were used not only as surrogates for the detailed calculations, but also to explore areas not currently treated by the STCP. When the XSOR codes were used in tandem with a statistical sampling method, Limited Latin Hypercube (LLH), quantitative estimates of source term uncertainties were generated.

The purpose of this report is to present the results of an independent assessment of the ability of the simplified methods to reasonably reproduce the results that have been (or would be) obtained with the STCP, as well as to evaluate the reasonableness of the results when extended beyond the scope of the available calculational models.

Since this assessment was being undertaken during the time period that the XSOR codes were undergoing continued development, much of the assessment effort was devoted to the DRAFT NUREG-1150 versions of these codes, with more limited attention focused on the final versions. This was necessitated by time and schedule constraints, as the final versions only became available near the end of the present assessment. This assessment was focused on SURSOR, the version of the XSOR codes tailored to the Surry plant, since it was the lead code in the series. More limited attention was devoted to the other versions: SEQSOR for the Sequoyah plant, ZISOR for Zion, PBSOR for Peach Bottom, and GGSOK for Grand Gulf.

PURPOSE OF THE XSOR CODES

As noted briefly above, the XSOR codes represent an effort to cope with two essential requirements of NUREG-1150:

- (1) Very large numbers of source term estimates (numbering into the thousands) were required for each of the NUREG-1150 plants. STCP calculations were generally available for only a small number (8-18) of specific accident scenarios. Because of time and resource requirements, it was not practical to generate such large numbers of source terms with the STCP.
- (2) It was recognized that significant uncertainties may be associated with the results of the STCP or any other calculational tool due to lack of knowledge, modeling limitations, uncertain boundary conditions, etc. A method was required for representing these uncertainties and propagating them through the risk calculations to determine their impact upon the uncertainty in the final results. The statistical sampling method adopted for the uncertainty analyses in NUREG-1150 required the calculation of very large numbers of source terms. The XSOR codes provide a convenient method of generating the large number of source terms required.

The XSOR approach is based on decomposing the processes of fission product release and transport into a number of major stages, and representing each stage in terms of specific parameters. Examples of such individual parameters include release from the fuel prior to vessel breach, release from the primary system, and release from the melt during concrete attack. Many of the XSOR code parameters are closely related to the output of the major modules of the STCP. The specific variables in the XSOR equation can be different for each of a number of radionuclide groups, and also depend on the definition of the accident scenario. By assembling and combining the individual factors in various permutations a large variety of accident scenarios, each with a particular source term, can be simulated. Similarly, by varying the individual parameters over their uncertainty ranges, the effects of such uncertainties on the overall source term can be assessed.

When the XSOR codes are used to simulate the STCP, the parameters appropriate for a given scenario are selected and assembled by XSOR based on the scenario definition to generate the required source term. The values of the individual parameters themselves are derived from existing STCP calculations. While the number of available STCP calculations for each individual plant is limited, the overall data base is quite substantial. For example, fission product behavior in the primary systems of the three PWR's considered is essentially the same; thus the available analyses for all three plants for this aspect of the problem are applicable to each one. Many of the other insights developed from the analyses for one plant are often applicable to others. The considerable experience with the STCP for a variety of reactor designs and accident sequences provides a substantial base on which to exercise sound engineering judgment when required.

The most important use of the XSOR codes in the WREG-1150 context is the quantification of source term uncertainties. Those parameters in XSOR for which the uncertainties were considered to be the most important were assigned distributions over the ranges of uncertainty. These uncertainty distributions were developed on the basis of a wide variety of inputs, including calculations with other source term methodologies, experimental observations, first principles analyses, as well as expert opinion. Such uncertainty distributions were developed for many of the STCP related parameters as well as for key issues not considered by the STCP. In the statistical sampling technique these parameters were varied over their assigned uncertainty distributions and the resulting distributions in the XSOR outputs were taken as measures of the source term uncertainty.

Given the foregoing, it is useful to make an important point regarding the role of the XSOR codes. While the structure of the decompositions used in XSOR reflects substantial understanding, based on extensive experience with the STCP as well as other sources of information, it is not the purpose of XSOR to incorporate the available body of source term phenomenology. It is the purpose of XSOR to take the understanding obtained from the STCP and elsewhere, as represented by the values assigned to the XSOR parameters, and generate the source terms corresponding to those parameters.

APPROACH TO THE ASSESSMENT

Given the purposes of the XSOR codes as described above, this assessment consisted of two phases. The first phase of the assessment addressed the question of how well XSOR could reproduce STCP results. This phase of the assessment was relatively straightforward and consisted largely of comparing XSOR predictions to available STCP results. The use of the XSOR codes as surrogates for the STCP is sometimes called the interpolation mode of their application.

The second phase of the assessment addresses uncertainties in source term predictions, both due to phenomena not explicitly considered in the STCP as well as phenomena included but poorly understood. This type of application is called the extrapolation mode of the XSOR codes. There were no STCP results with which to test the XSOR codes in this mode. Thus, the assessment of the reasonableness of the XSOR predictions in the extrapolation mode was much more difficult. It was accomplished by examining the range of XSOR predictions and determining which factors in the samples led to extreme values in the predicted source terms. The ranges for these factors were then compared to the values developed by the expert panels. The reasonableness was determined by the degree of agreement between the XSOR ranges and those of the expert panels.

Since this assessment was being undertaken while several versions of the XSOR codes were undergoing continuing development, the bulk of the present effort was devoted to the versions of the codes corresponding to those used in DRAFT NUREG-1150, with more limited attention given to the final versions as the latter became available.

SUMMARY DESCRIPTION OF THE XSOR CODES

In the XSOR codes the environmental source term for fission product species group I is approximated by an equation of the following general form:

$$\begin{aligned} ST(I) = & FCOR(I) * \{ FISG(I) * FOSG(I) + [1 - FISG(I)] * FVES(I) * FCONV(I) / DFE \\ & + FPART * [1 - FCOR(I)] * FCCI(I) * FCONC(I) / DFL \\ & + [1 - FCOR(I)] * FPME * FDCH(I) * FCONV \\ & + FLATE(I) * [FCOR(I) * (1 - FVES(I))] \\ & + FREM * [1 - FCOR(I)] \} * FCONRL(I) / DFL \end{aligned}$$

where,

- ST(I) = fraction of initial core inventory of species I released to the environment
- FCOR(I) = fraction of initial inventory released from the fuel prior to vessel breach
- FISG(I) = fraction of the initial inventory released to the steam generator
- FOSG(I) = fraction of initial inventory released from the steam generator
- FVES(I) = fraction of FCOR that is released from the reactor vessel into the containment
- FCONV = fraction of the early in-vessel release to the containment that would escape to the environment in the absence of decontamination mechanisms
- DFE = decontamination factor applicable to the releases from the primary system
- FPART = fraction of the core involved in concrete attack
- FCCI(I) = fraction of inventory remaining in the melt that is released during core-concrete interaction
- FCONC(I) = fraction of core-concrete interaction release escaping containment
- DFL = decontamination factor applicable to the corium-concrete interaction release
- FPME = fraction of the core involved in pressurized melt ejection

- FDCH(I) = fraction of material involved in pressurized melt ejection released from containment due to direct heating
- FLATE(I) = fraction of material remaining in the reactor coolant system after vessel breach which is revolatilized later
- FREM = fraction of the core material remaining in the reactor vessel after breach
- FCONRL(I) = fraction of late revolatilized material which would be released from containment in the absence of decontamination mechanisms

For iodine, an additional term is added:

$$+ \text{XLATE} * (\text{RELIV} - \text{RELIC})$$

where,

- XLATE = fraction of the iodine remaining in the containment late that is converted to organic iodides
- RELIV = fraction of initial inventory of iodine released to containment
- RELIC = fraction of initial inventory of iodine released from containment

FVES, the fraction of the in-vessel release from the fuel that escapes the containment, was described at four pressure levels: very high, high, intermediate, and low. The fraction of the core that is ejected into containment was discretized into four combinations of primary system pressure and quantity of water in the reactor cavity. Similarly, the fraction of the ejected material that participates in direct heating was considered at several levels. The decontamination factors considered are those appropriate to the reactor design and accident sequence being considered and included the effects of sprays, suppression pools, ice beds, water over the melt, etc., as appropriate.

In the DRAFT NUREG-1150 version of SURSOR there were seven fission product groups considered: noble gases, iodine, cesium, tellurium, strontium, ruthenium, and lanthanum. In later versions strontium and barium as well as lanthanum and cerium were tracked separately.

The parameters for each of the issues were set at six levels in DRAFT NUREG-1150. Levels 1-5 defined the cumulative distribution function for the uncertainty analyses; i.e., they were the minimum, twenty fifth, fiftieth, seventy fifth percentile, and maximum. Level six for any issue represents the central estimate; thus setting all issues in the sampling matrix to level six will yield the central estimates for the source term. The central estimate mimics the STCP parameters and results. In the final version of SURSOR the parameters to be set by issues have entries for ten levels. Levels one through

nine define the cumulative distribution function, i.e., they are the minimum, maximum, and seven intermediate percentiles (1%, 5%, 25%, 50%, 75%, 95%, 99%) of the CDF. The tenth level for any issue corresponds to the central estimate.

In addition to the above source term parameters, a number of other input parameters are provided to define the various accident categories or accident progression bins of interest. In the version of SORSOR which formed the principal basis of this review there were twenty accident progression bins considered.

COMPARISON OF XSOR AND STCP RESULTS

Given the uses that are being made of the XSOR codes in NUREG-1150, there are two questions that should be addressed:

- (1) Given input parameters that are appropriate to an accident scenario being considered, how well can XSOR reproduce source terms that would be calculated by the STCP for that scenario?
- (2) How much inaccuracy is introduced when XSOR is used to generate source terms for scenarios that differ from those for which STCP results are available?

The following discussion deals with the SURSOR code and its ability to mimic the STCP, as well as its extension to treat issues not explicitly modeled in the STCP. The other versions of the XSOR codes are reviewed in the appendices to this document.

Comparison of SURSOR Central Estimates with STCP Results

Figures 1 through 10 compare the SURSOR source term estimates with available STCP calculations. These comparisons are based on a SURSOR version very similar to that used in DRAFT NUREG-1150. Further comparisons with the predictions of the final version of SURSOR are presented later in this report. In an effort to present as many comparisons as possible, the calculated results from several versions of the STCP have been utilized; where significant changes in results are due to modifications in the STCP, they are noted in the discussion. In Figures 1 through 10 the vertical line represents the range of one hundred SURSOR estimates, with the horizontal line being the SURSOR central estimate. The discrete symbols represent the specific STCP results; in several of the cases more than one relevant STCP calculation was available.

Figure 1 compares SURSOR estimates with STCP calculations for the TMLB and S₃B sequences. These sequences represent accident scenarios in which core melting takes place at high primary system pressure, no containment safety features are operable, and containment failure occurs at the time of vessel breach. The results for TMLB were generated with the predecessor code suite to the STCP; those for S₃B were calculated by the reference version of the STCP. As can be seen, the agreement between the SURSOR central estimate and the STCP calculations is quite good; the only exception being the ruthenium release for S₃B. For the TMLB scenario the agreement is to be expected since this is one of the calculations used to derive the SURSOR parameters. The S₃B scenario is in many respects similar to TMLB, so again the agreement is not surprising. The lack of agreement for ruthenium arises from a change in the CORCOR-M release model in the reference version of the STCP, which was used for the S₃B sequence analyses.

The SURSOR estimates are compared with the STCP results for TMLB-beta in Figure 2. This is a station blackout with containment isolation failure. The comparison is only shown for the iodine, cesium, and tellurium groups since the other species were not explicitly tracked at the time this particular calculation was performed. It may be noted, however, that the iodine and

cesium releases take place predominantly during the in-vessel phase of the accident, whereas the tellurium release occurs mainly during concrete attack. Thus, the comparison for tellurium should be indicative of that for the other species also, since they too occur predominantly ex-vessel. The SORSOR central estimates are in good agreement with the STCP results.

Figure 3 illustrates the comparison of SORSOR with the STCP results for TMLB-epsilon, station blackout with containment meltthrough. Since this was again one of the calculations used to derive the SORSOR parameters, the good agreement is to be expected.

The SORSOR estimates are compared to TMLB with containment leak before break in Figure 4. In this case STCP results for only iodine, cesium, and tellurium are available for comparison. The agreement between the STCP and SORSOR central estimates is quite reasonable.

Figure 5 compares the SORSOR estimates with two STCP calculations for the S₂D-gamma sequence, an represents accident initiated by a small break in the primary coolant system accompanied by failure of emergency core cooling, the containment sprays are initially operating but fail following containment failure near the time of vessel breach. The two STCP calculations were based on containment spray drops of 400 and 1000 microns. As can be seen, the agreement between the SORSOR central estimate and the STCP results for the 1000 micron spray is excellent. This is again to be expected since these results were part of the data base used to derive the SORSOR parameters. The difference in the iodine and cesium releases for the 400 micron spray reflects the sensitivity of the results to the assumed spray size. This sensitivity is not reflected in the other release groups since they take place predominantly ex-vessel, after the sprays have failed in this particular scenario.

Figure 6 compares the SORSOR estimates with STCP calculations for the S₂D-gamma sequence under the assumption that the containment sprays continue to operate after the containment fails. The SORSOR central estimate results are again in excellent agreement with the STCP calculations for the 1000 micron spray. Again, this was one of the calculations used for the SORSOR data base.

The SORSOR predictions are compared with STCP calculations in Figure 7 for the S₂D-beta sequence, a small break with failure of the emergency core cooling system and failure of containment isolation, but the containment sprays operating. The STCP results for this case again explicitly tracked only three of the fission product groups. The 1000 micron spray case was used in the derivation of the SORSOR parameters, thus the excellent agreement. The comparison for the 400 micron spray shows the previously noted sensitivity of the releases to spray droplet size.

The SORSOR results are compared with the STCP results for AG-delta in Figure 8. The AG-delta sequence is characterized by a large pipe break and failure of the containment heat removal system, with containment failure leading to the failure of the emergency core cooling system; core melting thus takes place in a failed containment. With the exception of the ruthenium release, the agreement between SORSOR central estimate and the STCP is quite good. The difference in ruthenium release stems from the previously noted

change in the model for ruthenium release from the fuel. This change was made after the initial SURSOR parameters had been derived.

The results of the STCP calculation for the V sequence with a submerged release path are compared to the SURSOR estimates in Figure 9; the corresponding results for a dry release path are compared with SURSOR estimated in Figure 10. Generally good agreement is seen except for the lanthanum group. The STCP results for these cases were generated with an early version, with further changes in the modeling of the refractory species taking place subsequently.

FIGURE 1.
 COMPARISON OF SURSOR WITH STOP
 RESULTS FOR TMLB-delta AND S3B-delta

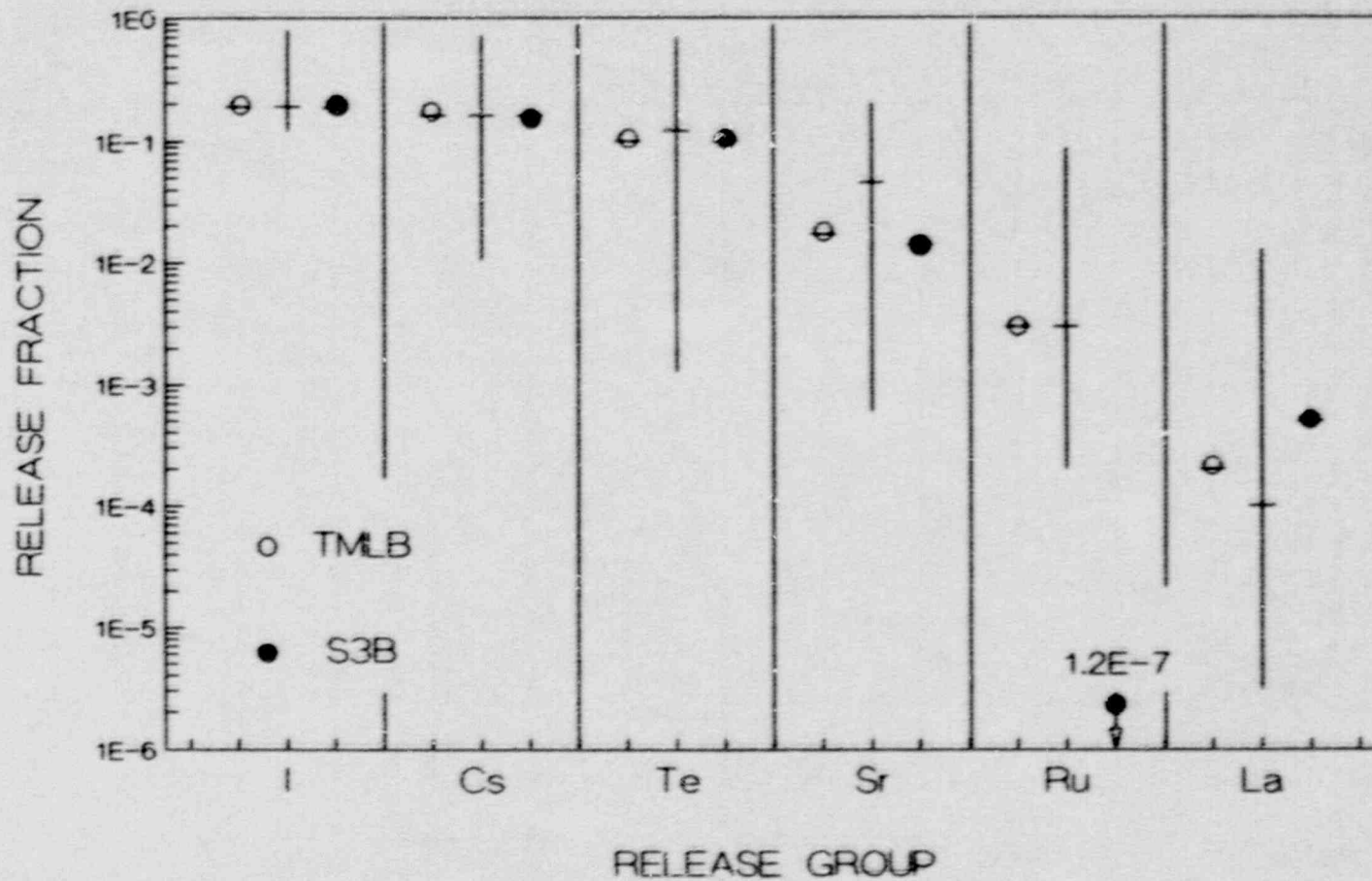


FIGURE 2.
COMPARISON OF SURSOR WITH STOP
RESULTS FOR TMLB-beta

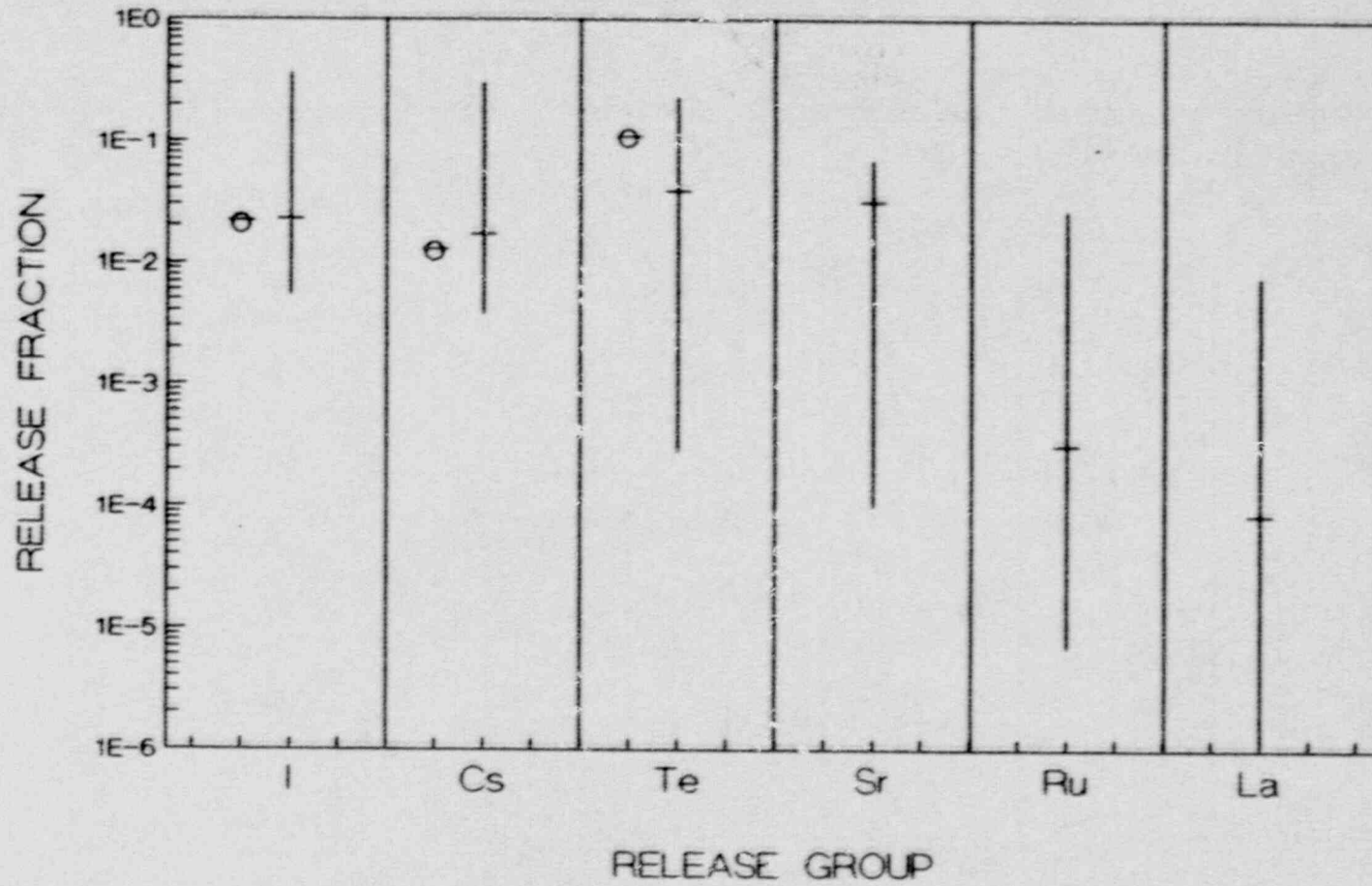


FIGURE 3.
COMPARISON OF SURSOR WITH STOP
RESULTS FOR TMLB-epsilon

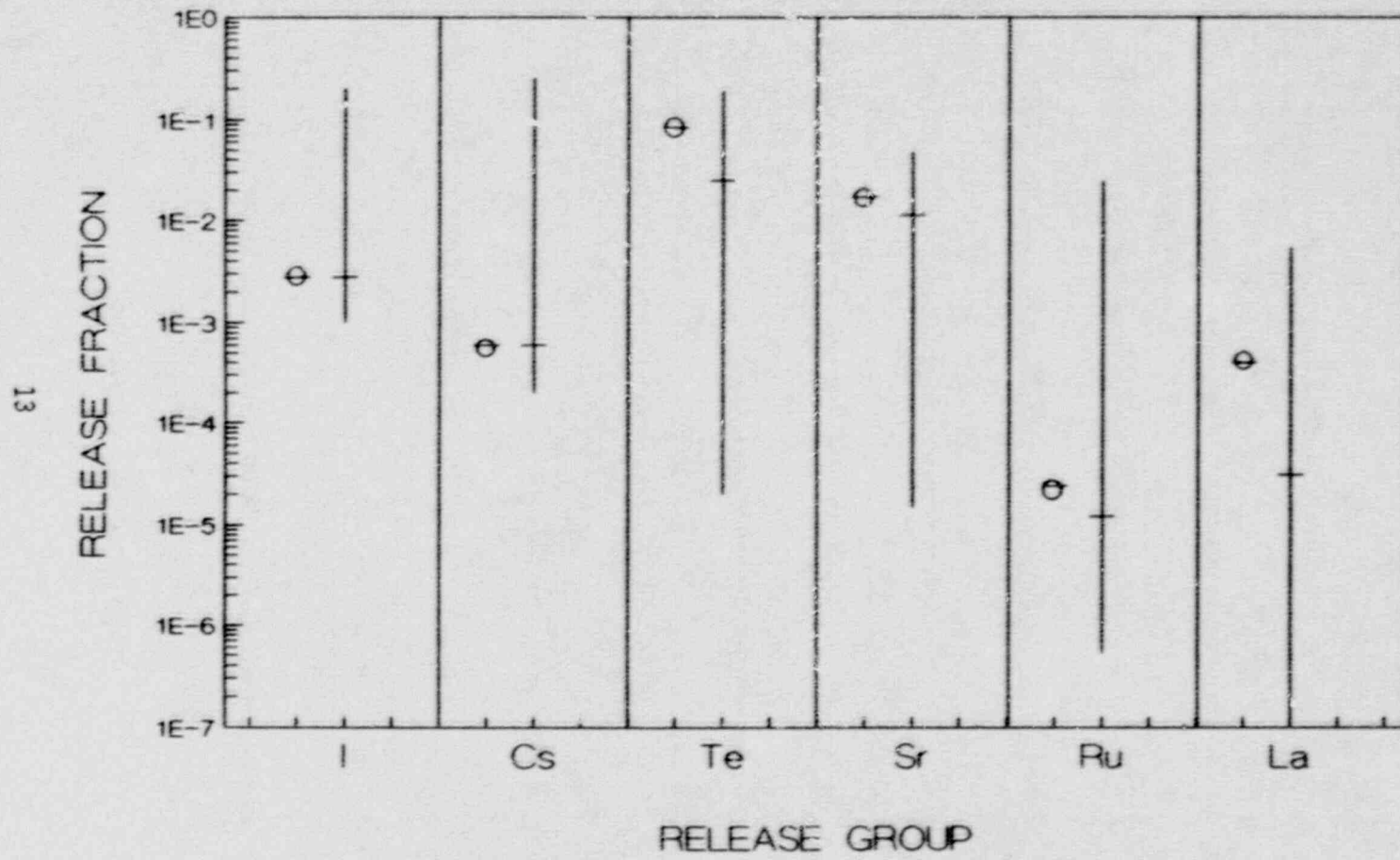


FIGURE 4.
COMPARISON OF SURSOR WITH STOP
RESULTS FOR TMLB-leak-before-break

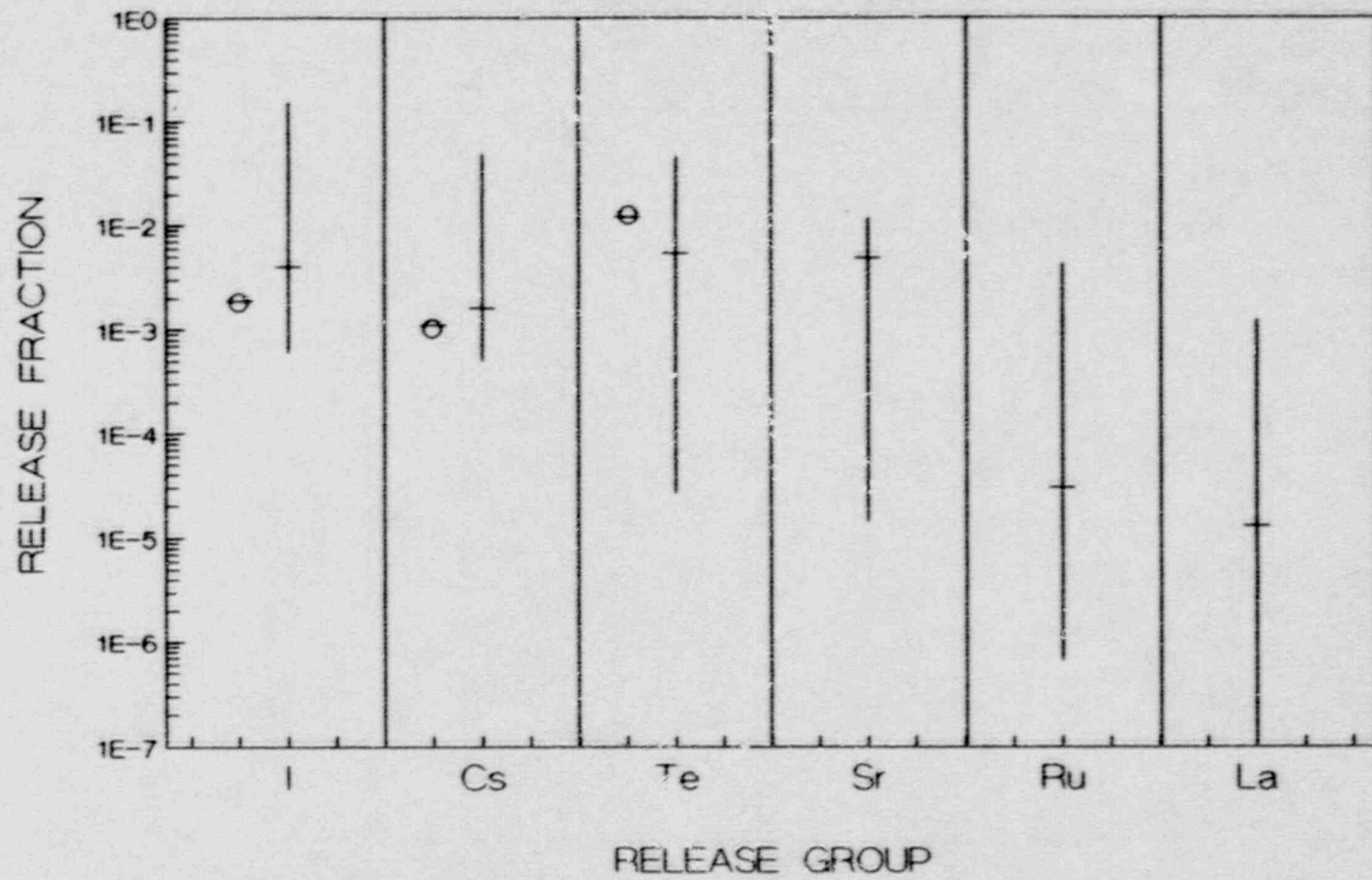


FIGURE 5.
COMPARISON OF SURSOR WITH STOP
RESULTS FOR S2D-gamma W/SPRAY FAILURE

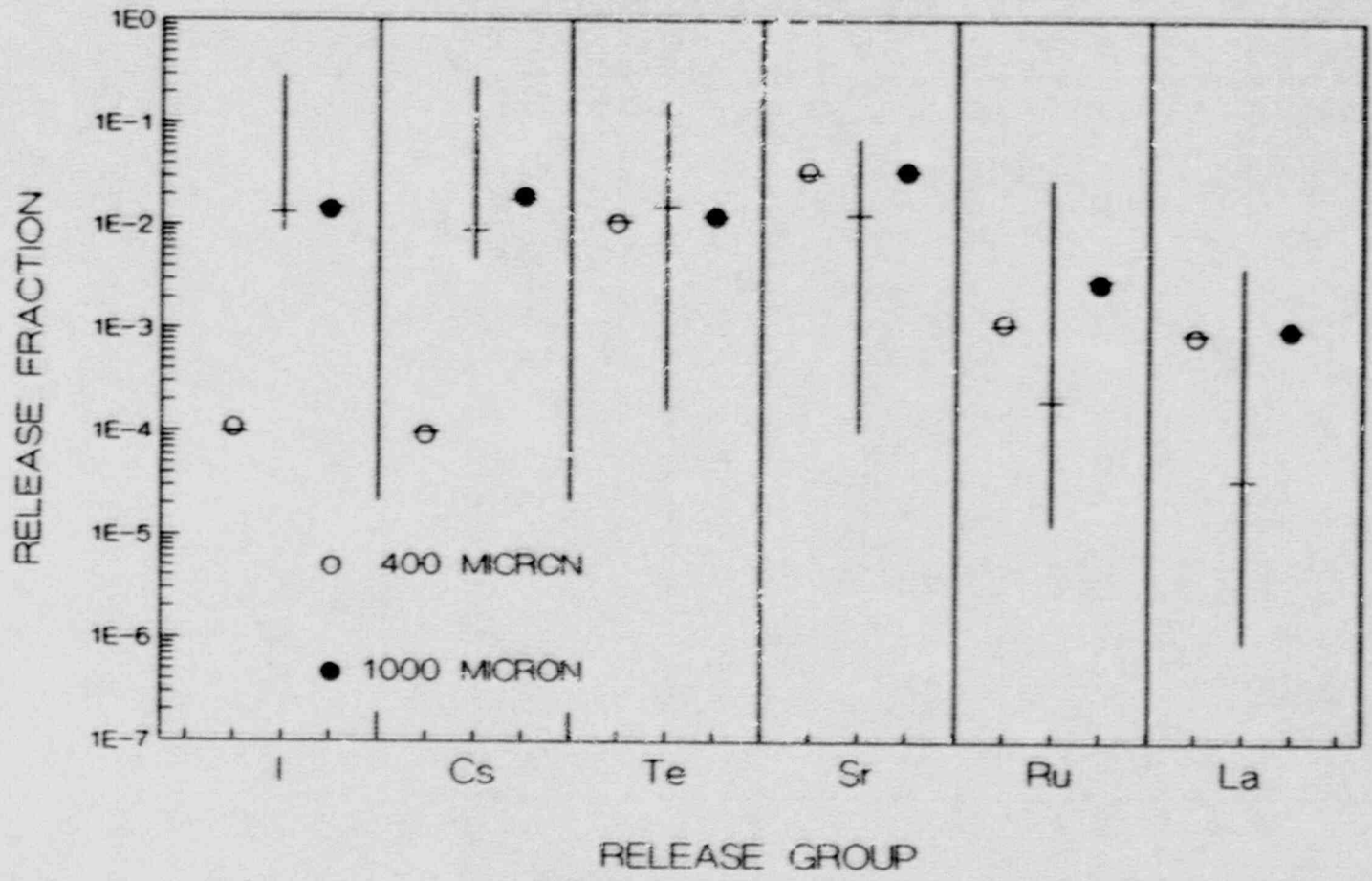


FIGURE 6.
 COMPARISON OF SURSOR WITH STCP
 RESULTS FOR S2D-gamma

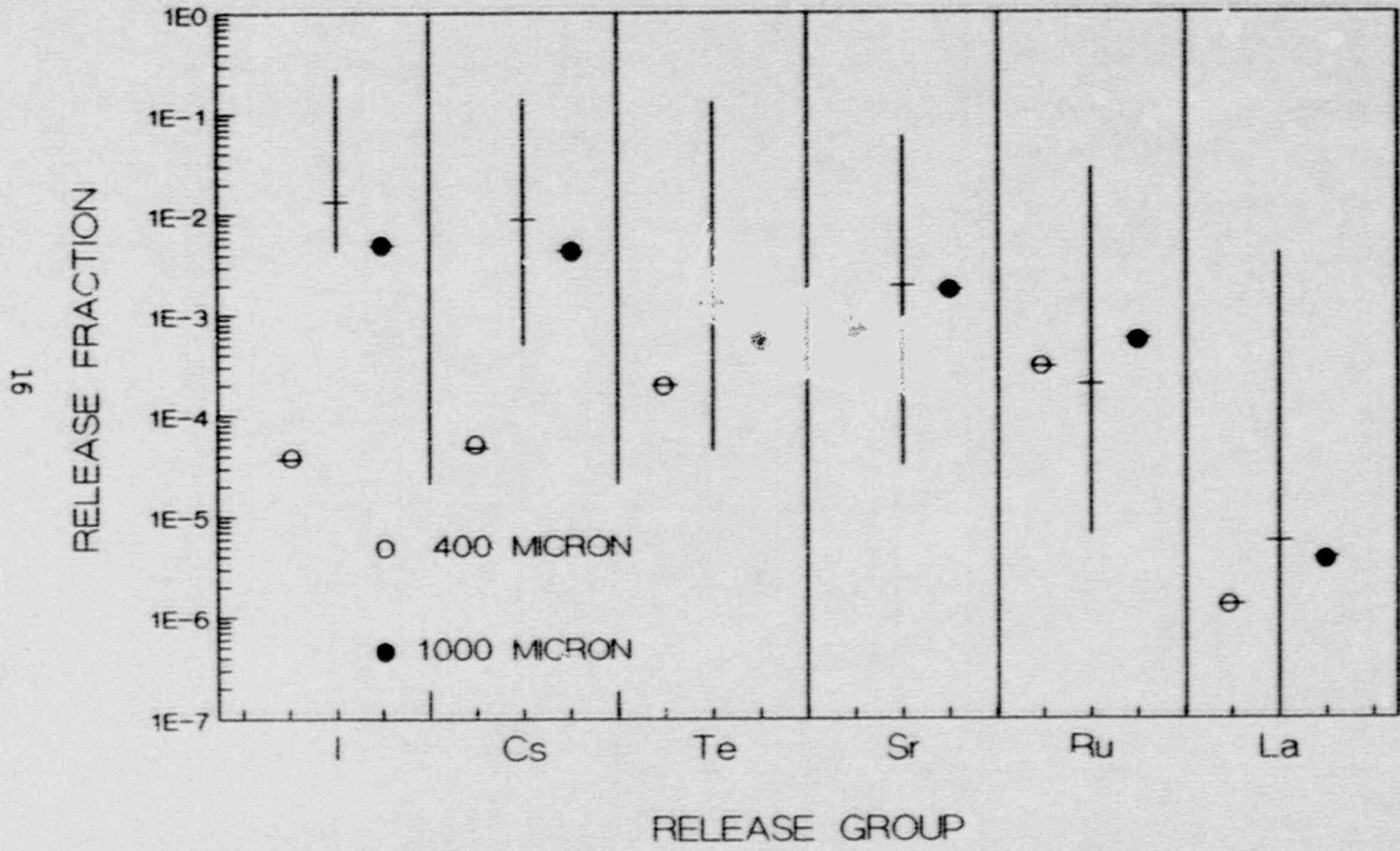


FIGURE 7.
 COMPARISON OF SURSOR WITH STCF
 RESULTS FOR S2D-beta

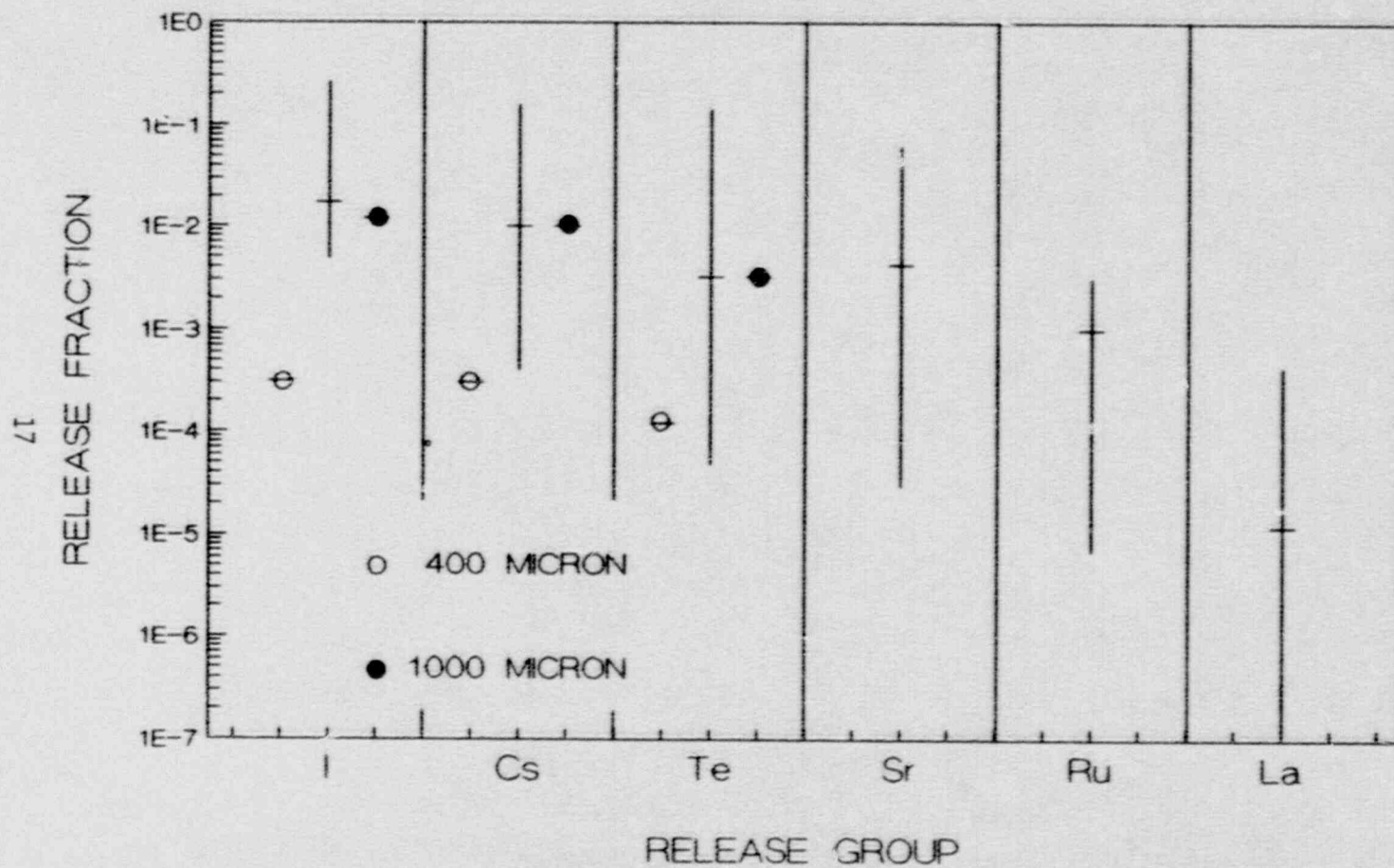


FIGURE 8.
COMPARISON OF SURSOR WITH STCP
RESULTS FOR AG-delta

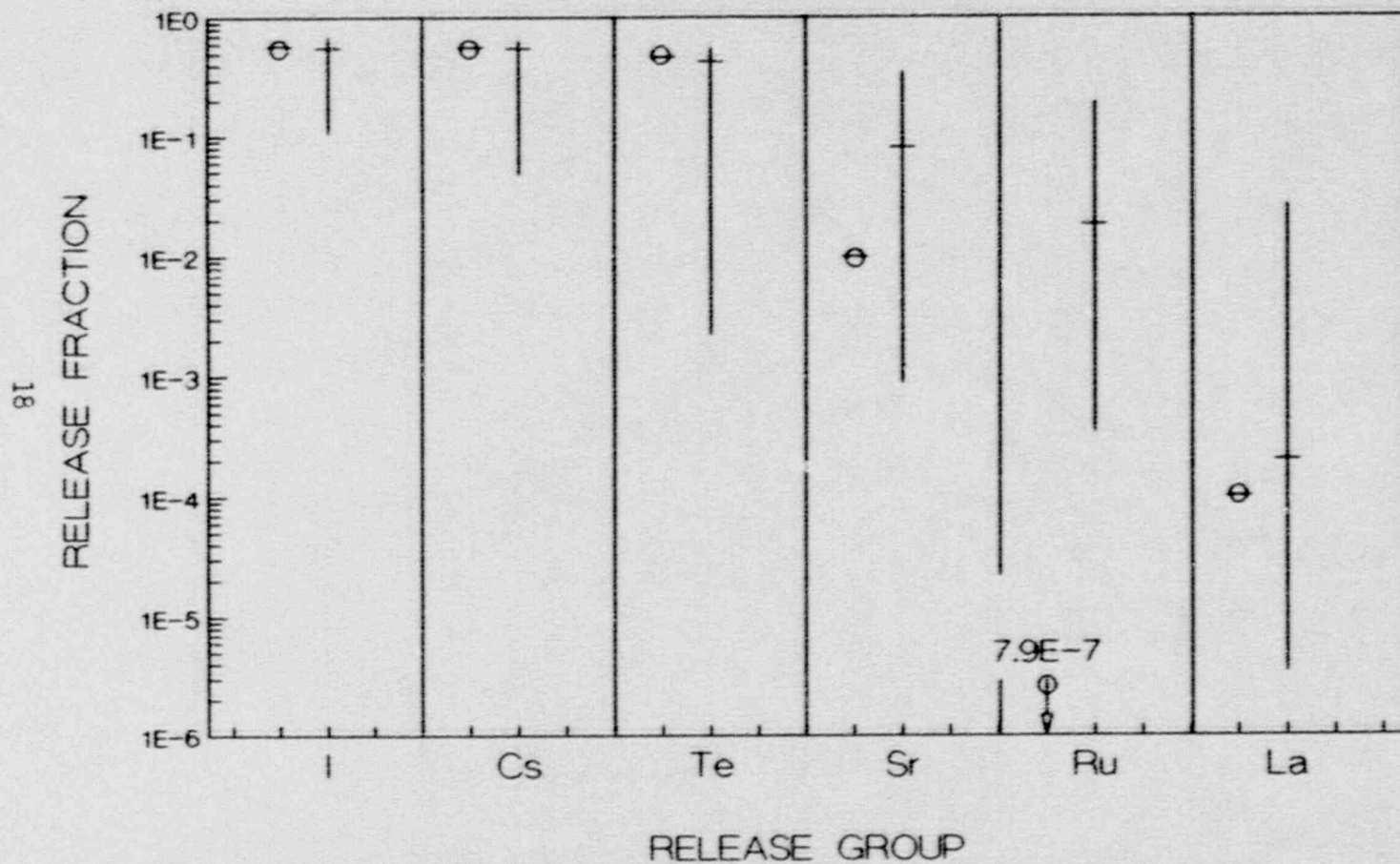


FIGURE 9.
COMPARISON OF SURSOR WITH STCP
RESULTS FOR V-wet

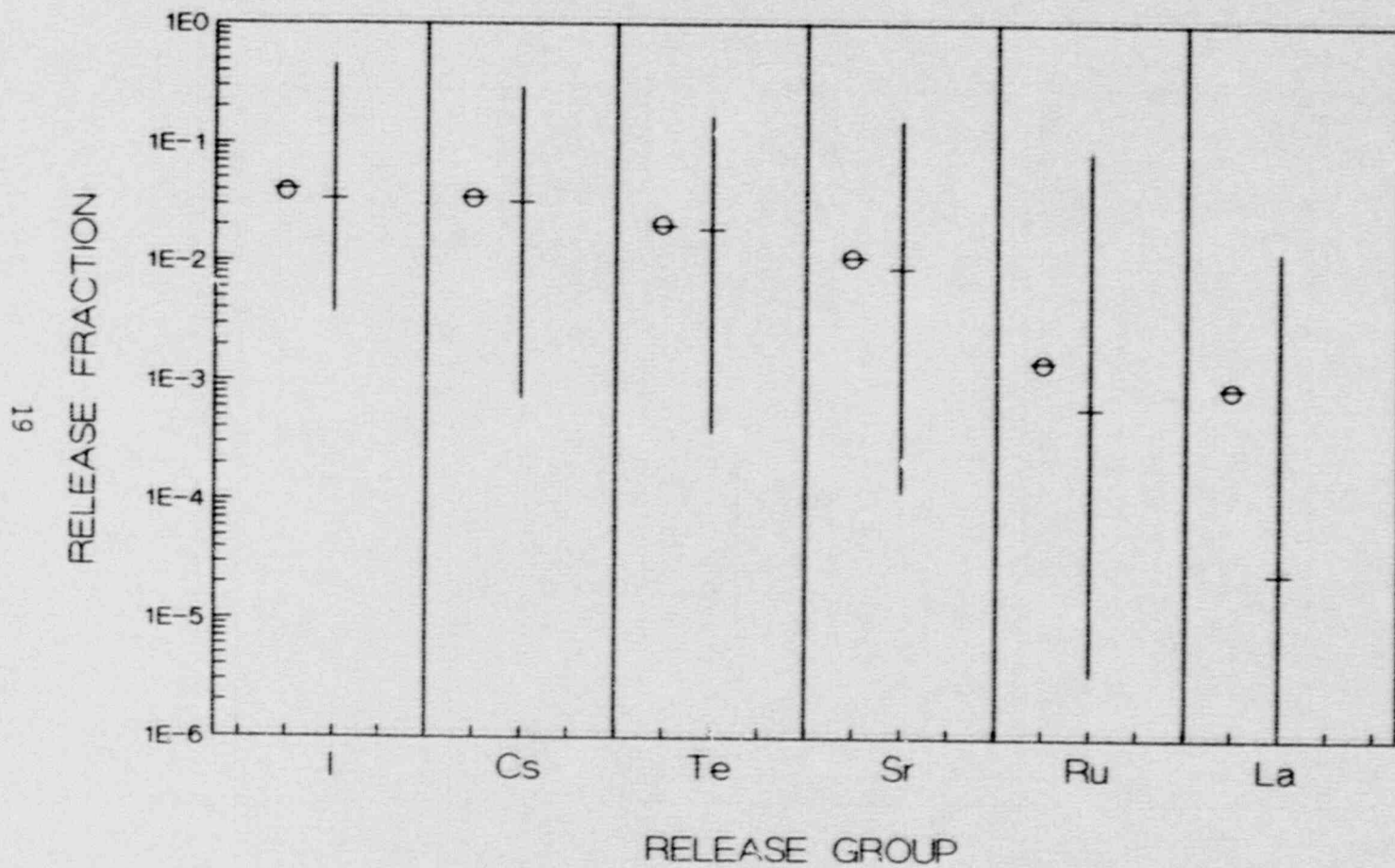
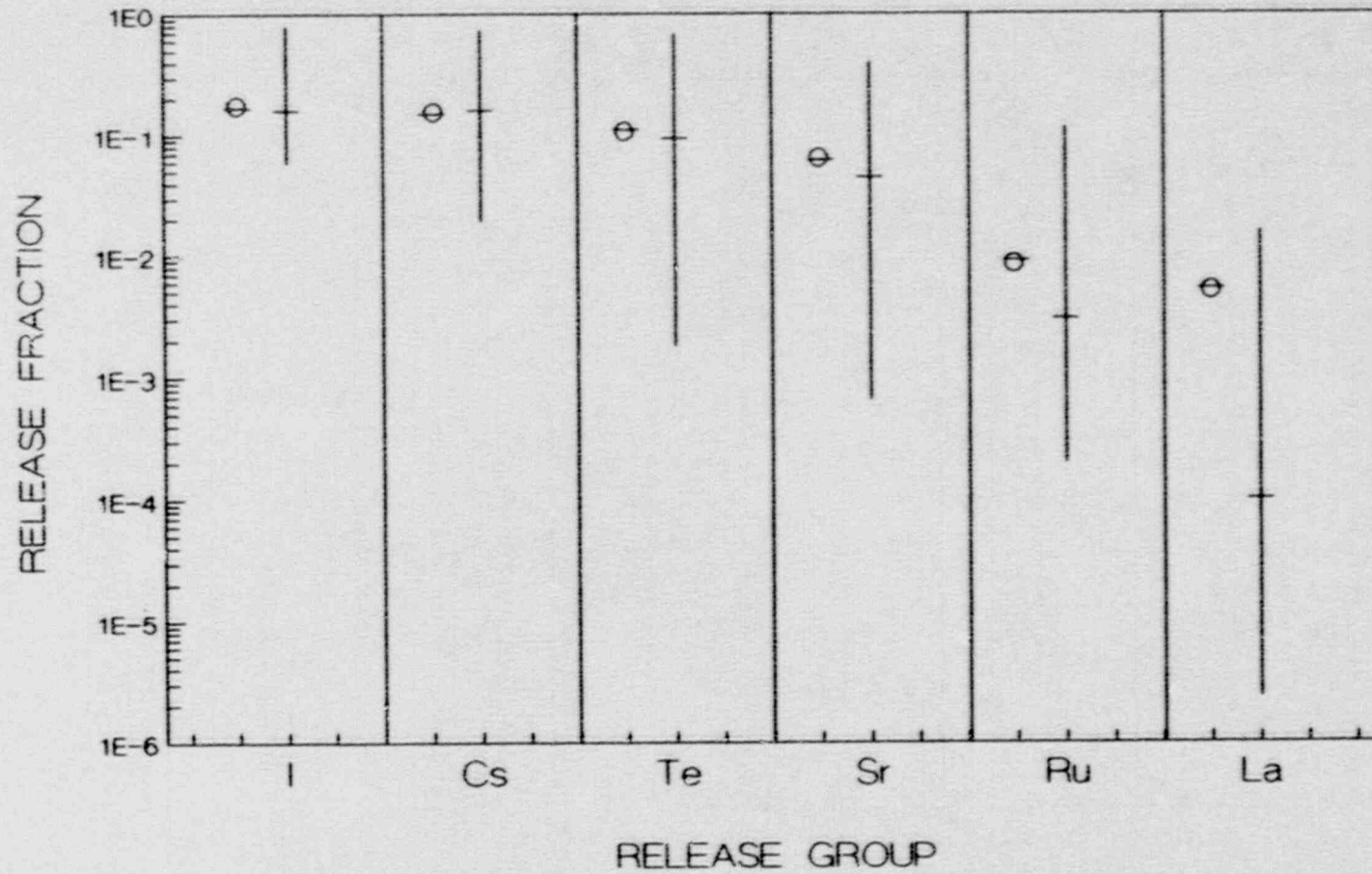


FIGURE 10.
COMPARISON OF SURSOR WITH STCP
RESULTS FOR V-dry



SURSOR Source Term Distributions

The foregoing discussion focused on the comparison between the SURSOR central estimates and corresponding STCP results. The following addresses the source terms distributions generated by SURSOR taking into account phenomena not considered by the STCP as well as uncertainties in the phenomena that are considered. The results discussed below were generated with one hundred runs of the DRAFT NUREG-1150 version of SURSOR, with the input parameters varied according to a statistical sample.

Figures 11 through 30 display the SURSOR generated source term distributions in two forms: histograms as well as smooth curves. The histograms were generated by dividing the range of values for each release group into five logarithmically equal intervals, counting the number of individual sample members in each interval, and dividing by the total number of sample members. The choice of five intervals was based on the fact that the SURSOR input variables were sampled over five intervals, representing the minimum, twenty-fifth, fiftieth, seventy-fifth, and maximum values of the individual variables.* The smooth curves represent the fitted normal or log-normal distributions for the one hundred sample members for each release group for each of the accident categories or accident progression bins. The normal distributions were found to provide reasonable fits for only a few of the cases; these are the asymmetrical distributions in the plots. The log-normal distributions appeared to provide better fits for the majority of the cases. Obviously, other possible distributions could have been considered, but the effort was not deemed warranted for the present purposes. The STCP results are indicated by the arrows for those accident progression bins for which they were available. Twenty accident categories (accident progression bins) were used for the Surry analyses. The discussion below addresses only the accident categories that have been indicated to be risk significant for the Surry plant.

Some general observations regarding the comparison between the SURSOR distributions and the available STCP results are as follows:

- (1) The spread or range of the calculated releases is considerably greater for the non-volatile species than it is for the more volatile ones. This is consistent with previous estimates and is to be expected. The volatile species are generally completely released from the fuel; thus the uncertainties are largely associated with attenuation along the release path. The releases of the nonvolatiles from the fuel, on the other hand, are generally quite small; thus the uncertainties in their environmental releases are compounded by uncertainties in their releases from the fuel as well as attenuation mechanisms.

*Care should be taken in the comparison of these histograms with the smooth curves. The histograms represent the probabilities that the release fractions lie in the given intervals. Note that the smooth curves show the probability density functions over the logarithm of the release fractions rather than over the absolute values.

- (2) The SURSOR calculated distributions for iodine and cesium generally lie above the point values calculated by the STCP. This is due to the fact that SURSOR takes into account such factors as late revolatization of these species from the primary system, decomposition of cesium iodide, formation of organic iodides, etc.; these factors are not modeled by the STCP.
- (3) For the less volatile species there does not appear to be a consistent pattern between the SURSOR distributions and the STCP point estimates.

In order to gain further insight on the factors that lead to the prediction of the upper range of SURSOR releases, the SURSOR calculated source term distributions for a number of the accident progression bins have been examined in detail. The accident progression bins considered are those indicated to be risk significant in DRAFT NUREG-1150. The observations are discussed below.

Bin 1

Surry Bin 1 is characterized by a station blackout with early containment failure. The examination of the upper range of SURSOR source term distributions yields the following observations.

- The highest predicted iodine release fractions are all determined by LLH samples in which all the cesium iodide is assumed to decompose; the resulting volatile forms of iodine are released from the primary system and are available for release to the environment upon containment failure,
- The highest cesium releases are determined by the LLH samples in which primary system retention for this group is very low. The high release from the primary system leads directly to high environmental releases.
- The upper range of tellurium releases is determined by two types of samples: low primary system retention and high ex-vessel release, and low in-vessel release together with high ex-vessel release.
- The upper range of strontium releases are determined by samples characterized by various combinations of high in-vessel and high ex-vessel releases from the fuel.
- The highest ruthenium releases are determined by samples with very high in-vessel release fractions from the fuel, and to a lesser extent high ex-vessel releases.
- The upper range of predicted lanthanum group releases appears to be dominated by high ex-vessel releases.

Bin 2

This bin is characterized by sequences with total loss of makeup to the primary and secondary systems and early containment failure due to hydrogen combustion.

- The upper range of iodine releases is determined by samples in which all the cesium iodide in the primary system decomposed into more volatile forms and is released to the containment.
- The highest cesium releases are determined by LLH samples with low primary system retention.
- The upper range of tellurium releases appears to be driven by samples with low primary system retention for this group.
- The highest strontium releases are determined by samples with combinations of high in-vessel and ex-vessel releases.
- High ruthenium releases are the result of samples with very high in-vessel releases and, to a lesser extent, high ex-vessel releases.
- The highest lanthanum releases are associated with samples having combinations of high in-vessel and ex-vessel releases.

Bin 5

This bin involves containment failure prior to core melt and release of fission products in a failed containment in the absence of operating safety features.

- The upper range of iodine source terms is determined by complete in-vessel releases with essentially no primary system retention. There are some samples, however, which have very low in-vessel releases, with the bulk of the iodine released ex-vessel.
- The factors leading to high cesium source terms are essentially the same as those for iodine.
- The highest tellurium releases are determined by factors similar to the above for iodine and cesium, i.e., high in-vessel releases with little or no primary system retention.
- The highest strontium releases are primarily the result of high in-vessel releases and low primary system retention, with some samples characterized by high ex-vessel releases.
- The upper range of ruthenium releases appears to be determined by high in-vessel release fractions, with little primary system retention.

- The highest releases for the lanthanum group are associated with two types of samples: high in-vessel releases, or high ex-vessel releases.

Bin 11

This bin is representative of interfacing systems loss-of-coolant-accidents with submerged release paths.

- All of the highest iodine source terms are associated with low decontamination factors for the water submergence. Additional factors include: high fractions of cesium iodide decomposition, low primary system retention, and the combination of low in-vessel and high ex-vessel releases.
- As with iodine, all the highest cesium source terms are associated with low decontamination factors for the submerged path. Other factors include: low primary system retention, the combination of low in-vessel and high ex-vessel releases, and late cesium volatilization.
- In addition to low decontamination factors for the submerged release path, the upper range of tellurium releases involve samples with high ex-vessel releases. An additional factor is low primary system retention.
- The upper range of strontium releases are governed by low to moderate water decontamination factors as well as including high in-vessel releases and/or low primary system retention.
- The highest ruthenium releases are associated with low to moderate water decontamination factors, and high in-vessel releases, with some contribution from low primary system retention.
- In addition to low to moderate water decontamination factors, the upper range of lanthanum releases is associated with high in-vessel releases or high ex-vessel releases.

Bin 12

This bin is characteristic of interfacing systems loss-of-coolant-accidents with dry release paths.

- The upper range of iodine releases in this case is associated with high fractions of cesium iodide decomposition, low primary system retention, and large fractions of late iodine volatilization from the primary system.
- The highest cesium source terms are the result of low primary system retention, high fractions of late cesium volatilization, and the combination of low in-vessel and high ex-vessel releases.

- The highest tellurium source terms are determined by low primary system retention and the combination of low in-vessel and high ex-vessel releases.
- The upper range of strontium source terms all include high in-vessel releases and, in a number of cases, low primary system retention.
- The highest ruthenium releases are associated with various combinations of high in-vessel releases and low primary system retention, with high ex-vessel releases a contributing factor also.
- The highest releases of the lanthanum group include high releases in- and ex-vessel.

Bin 16

Bin 16 is characteristic of station blackout with early containment failure due to direct heating.

- The upper range of iodine source terms is determined by complete decomposition of cesium iodide and its release from the primary system.
- The upper range of cesium source terms arises from low primary system retention factors.
- The upper range of tellurium releases is associated with two types of samples: low primary system retention and high ex-vessel release, and low in-vessel release together with high ex-vessel release.
- The highest strontium releases are associated with various combinations of high in-vessel and high ex-vessel releases.
- The upper range of ruthenium releases is associated with samples having high direct heating releases, as well as with high in-vessel releases and low in vessel retention.
- The highest releases for the lanthanum group involve high direct heating contributions.

It is interesting to note that direct heating only influences the upper ranges of ruthenium and lanthanum releases, with little obvious impact on the source terms for the other groups.

Bin 17

Bin 17 is representative of accident scenarios with loss of makeup to the primary and secondary systems, containment safety features available, and containment failure due to direct heating.

- The upper range of iodine releases is governed by complete decomposition of cesium iodide into more volatile forms.
- The highest cesium releases are associated with samples having very low primary system retention.
- The upper range of tellurium release is determined by two types of samples: low primary system retention and high ex-vessel release, and low in-vessel release combined with high ex-vessel release.
- The upper range of strontium releases was determined by various combinations of high in-vessel and high ex-vessel releases, with some contribution from samples with high direct heating releases.
- The highest ruthenium releases involved large contributions to the source term from direct heating, as well as from samples with high in-vessel releases.
- The highest releases for the lanthanum group involve significant contribution from direct heating, as well as from high ex-vessel releases.

FIGURE 11.
 LLH SAMPLE SOURCE TERM DISTRIBUTIONS
 SURRY BIN 1

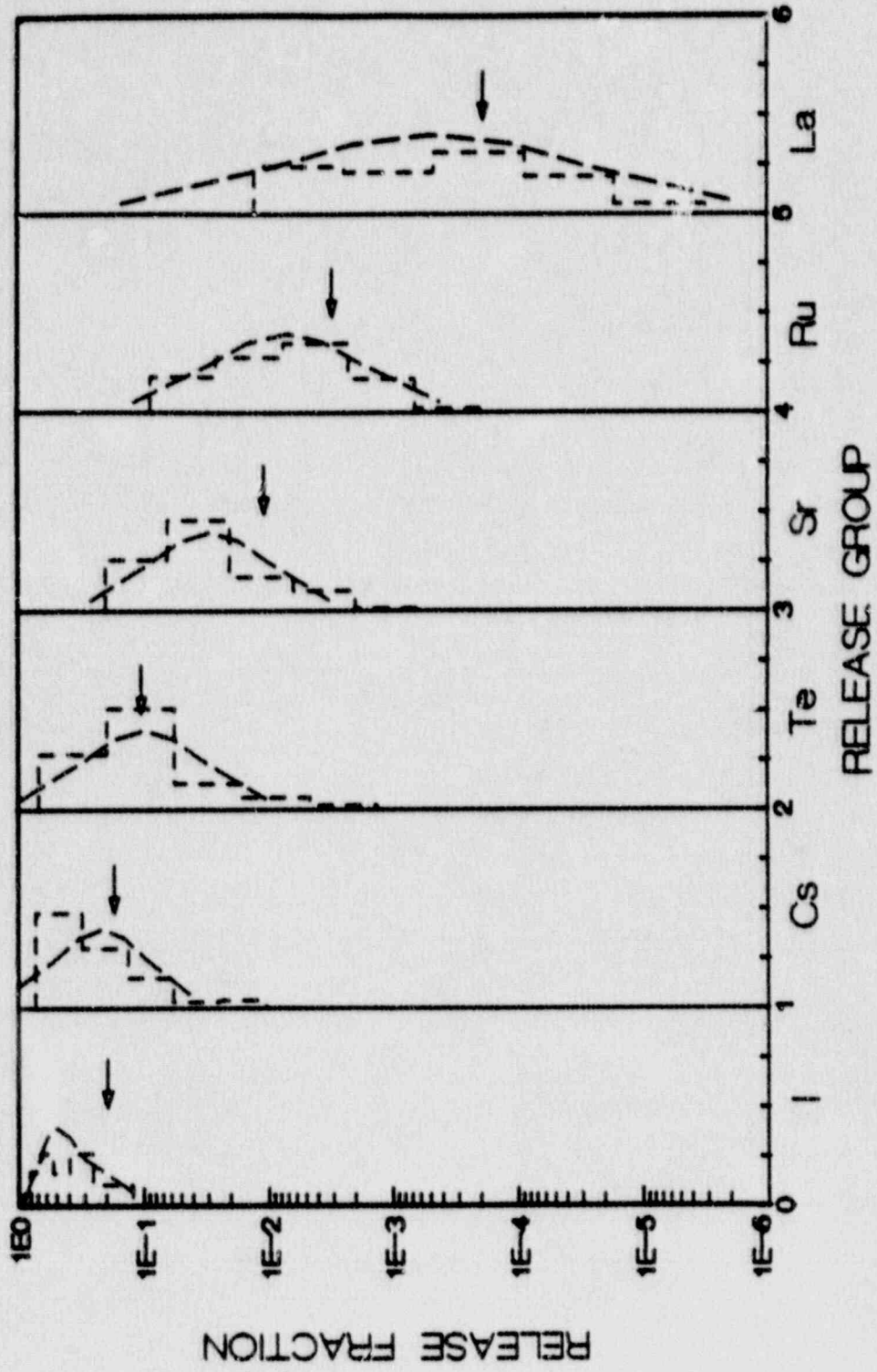


FIGURE 12.
 LLH SAMPLE SOURCE TERM DISTRIBUTIONS
 SUPPLY BIN 2

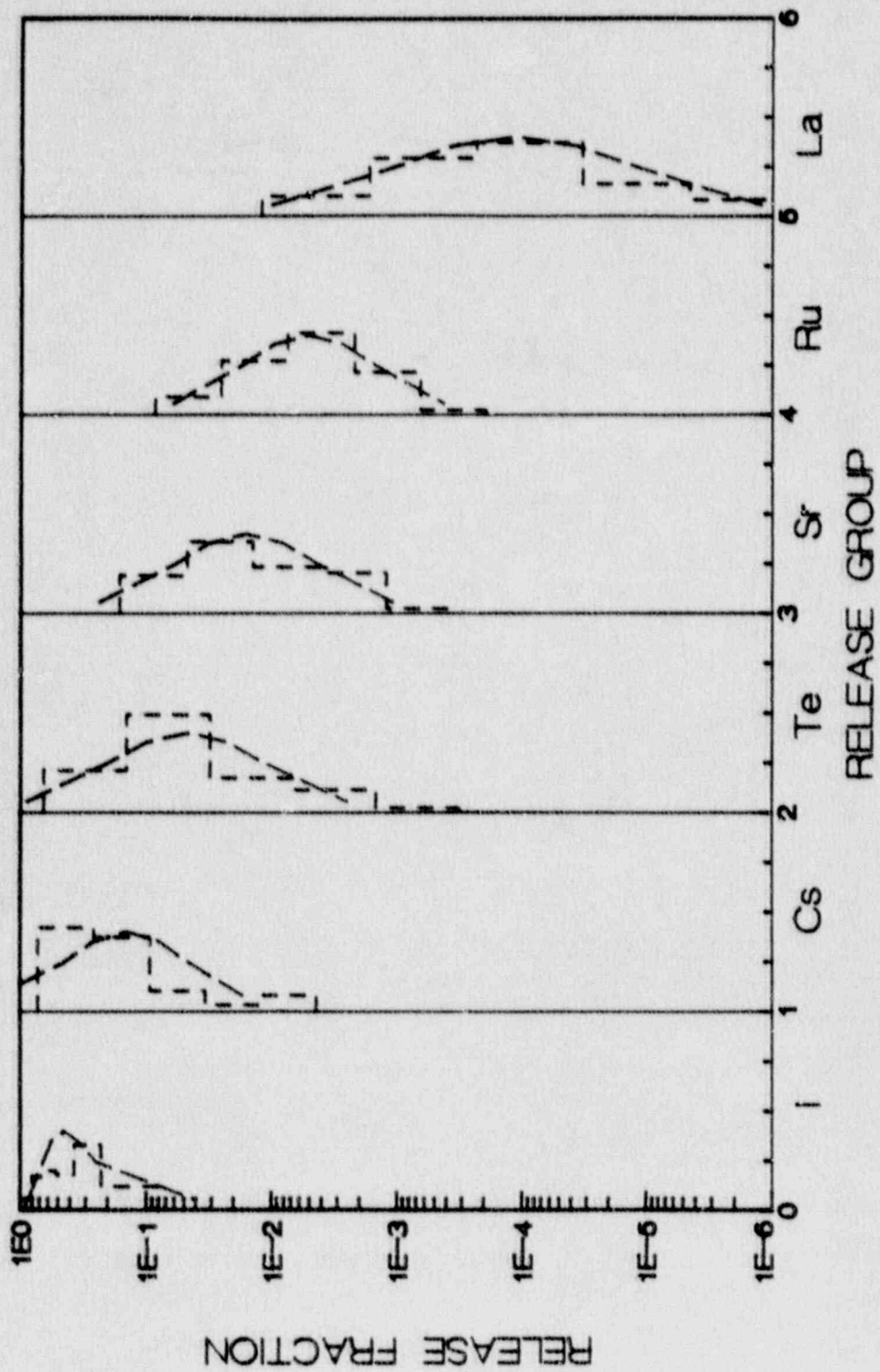


FIGURE 13.
LLH SAMPLE SOURCE TERM DISTRIBUTIONS
SURRY BIN 3

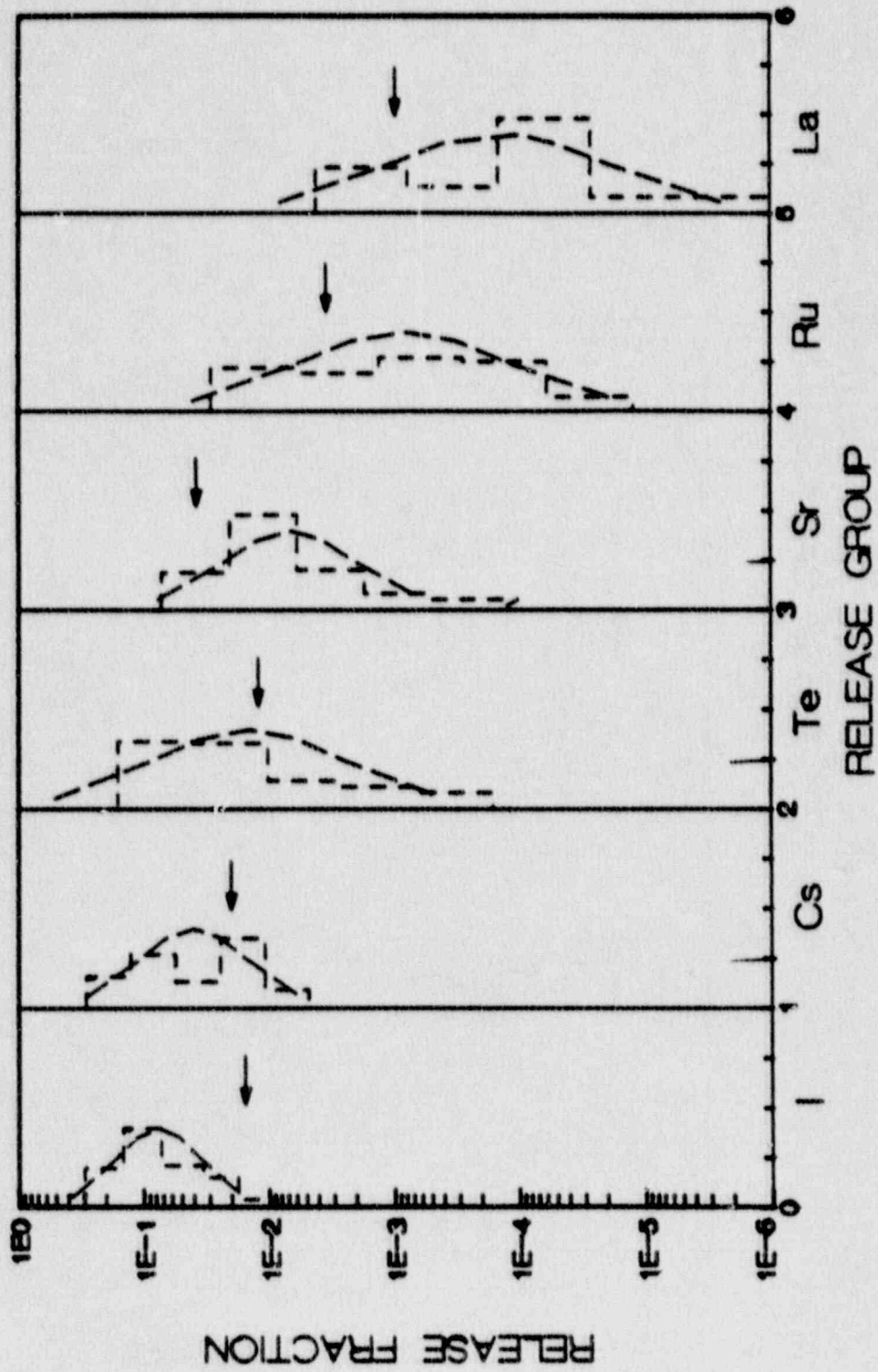


FIGURE 14.

LLH SAMPLE SOURCE TERM DISTRIBUTIONS
SURRY BIN 4

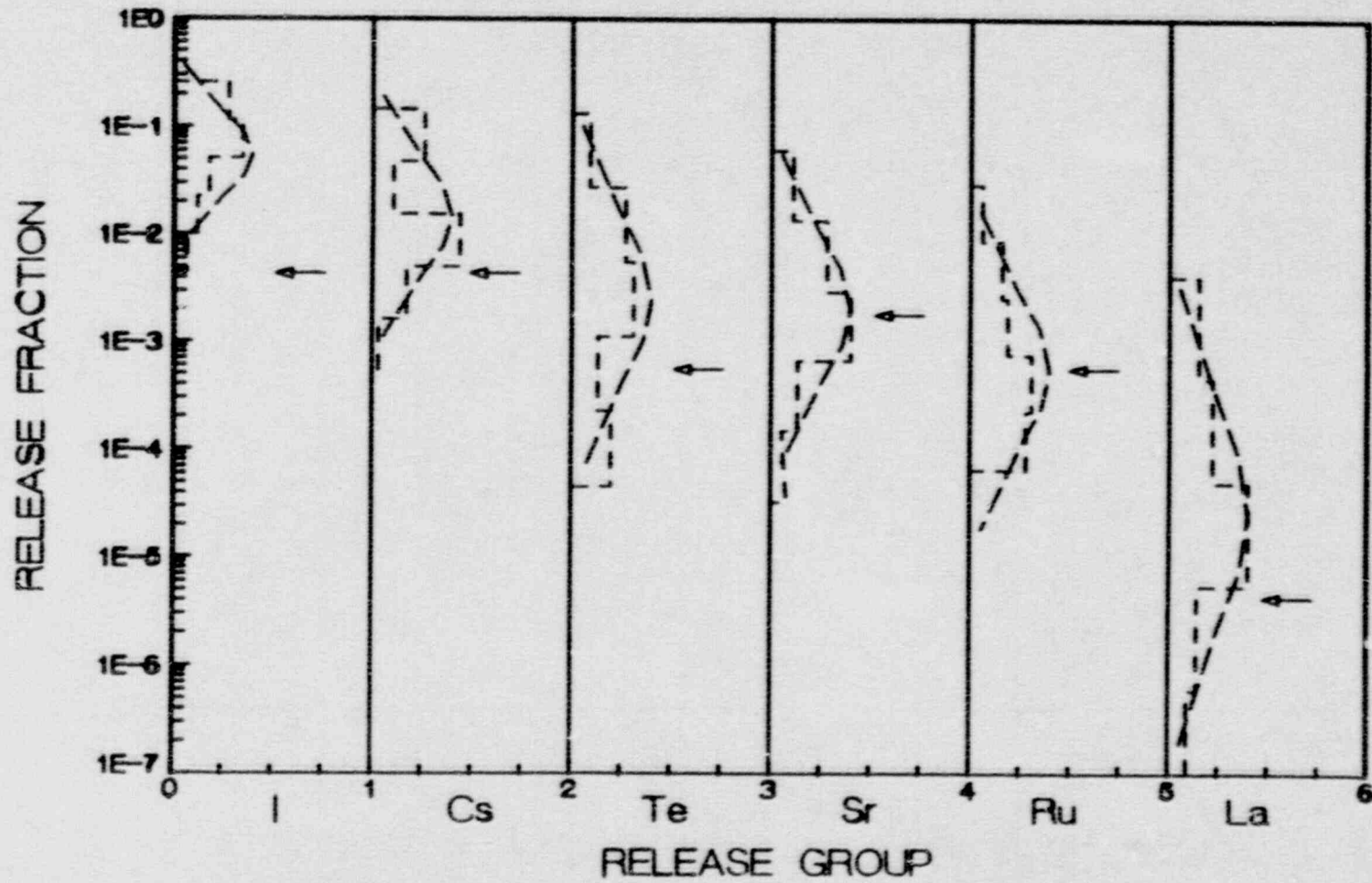


FIGURE 15.
LLH SAMPLE SOURCE TERM DISTRIBUTIONS
SURRY BIN 5

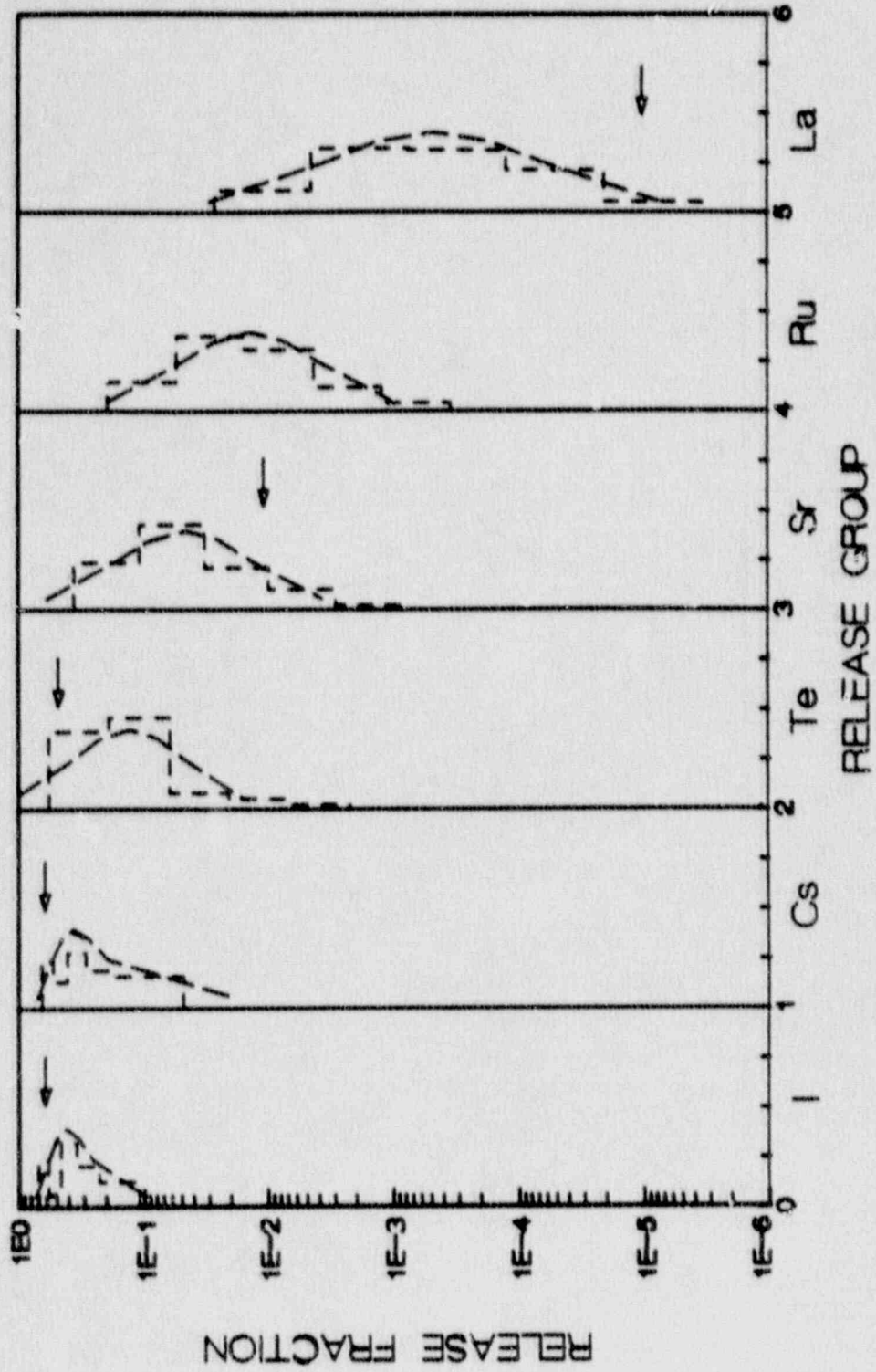


FIGURE 16.
LLH SAMPLE SOURCE TERM DISTRIBUTIONS
SURRY BIN 6

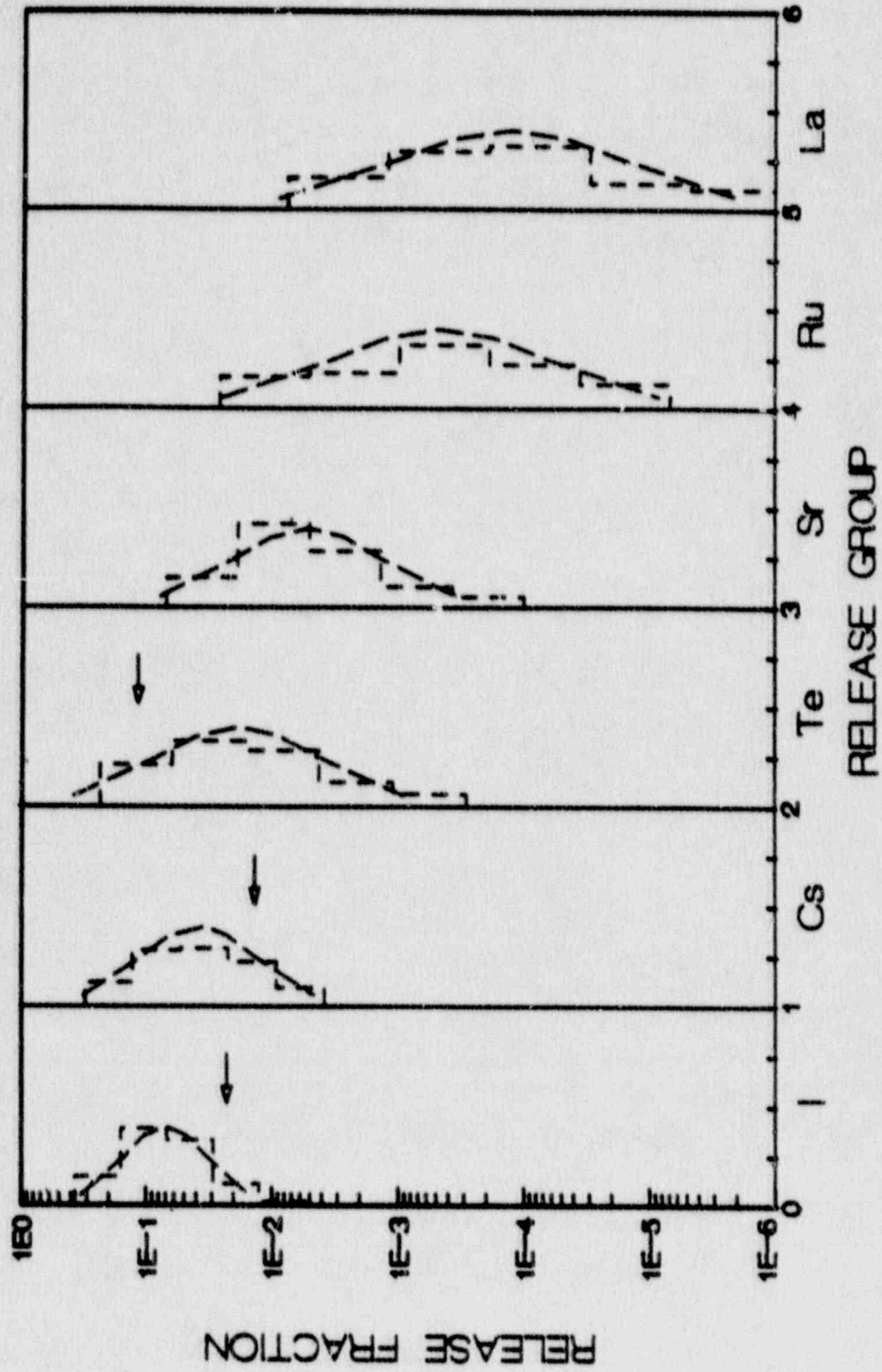


FIGURE 17.

LLH SAMPLE SOURCE TERM DISTRIBUTIONS
SURRY BIN 7

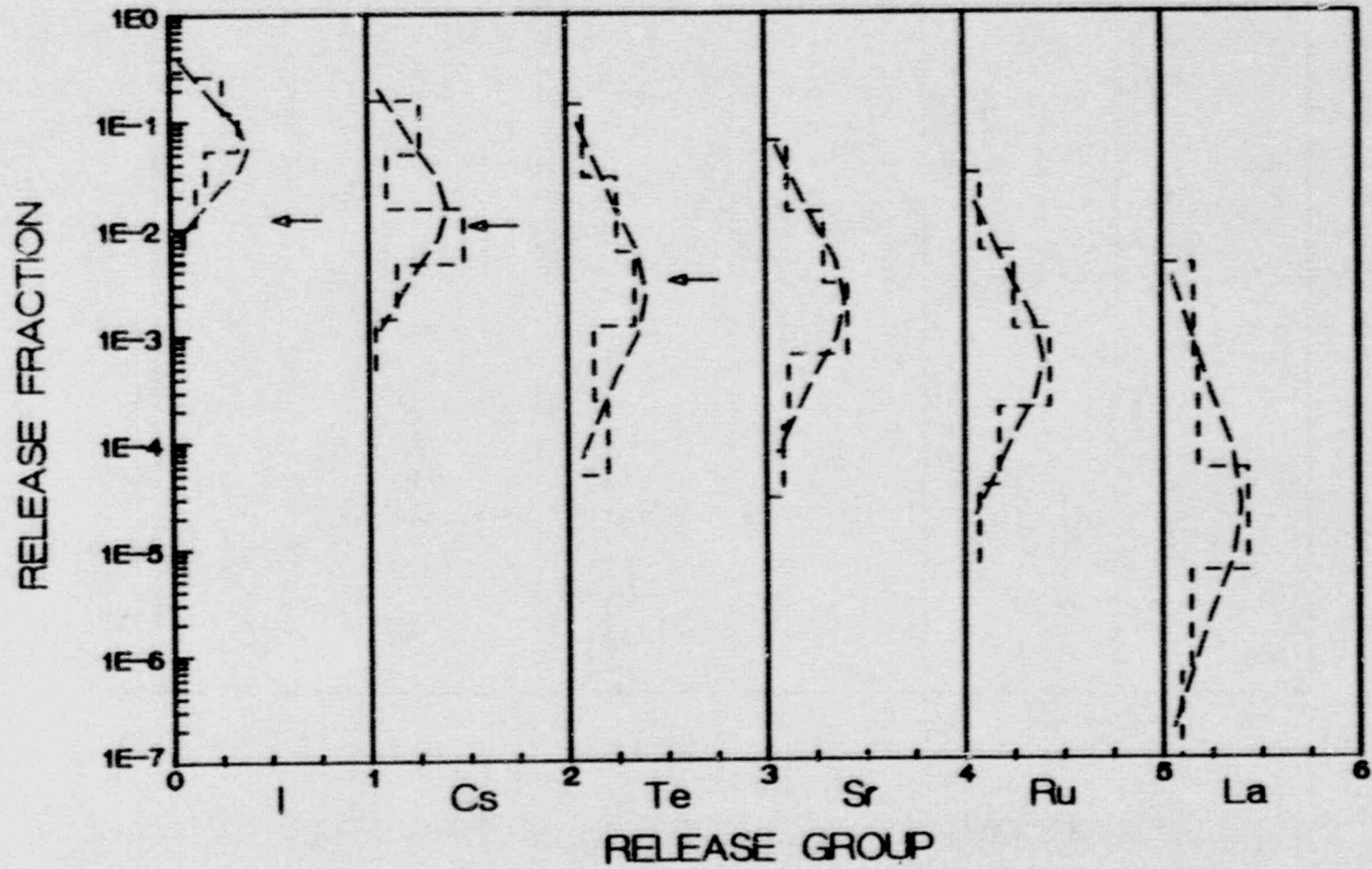


FIGURE 18.
 LLH SAMPLE SOURCE TERM DISTRIBUTIONS
 SURRY BIN 8

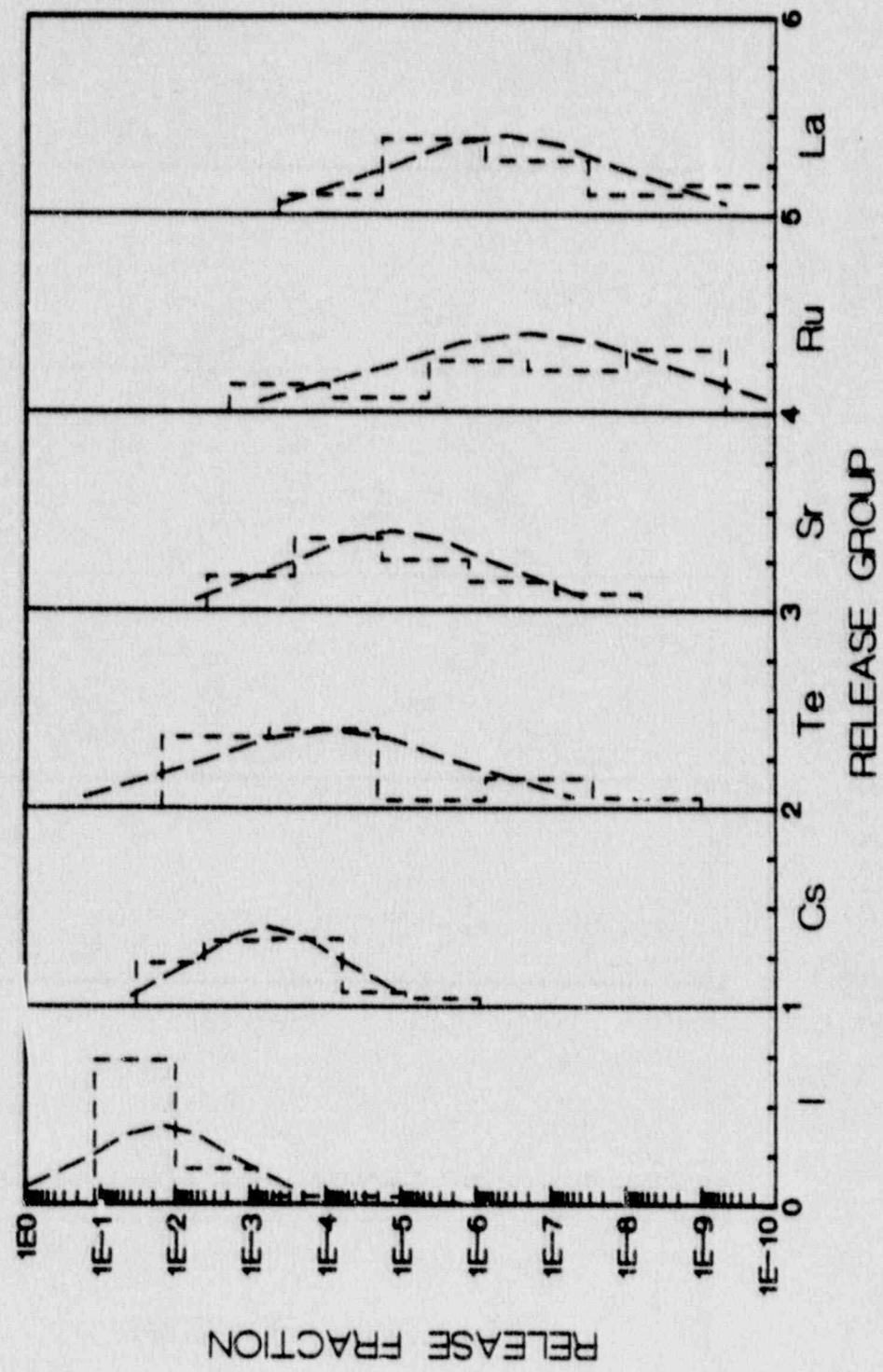


FIGURE 19.
 LLH SAMPLE SOURCE TERM DISTRIBUTIONS
 SURRY BIN 9

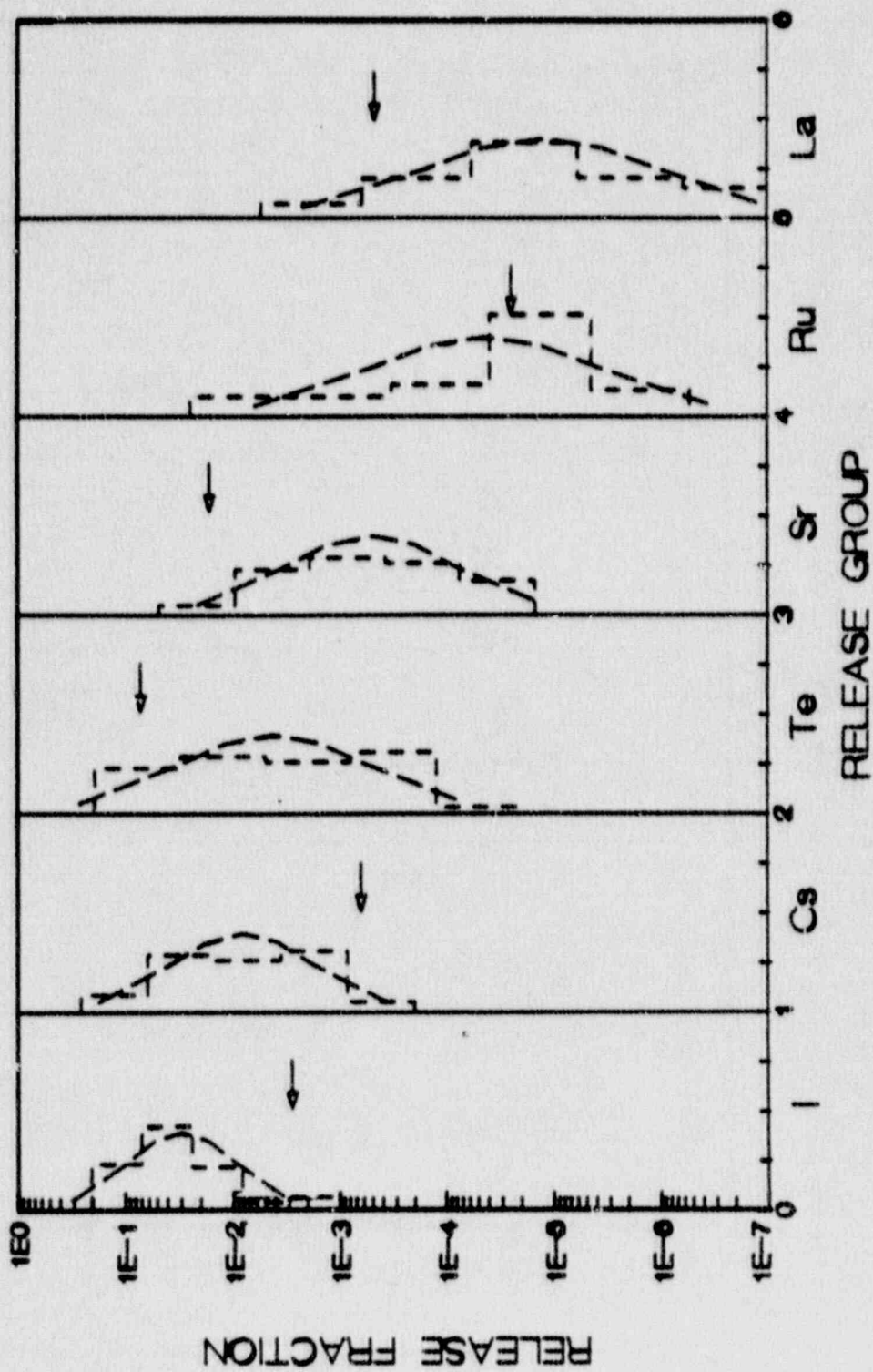


FIGURE 20.
 LLH SAMPLE SOURCE TERM DISTRIBUTIONS
 SURRY BIN 10

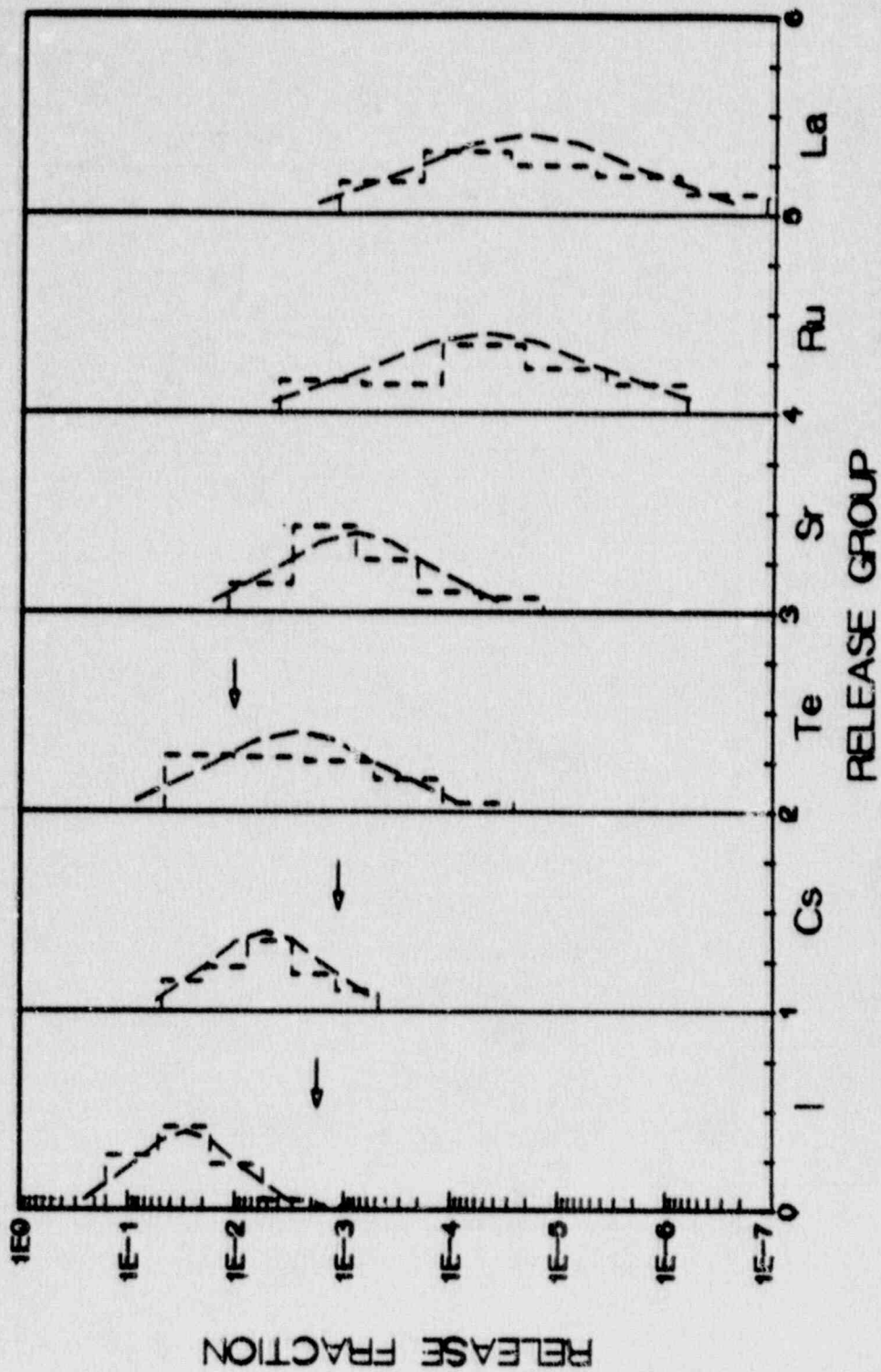


FIGURE 21.
LLH SAMPLE SOURCE TERM DISTRIBUTIONS
SURRY BIN 11

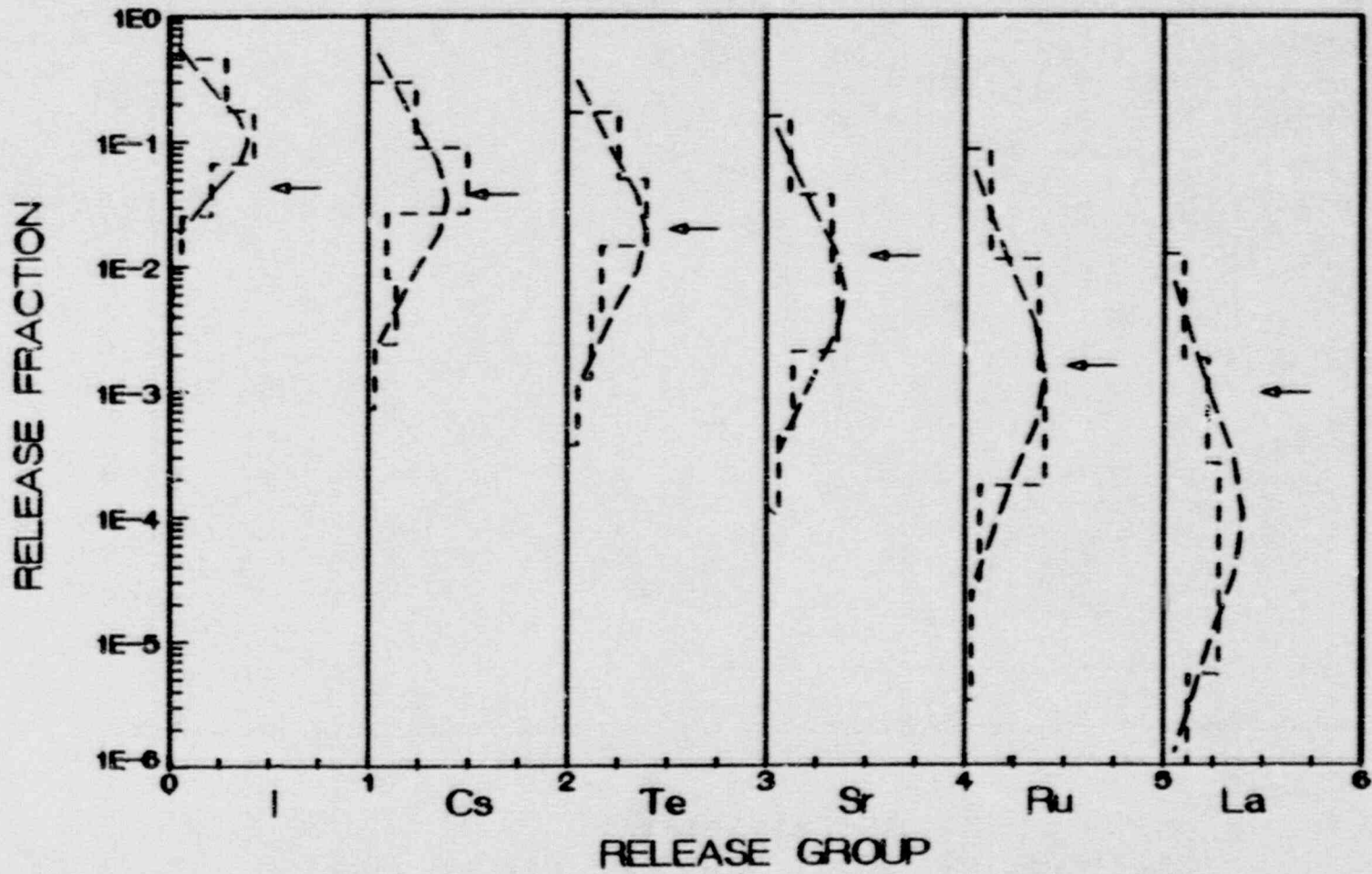


FIGURE 22.
 LLH SAMPLE SOURCE TERM DISTRIBUTIONS
 SUPPLY BIN 12

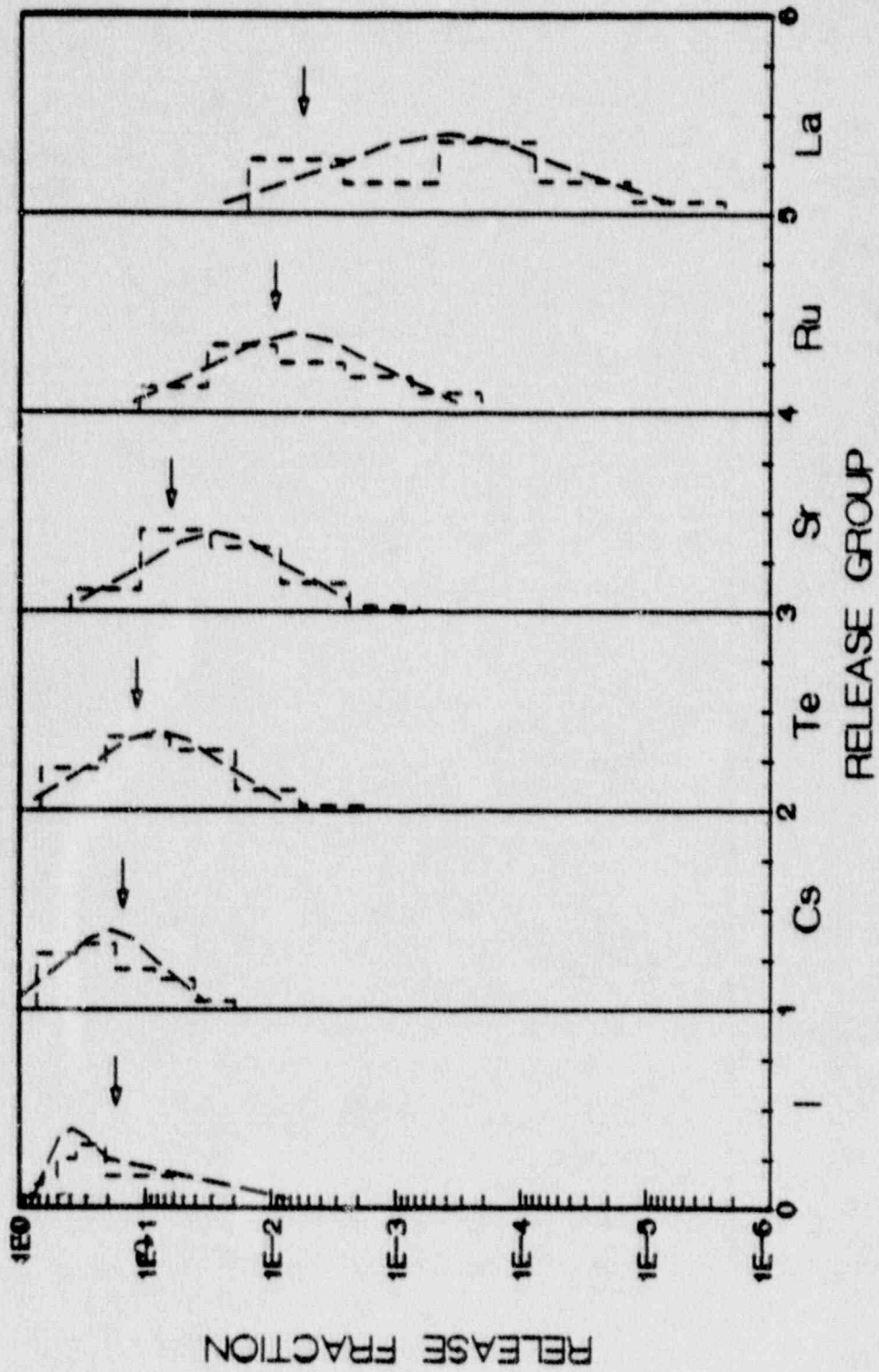


FIGURE 23.
LLH SAMPLE SOURCE TERM DISTRIBUTIONS
SURRY BIN 13

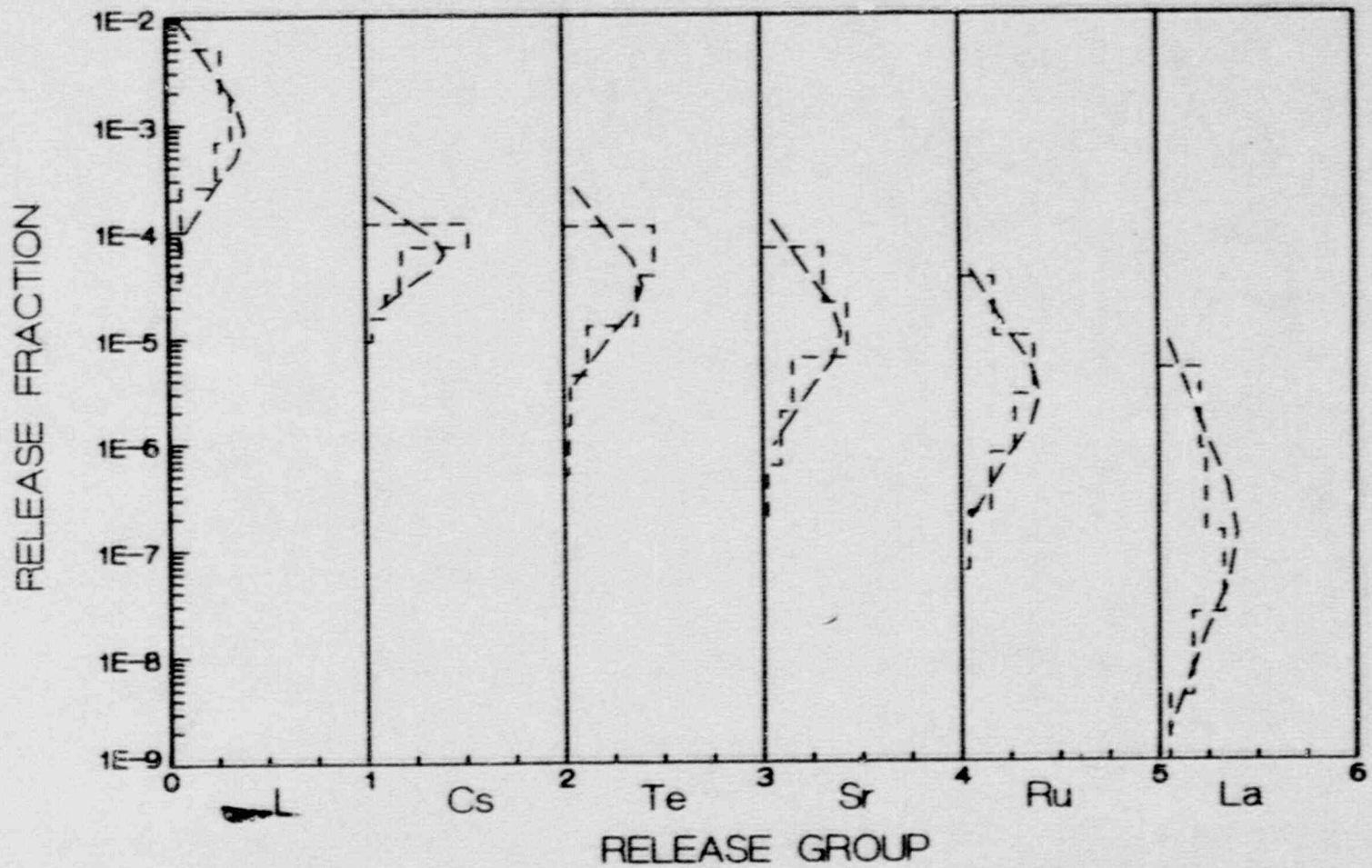


FIGURE 24.
LLH SAMPLE SOURCE TERM DISTRIBUTIONS
SURRY BIN 14

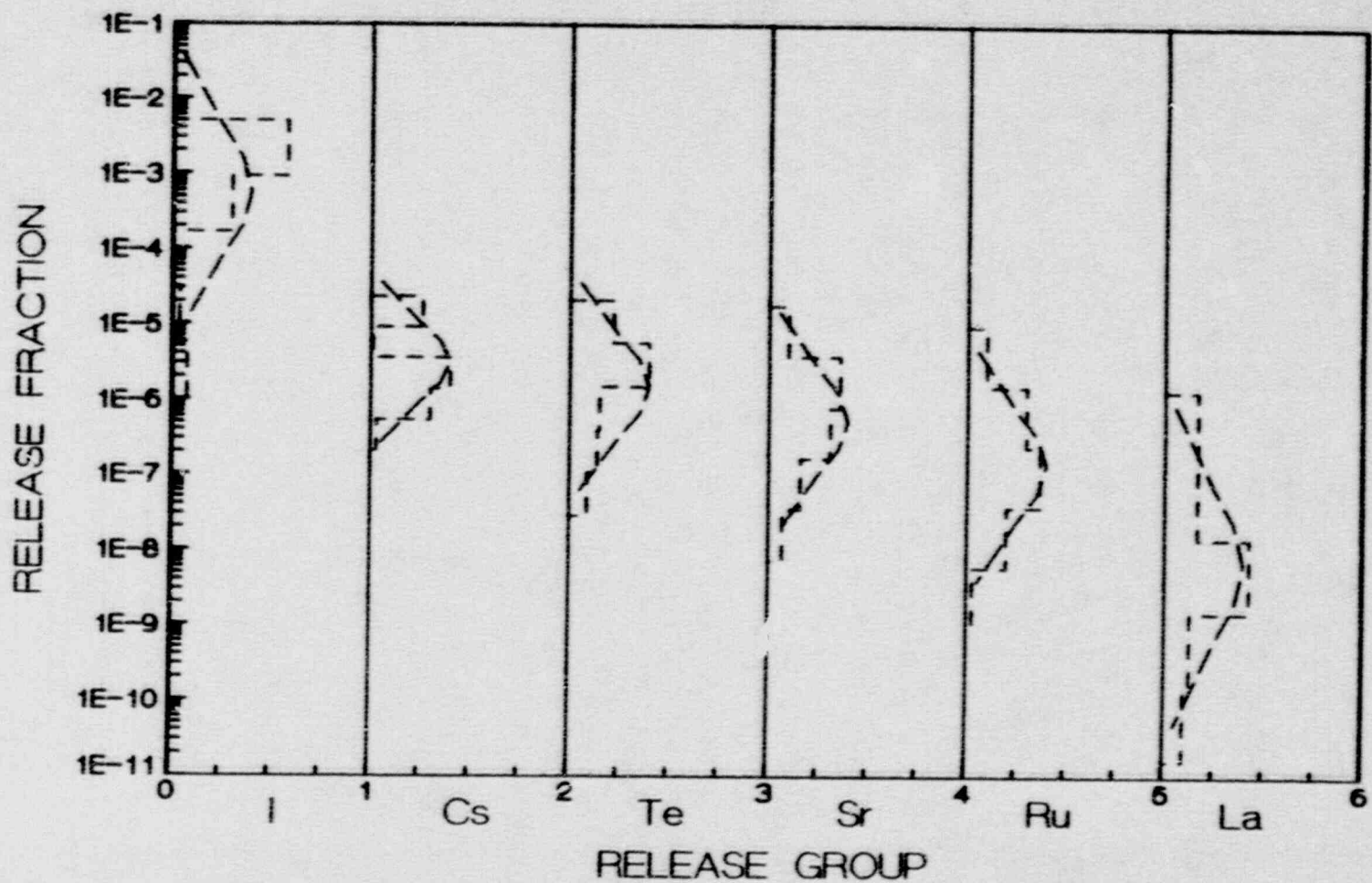


FIGURE 25.
LLH SAMPLE SOURCE TERM DISTRIBUTIONS
SURRY BIN 15

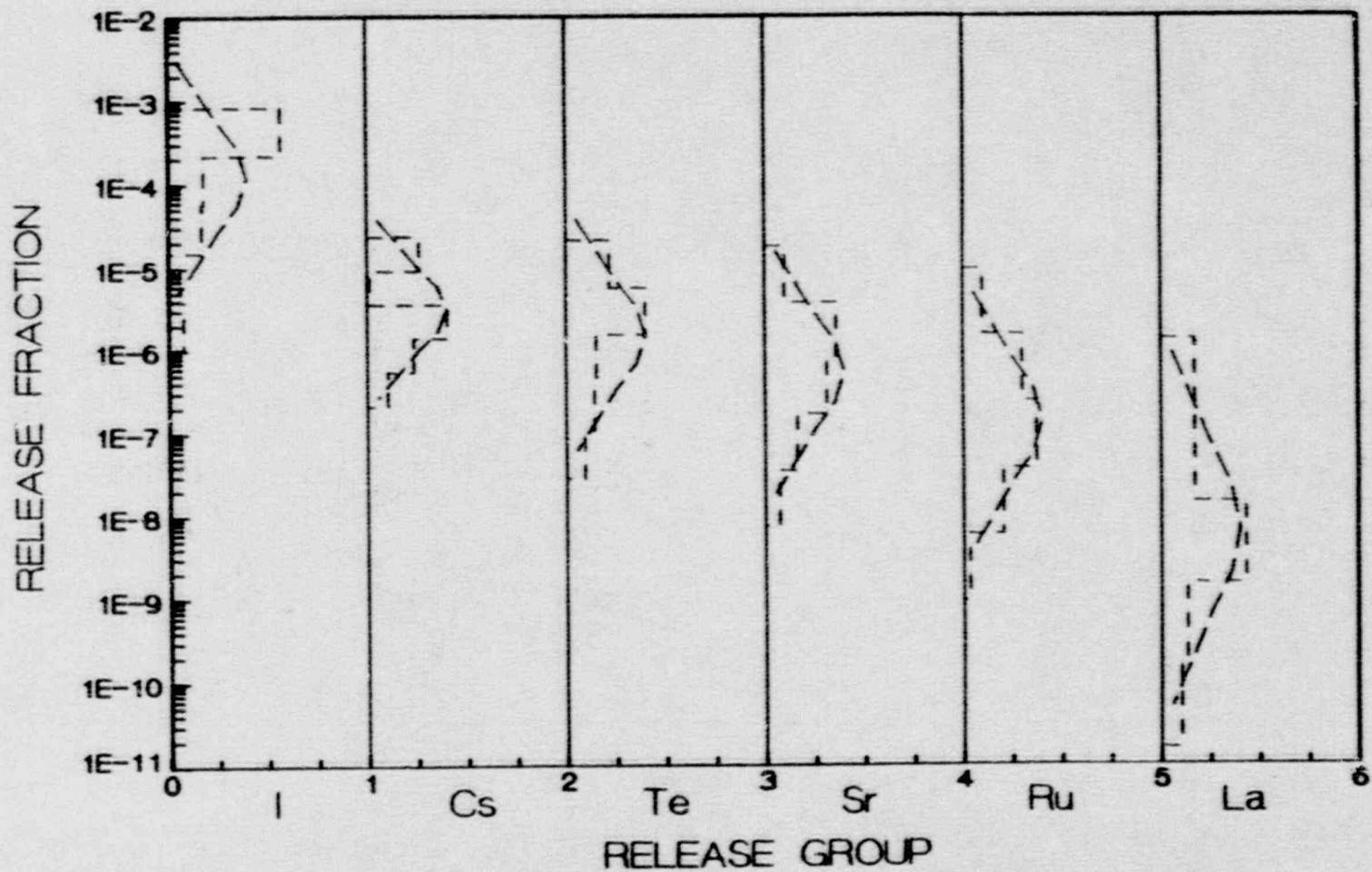


FIGURE 26.
LLH SAMPLE SOURCE TERM DISTRIBUTIONS
SURRY BIN 16

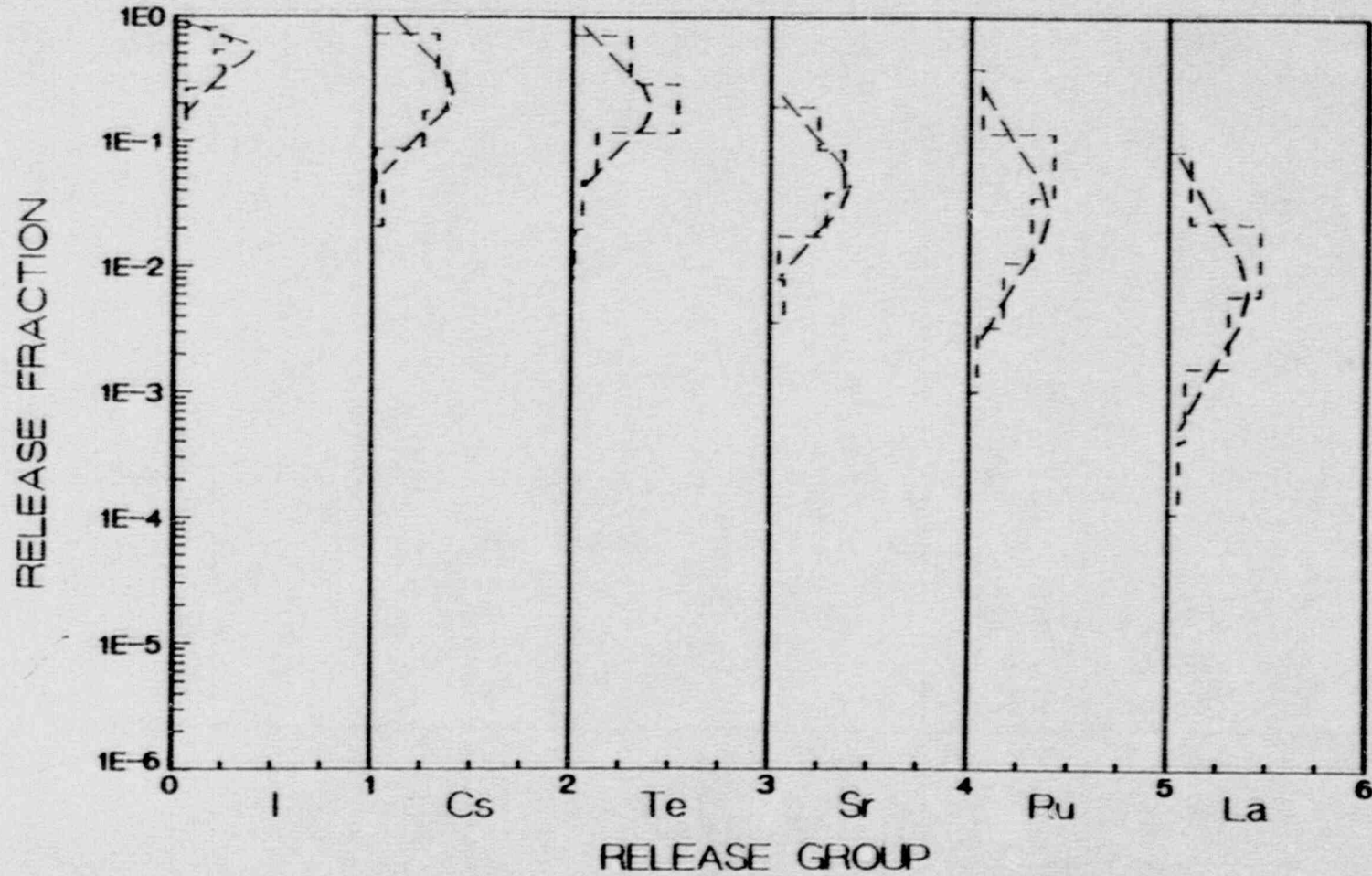


FIGURE 27.
LLH SAMPLE SOURCE TERM DISTRIBUTIONS
SURRY BIN 17

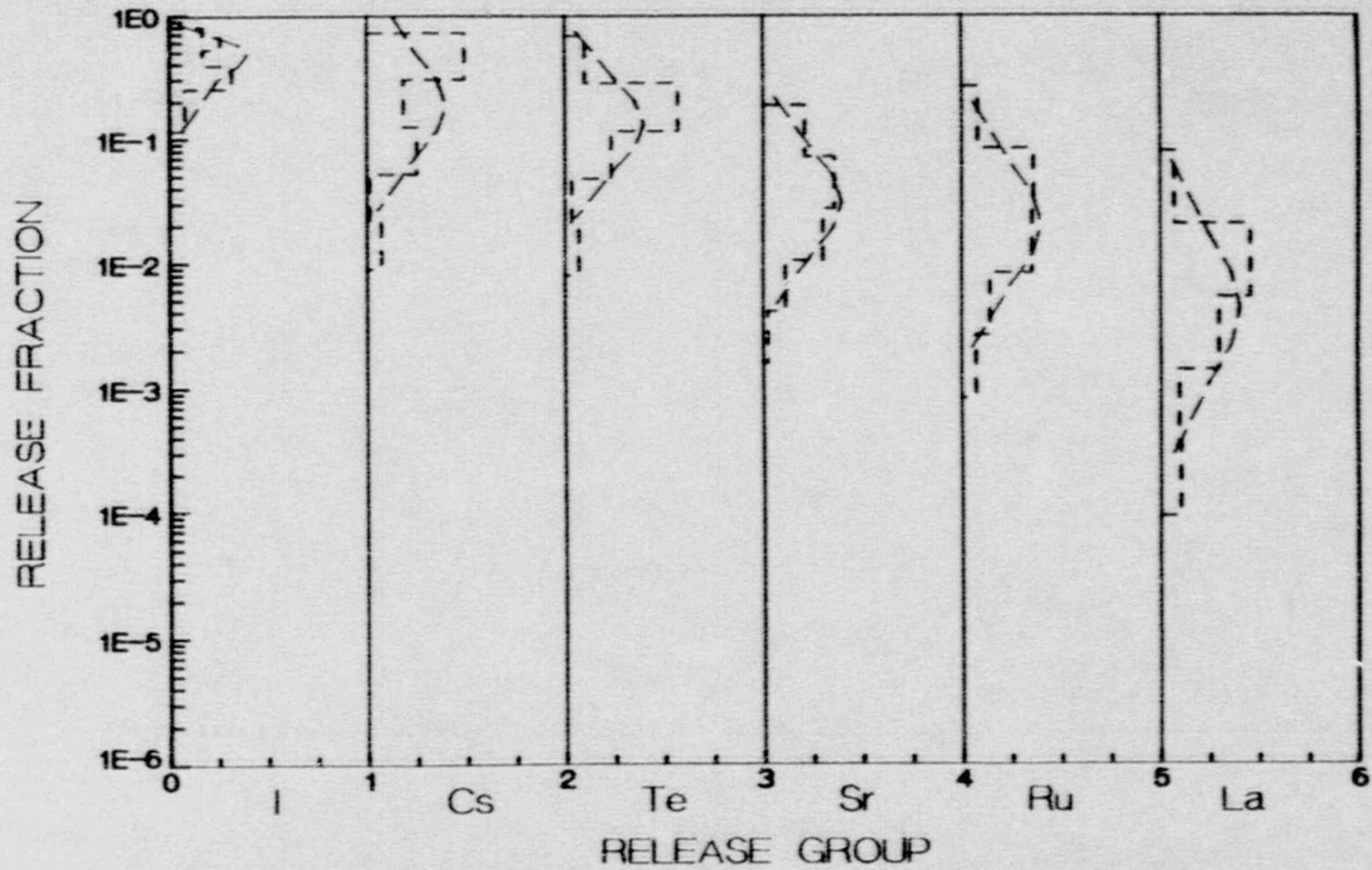


FIGURE 28.
 LLH SAMPLE SOURCE TERM DISTRIBUTIONS
 SURRY BIN 18

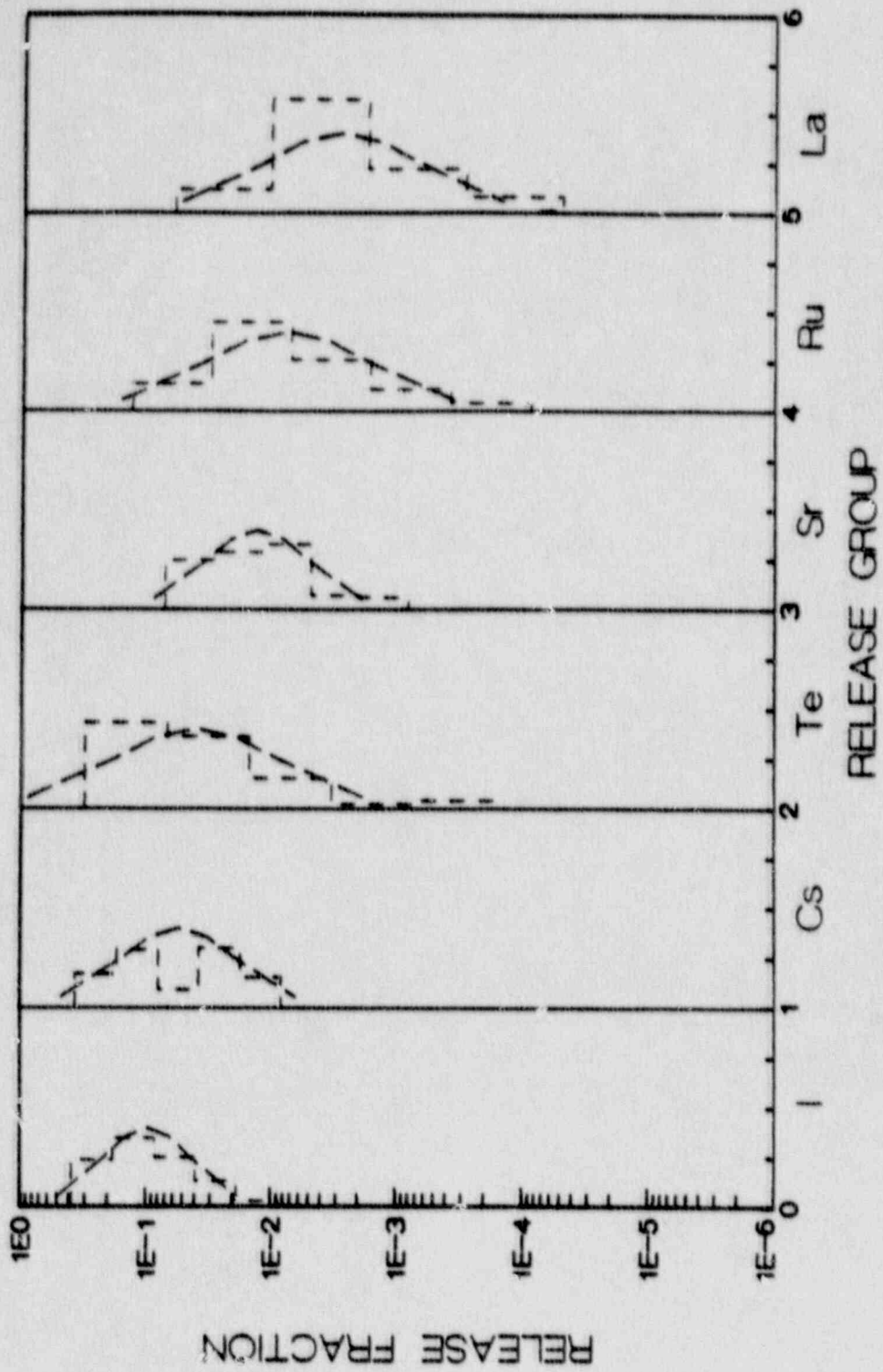


FIGURE 29.
LLH SAMPLE SOURCE TERM DISTRIBUTIONS
SURRY BIN 19

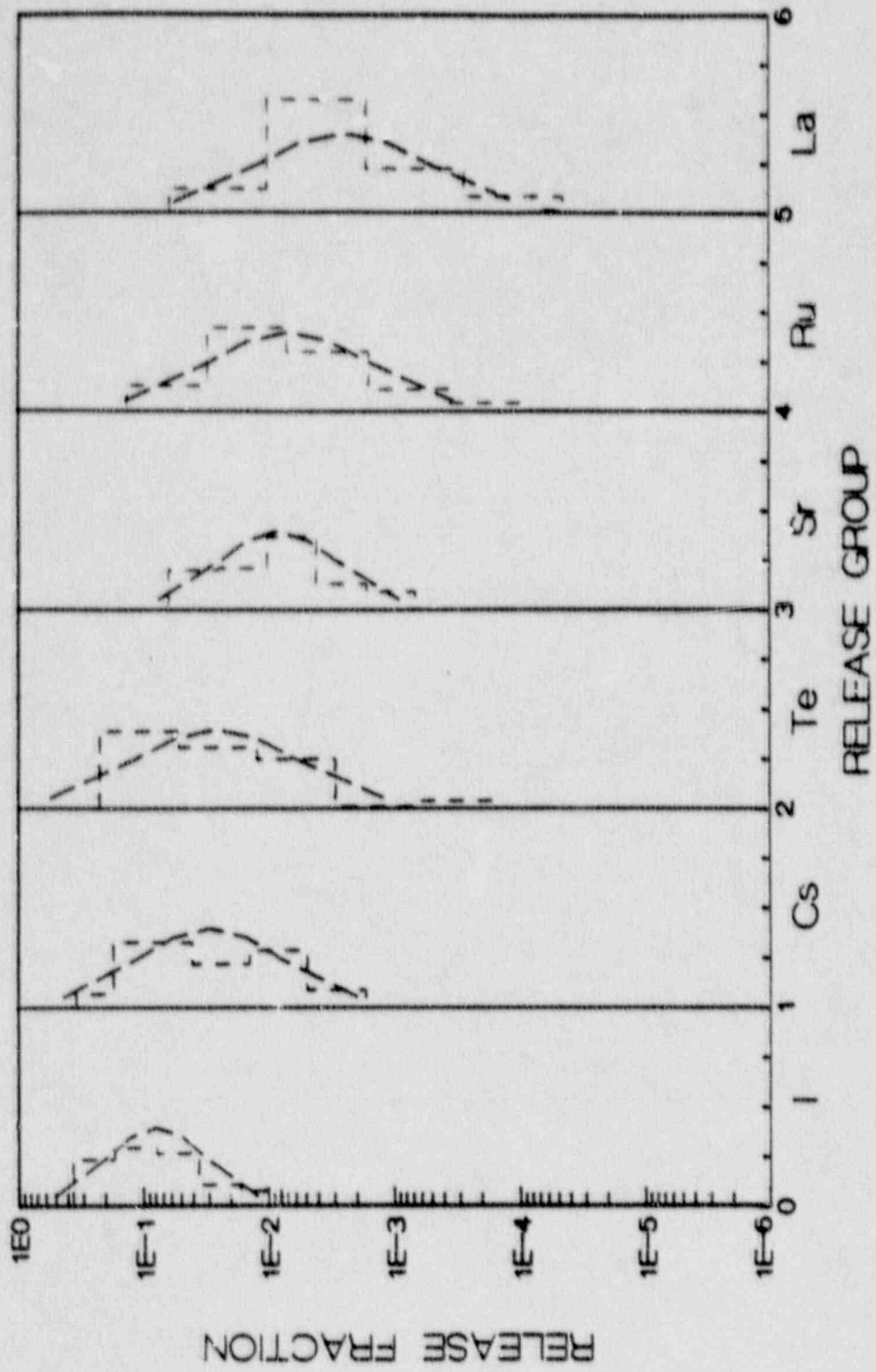
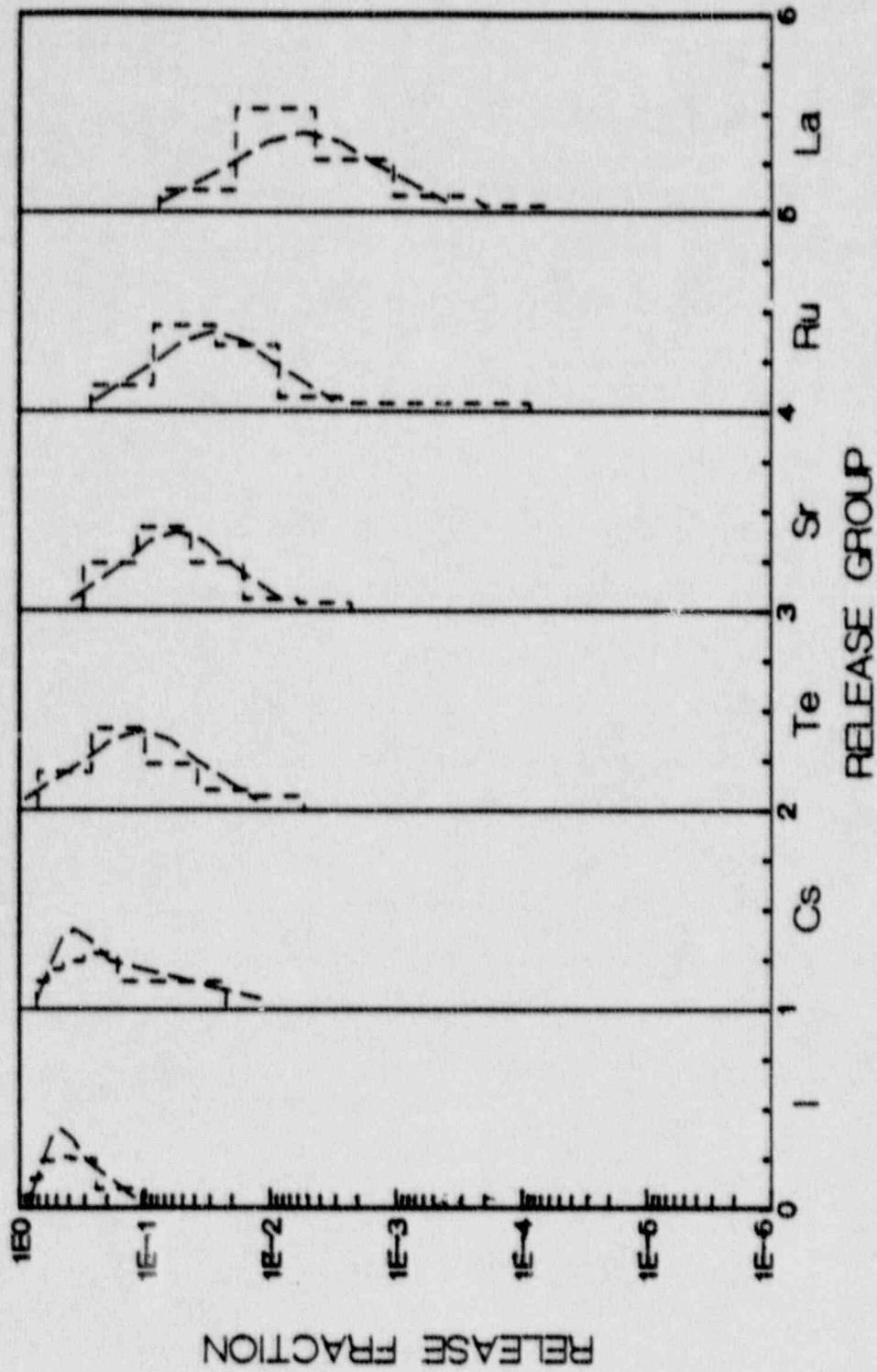


FIGURE 30.
 LLH SAMPLE SOURCE TERM DISTRIBUTIONS
 SURRY BIN 20



Results of Final Version of SURSOR

The foregoing discussions are based on the results with draft versions of SURSOR as the code was undergoing continued development during the course of this assessment. The following comparisons are based on the version that was used for the second draft of NUREG-1150. In this version the data base includes the results of the expert elicitation process. The specific issues considered as uncertain in the final version of SURSOR included:

- In-vessel release of fission products,
- In-vessel retention of fission products,
- Decontamination factor for submerged release for the interfacing systems loss-of-coolant accident,
- Escape from the containment of the species released from the primary system,
- Fission product release from the melt during concrete attack,
- Escape from the containment of the species released ex-vessel,
- Spray decontamination factors,
- Late iodine release from the containment,
- Late revolatilization of fission products initially deposited in the primary system,
- Release due to direct containment heating by core materials,
- Releases due to steam generator tube rupture events, and
- Scrubbing of ex-vessel releases by overlying water pools.

For the comparisons discussed below the SURSOR input parameters were selected to match as closely as possible the accident sequences that had been previously analyzed with the STCP.

Figure 31 compares the STCP results for TMLB-delta (station blackout with early containment failure) and S3B-delta (station blackout with pump seal failure and early containment failure) with SURSOR results. Shown are the STCP results together with the SURSOR central and median estimates, as well as the ranges of SURSOR estimates. The latter are based on two-hundred samples and consider source term uncertainties only. As noted previously, the SURSOR central estimates should correspond to the STCP calculations, whereas the median estimates take into account the results of the expert elicitation process. The latter addresses uncertainties in the STCP as well as phenomena not included in the STCP. The agreement among the various results presented in Figure 31, with the notable exception of the ruthenium group, is quite good. The STCP results for TMLB were based on an earlier version than those for S3B;

the difference in the ruthenium results is attributable to code changes. The uncertainty bands for all the species, particularly the nonvolatiles, are seen to be quite large.

The comparison for TMLB-beta (station blackout with containment isolation failure) is shown in Figure 32. The STCP results for this case explicitly tracked only the more volatile species. The SORSOR results for the iodine and cesium groups are higher than the STCP calculations. This is believed to be due to the consideration of late revolatilization from the primary system by SORSOR as well as the reflection of the view that some of these species may be released during concrete attack, rather than being completely released in-vessel. The tellurium results are in good agreement. Since the tellurium release takes place mostly during concrete attack, it should be indicative of the behavior of the other species. The SORSOR uncertainty bands are again seen to be large.

The results for a station blackout sequence with containment meltthrough are shown in Figure 33. The SORSOR predictions for iodine and cesium releases are again higher than those of the STCP for the same reasons as cited above. The agreement for the other species is reasonable. Very large uncertainty bands are again seen.

The results for TMLB, station blackout, with leak-before-break mode of containment failure are given in Figure 34. This STCP calculation again tracked only the more volatile species. The SORSOR results for cesium and iodine lie significantly above the STCP releases. Again, this is believed due to the consideration of late revolatilization of these species from the primary system by SORSOR. The tellurium results are in reasonable agreement. Large uncertainty bands are again evident.

Figure 35 presents the SORSOR-STCP comparison for TMLB-gamma, station blackout with containment failure due to a late hydrogen burn; in the scenario assumed here the electric power is recovered late in the sequence, the containment spray is activated and leads to containment deinerting, with containment failure from the subsequent large hydrogen burn. The STCP results for iodine and cesium are substantially below the SORSOR estimates. This is due to the fact that the STCP does not take into account the revolatilization of these species from the primary system, a factor addressed by SORSOR. Also, the possibility of the formation of organic iodides is reflected in SORSOR, but not in the STCP. The calculated releases for the other species show considerable scatter, with SORSOR results above those of the STCP. The predictions for a scenario of this type would be expected to be sensitive to the relative timing of spray actuation and containment failure. The results are again characterized by large uncertainty bands.

The comparison of results for S2D-gamma, small break with emergency core cooling failure and early containment failure due to a hydrogen burn is shown in Figure 36. In this variation the containment sprays are assumed to fail at the time of containment failure. The SORSOR median estimates for iodine, cesium, and tellurium are well above the SORSOR central and STCP results, reflecting higher ex-vessel release estimates; the latter would take place after spray failure. The strontium and lanthanum predictions are in

reasonable agreement, with the ruthenium results showing significant differences. The STCP calculations were performed with two spray droplet sizes. The results illustrate the sensitivity for spray size for short periods of spray operation. The SORSOR parameters are clearly based on the larger of the two spray sizes.

The results for S2D-gamma, again a small break with emergency core cooling failure and early containment failure due to a hydrogen burn are shown in Figure 37. In this variation the sprays were assumed to continue operation after containment failure. The results for this case show much better agreement than the previous case. The consideration of the formation of organic iodides is believed to lead to the higher SORSOR median estimate in comparison to the central and STCP values. Cesium, strontium, and lanthanum show reasonable agreement. The median release for tellurium is considerably higher than the other estimates. The STCP results for this case were again obtained with an early version; thus the difference in the STCP and SORSOR results for ruthenium.

The results for S2D-beta, small break with emergency core cooling failure as well as failure of the containment to isolate, are illustrated in Figure 38. As has been previously noted, the SORSOR results are obviously tuned to the 1000 micron spray droplet size. The SORSOR median release for iodine is believed to be above the other estimates due to consideration of the formation of organic iodides. The less volatile species were not explicitly tracked in this STCP calculation.

Figure 39 illustrates the results for S2D-epsilon, small break with emergency core cooling failure and containment meltthrough. The STCP results for iodine are well below the SORSOR estimates since they do not take into account formation of organic iodides or the late revolatization of iodine. The cesium and tellurium releases are both at very low levels and the agreement should be considered reasonable. It may be noted that in this case the in-vessel releases are subject to scrubbing by the sprays, and the ex-vessel releases are scrubbed by an overlying water pool as well as the sprays. The less volatile species were not explicitly tracked in this STCP calculation. The SORSOR uncertainty results still display considerable ranges for the releases.

The results for AG-delta, a large break with loss of containment heat removal, are shown in Figure 40. In this scenario the loss of containment heat removal leads to long term containment overpressure failure, with subsequent failure of the core cooling systems; core meltdown thus takes place in a failed containment. The SORSOR median estimates, except for ruthenium, are seen to be below the STCP and SORSOR central estimates. The overall agreement is believed to be reasonable, but the uncertainty bands are typically very large.

Figures 41 compare the results for the interfacing systems loss-of-coolant scenario with a submerged release path, V-wet. The SORSOR median results for the more volatile species are somewhat higher than the central and STCP estimates, but are reasonably close. The results for the less volatile

species, particularly ruthenium, show more scatter. The uncertainty bands are typically large.

Figure 42 illustrates the results for the interfacing systems loss-of-coolant scenario assuming a dry release path, V-dry. The results are comparable to the foregoing, but expectedly somewhat higher.

The results for AB-epsilon, a large break and complete loss of electric power leading to containment meltthrough, are shown in Figure 43. This set of results shows more scatter than the others. The higher iodine releases from SURSOR in comparison to the STCP are due to the consideration of the formation of organic iodides. The differences for the other species are not as obvious.

The results for AB-gamma, large break with complete loss of electric power and containment failure due to a hydrogen burn, are shown in Figure 44. The SURSOR and STCP results for the volatile species are in good agreement; those for the nonvolatile groups show more scatter. The uncertainty bands, particularly for the nonvolatile groups are again very large.

The results for AB-beta, large break with complete loss of electric power and containment isolation failure, are shown in Figure 45. In this case the SURSOR estimates for the volatile species are above those of the STCP, whereas those for the nonvolatile groups are lower than the STCP results. The uncertainty bands are again large.

The results for SGTR1, a steam generator tube rupture event with the secondary side steam dump valve sticking open and leading to the eventual failure of the emergency core cooling system, are shown in Figure 46. For the volatile species SURSOR predictions are somewhat below those of the STCP. For the nonvolatiles, on the other hand, the SURSOR results are substantially higher than the STCP calculation. The latter reflects the expert panel view of the potential for greater in-vessel releases for these species than is currently calculated.

The results for SGTR2, a steam generator tube rupture event with failure of the emergency core cooling system and the secondary side steam dump valves reclosing, are shown in Figure 47. In this case the SURSOR and STCP results agree quite closely for the volatile species. The results for the nonvolatiles display the same differences as were noted in the previous case.

The results for SGTR3, a steam generator tube rupture event with failure of the pressurizer relief valve as well as the secondary side steam dump valve to reclose, are given in Figure 48. The SURSOR and STCP results for the volatile species agree quite closely. The results for the nonvolatiles show the same large differences noted above.

FIGURE 31.
 COMPARISON OF SURSOR WITH STOP RESULTS
 FOR TMLB-delta AND S3B-delta

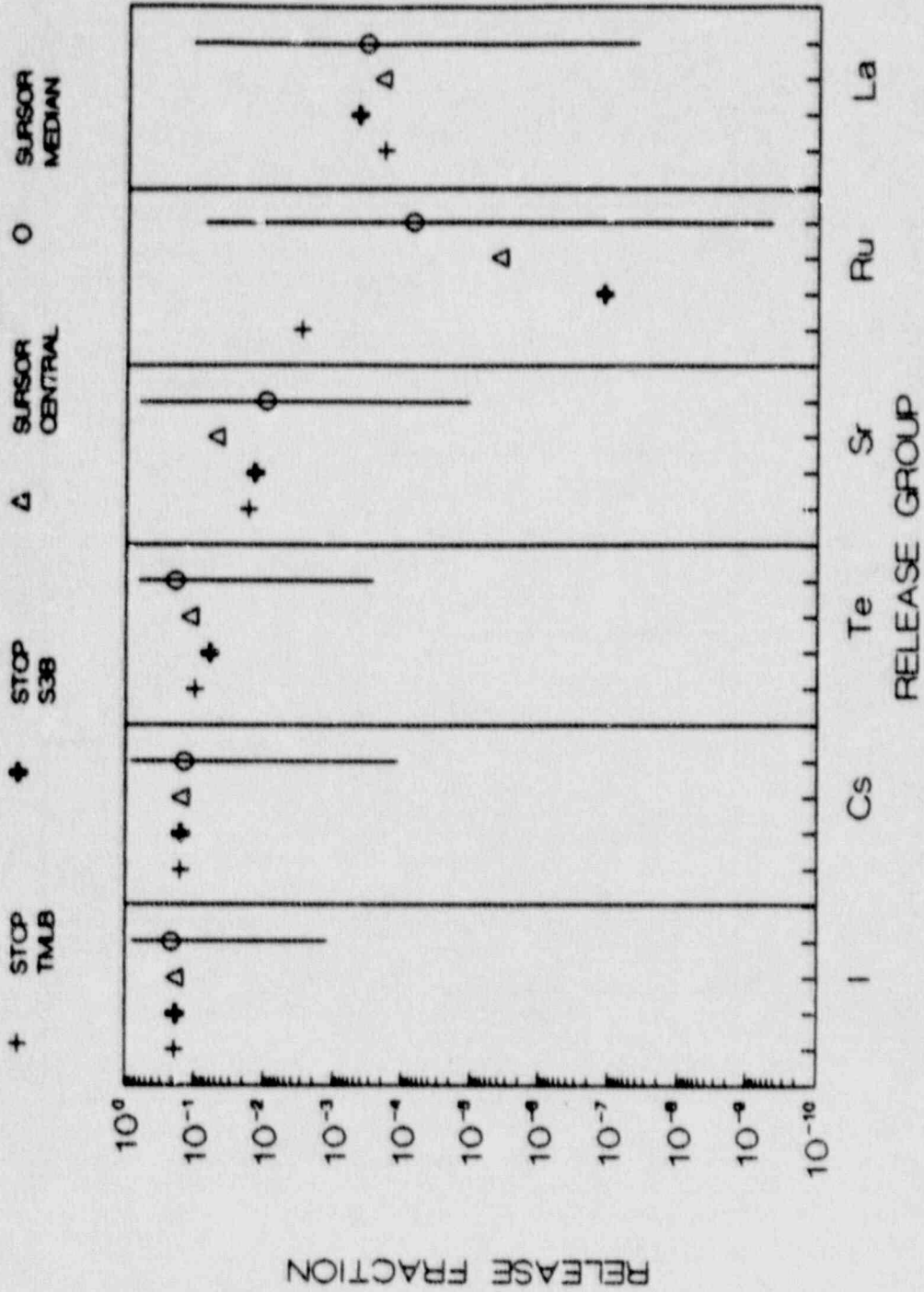


FIGURE 32.

COMPARISON OF SURSOR WITH STOP
RESULTS FOR TMLB-beta

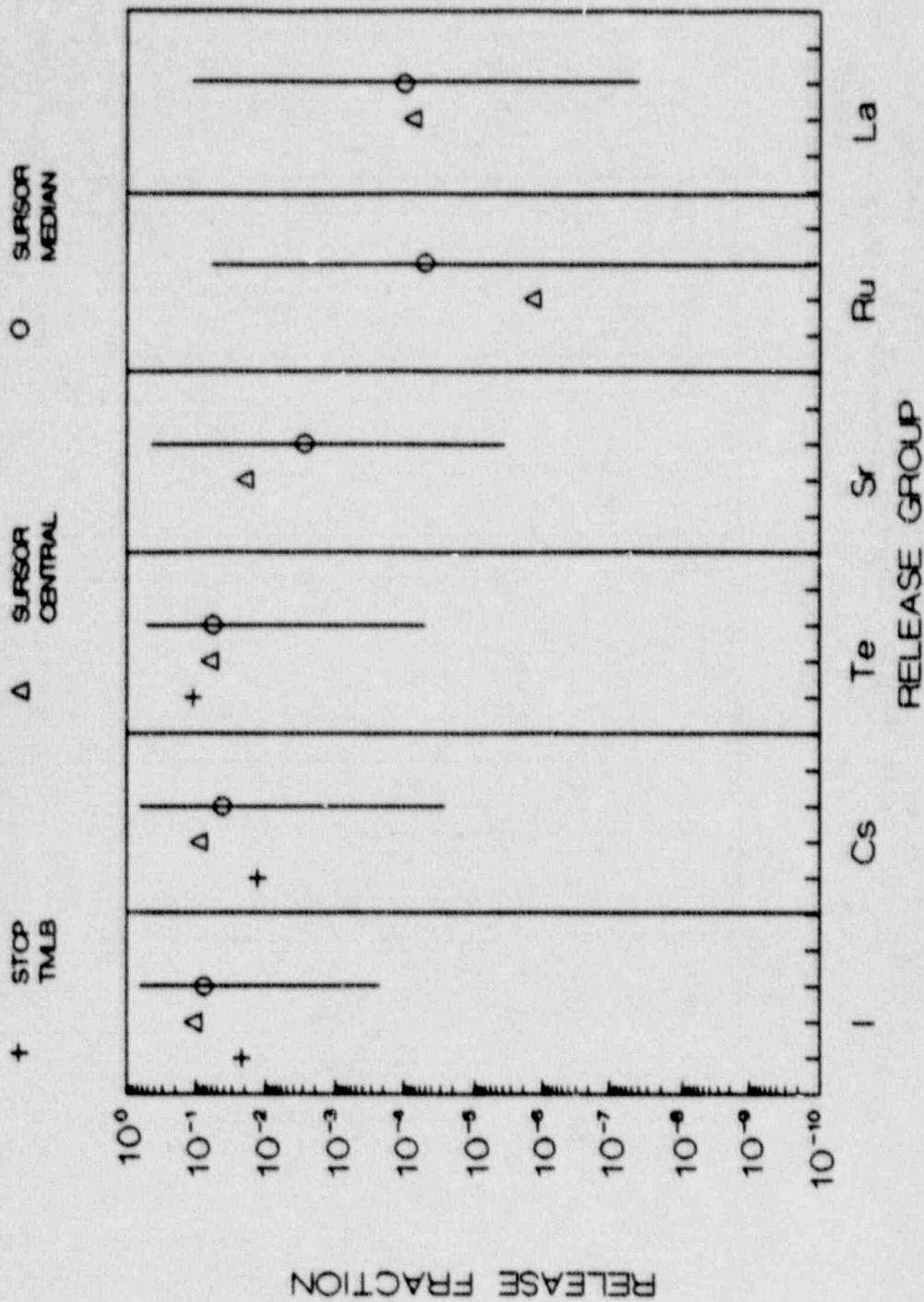


FIGURE 33.

COMPARISON OF SURSOR WITH STOP RESULTS
FOR TMLB-epsilon

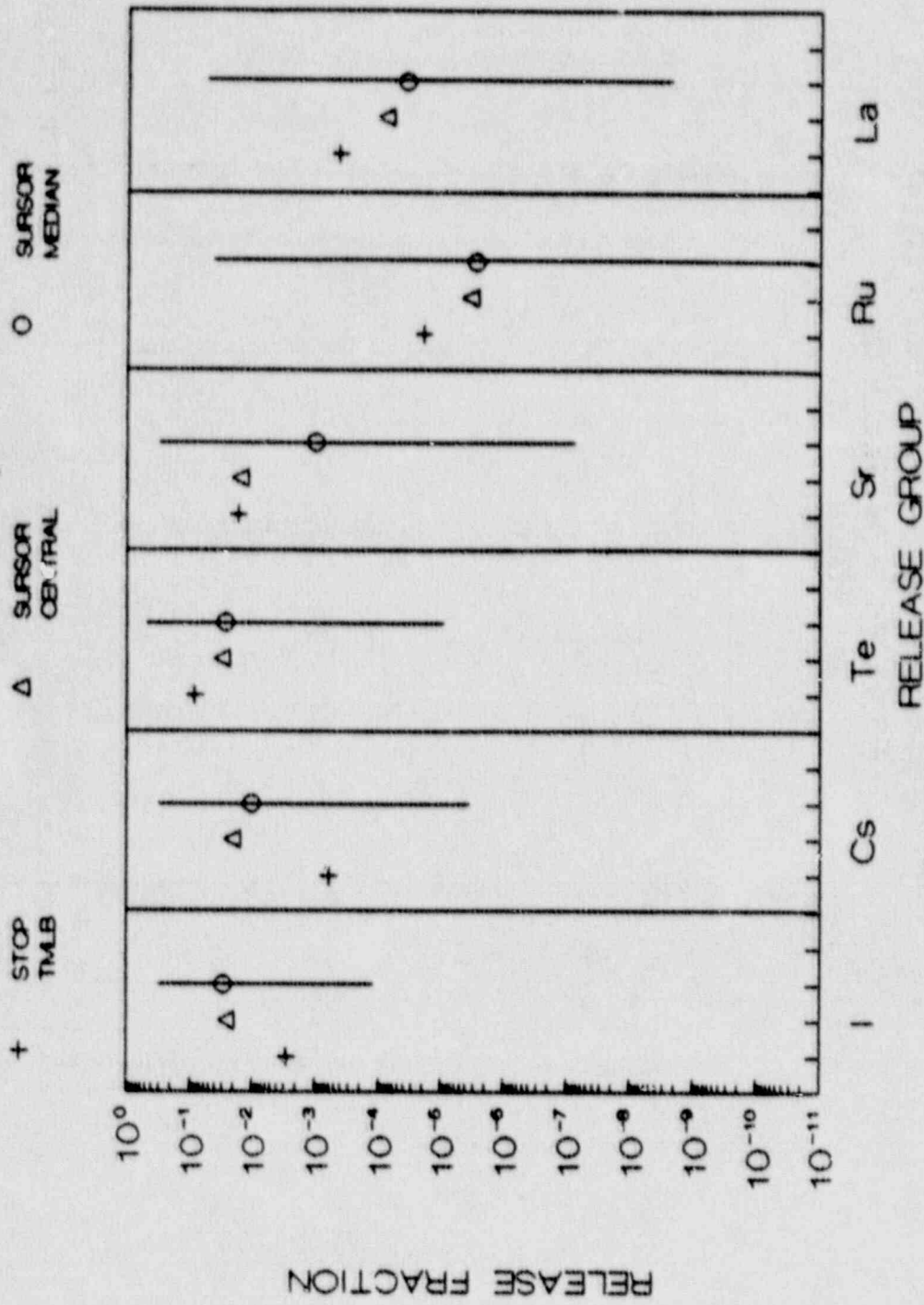


FIGURE 34.

COMPARISON OF SURSOR WITH STOP RESULTS
FOR TMLB-leak-before-break

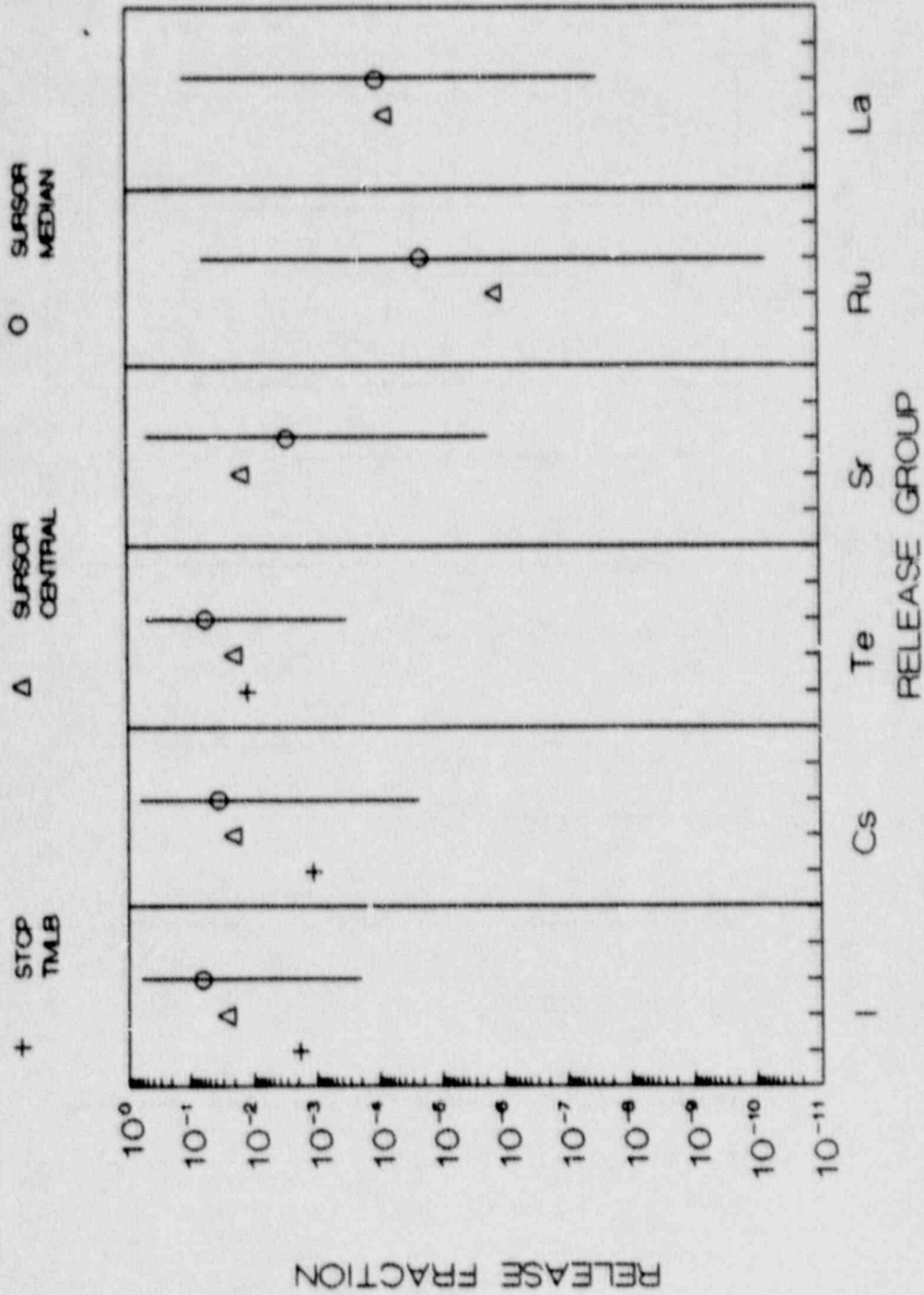


FIGURE 35.

COMPARISON OF SURSOR WITH STOP RESULTS
RESULTS FOR TMLB-gamma

+ STOP TMLB-400 + STOP TMLB-1000 Δ SURSOR CENTRAL ○ SURSOR MEDIAN

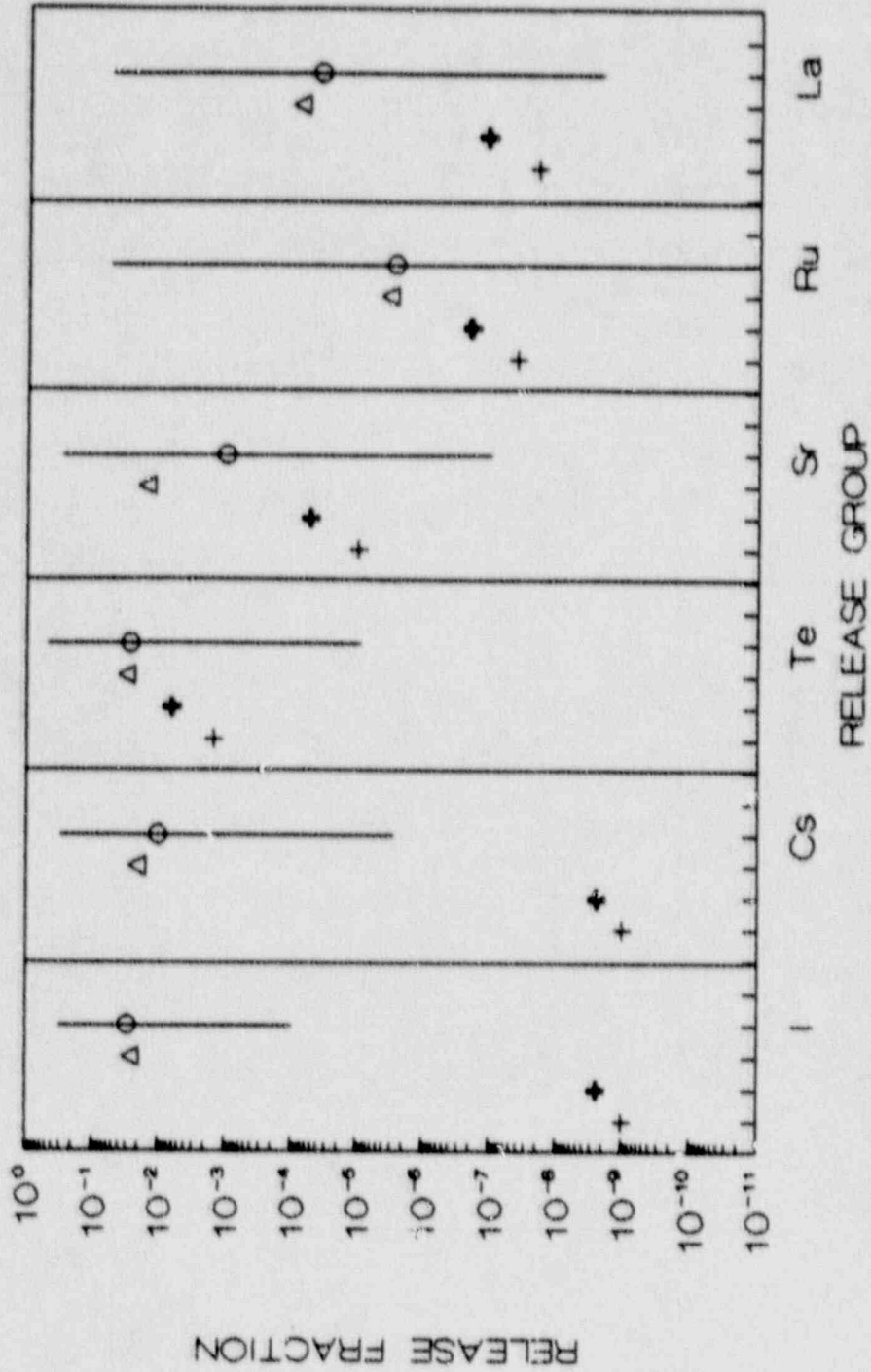


FIGURE 36.

COMPARISON OF SURSOR WITH STOP RESULTS
S2D-gamma (w/spray fail)

+ STOP S2D-400 ◆ STOP S2D-1000 Δ SURSOR CENTRAL ○ SURSOR MEDIAN

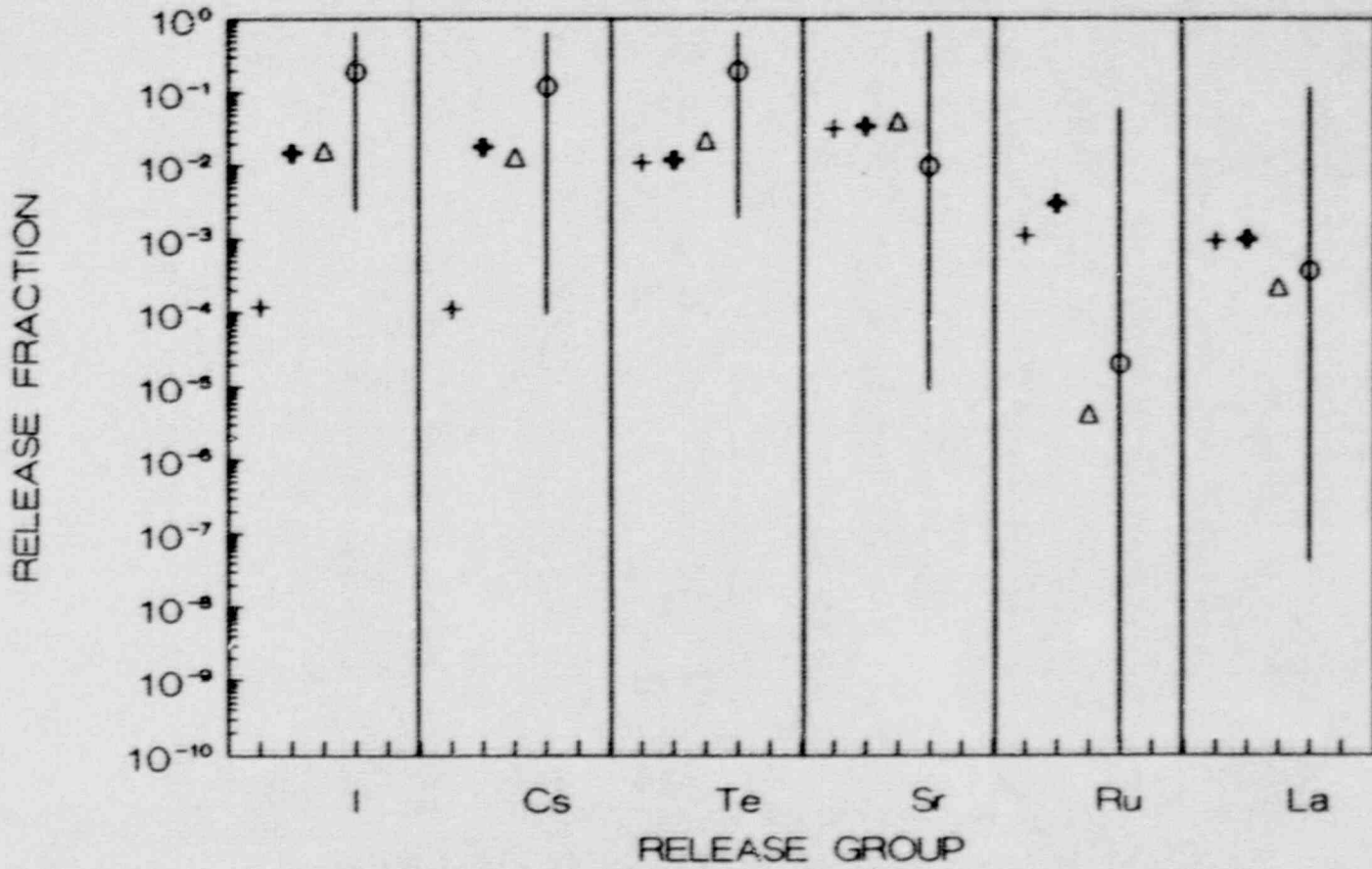


FIGURE 37.

COMPARISON OF SURSOR WITH STOP RESULTS
FOR S2D-gamma (w/spray on)

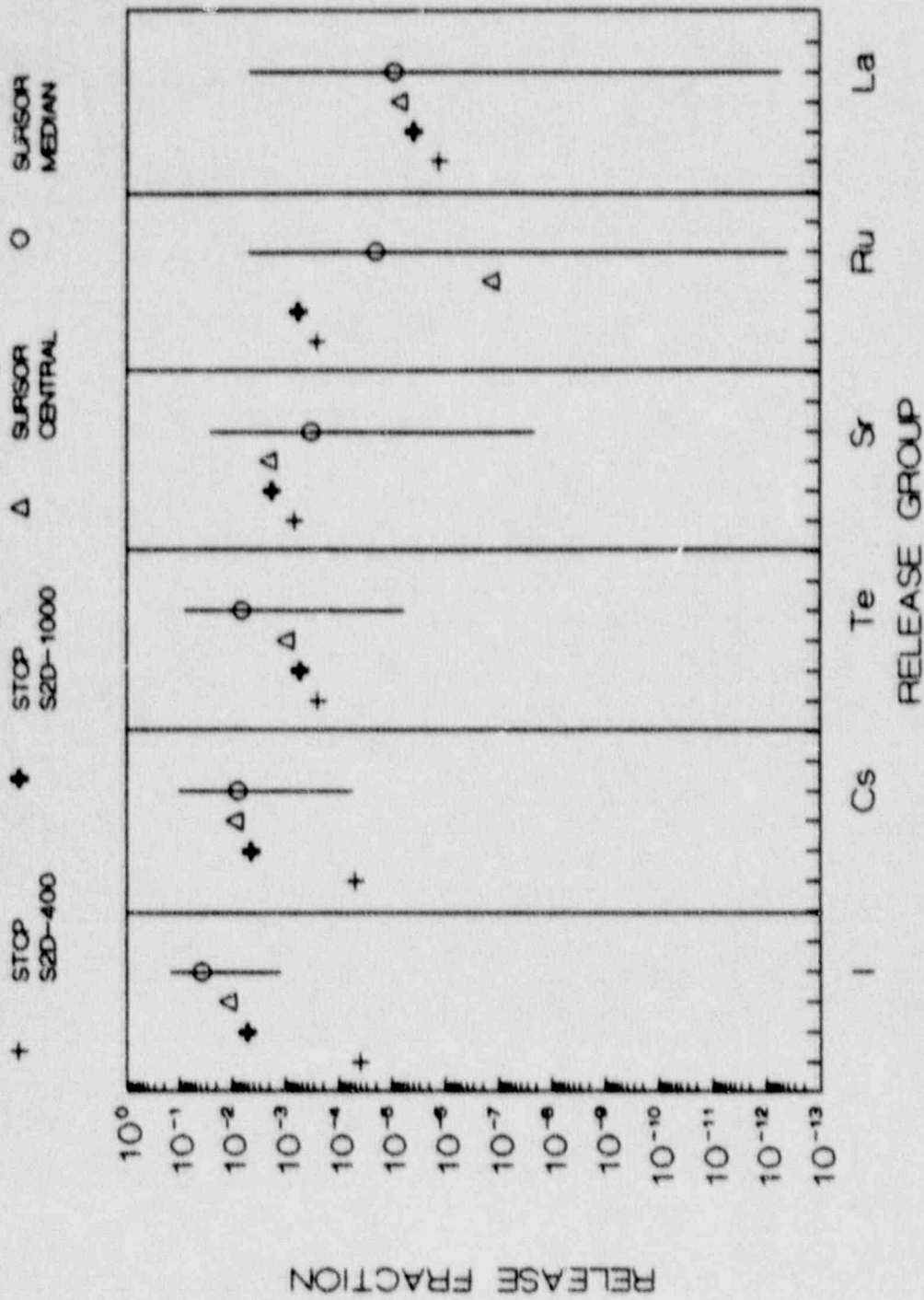


FIGURE 38.

COMPARISON OF SURSOR WITH STOP RESULTS
FOR S2D-beta

+ STOP S2D-400 ♦ STOP S2D-1000 Δ SURSOR CENTRAL ○ SURSOR MEDIAN

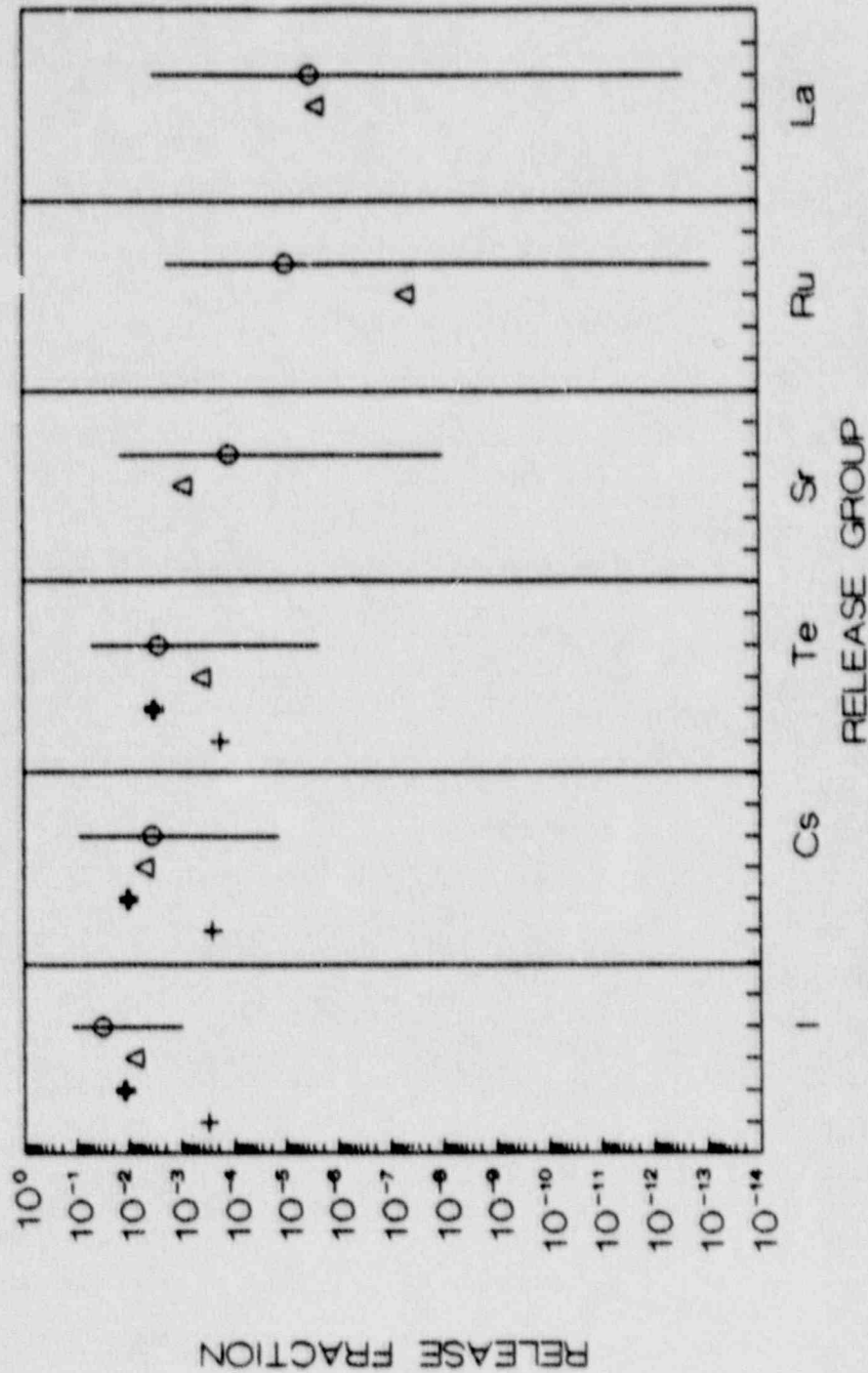


FIGURE 39.

COMPARISON OF SURSOR WITH STOP RESULTS
FOR S2D-epsilon

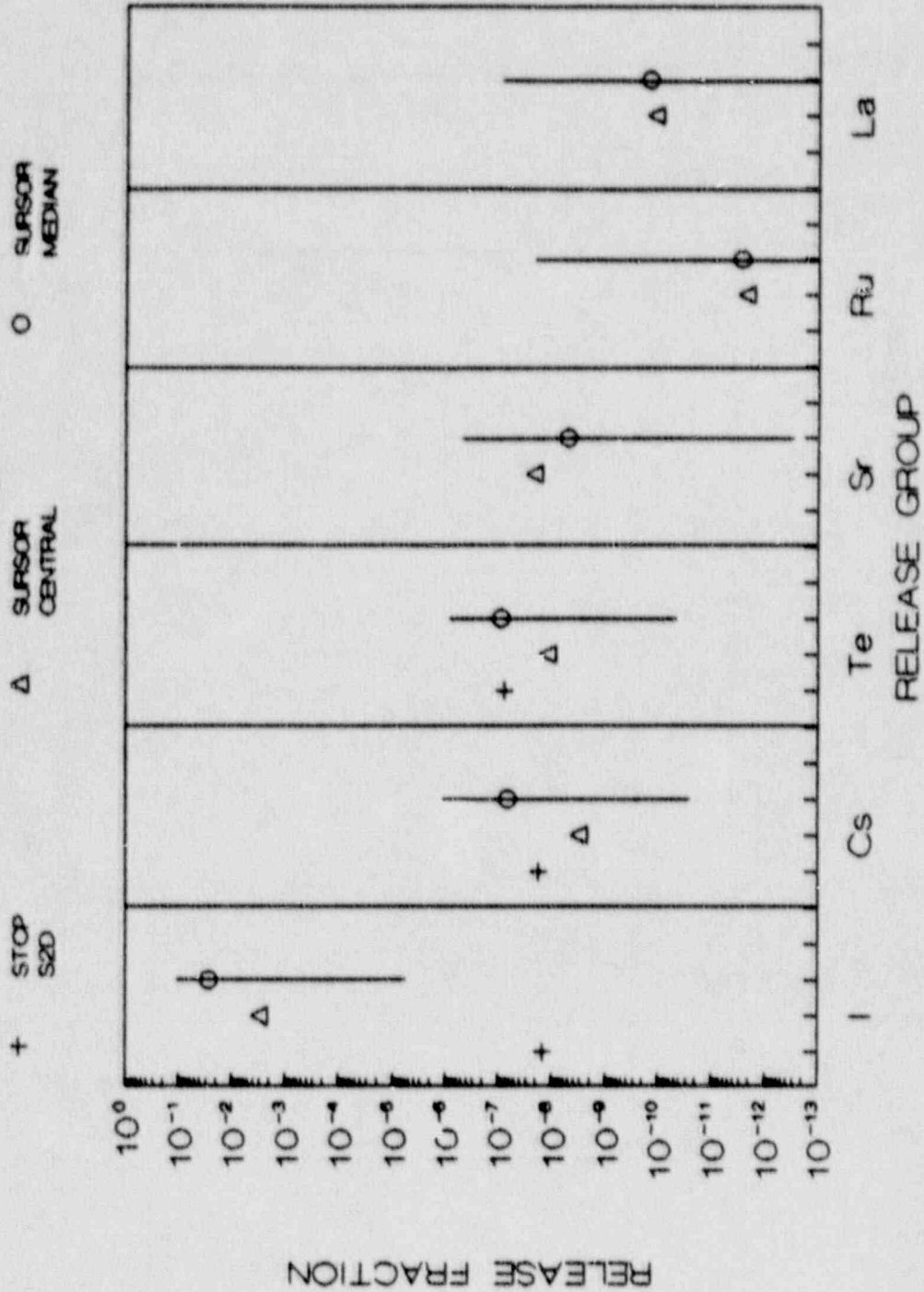


FIGURE 40.

COMPARISON OF SURSOR WITH STCP RESULTS
RESULTS FOR AG-delta

+ STCP AG Δ SURSOR CENTRAL O SURSOR MEDIAN

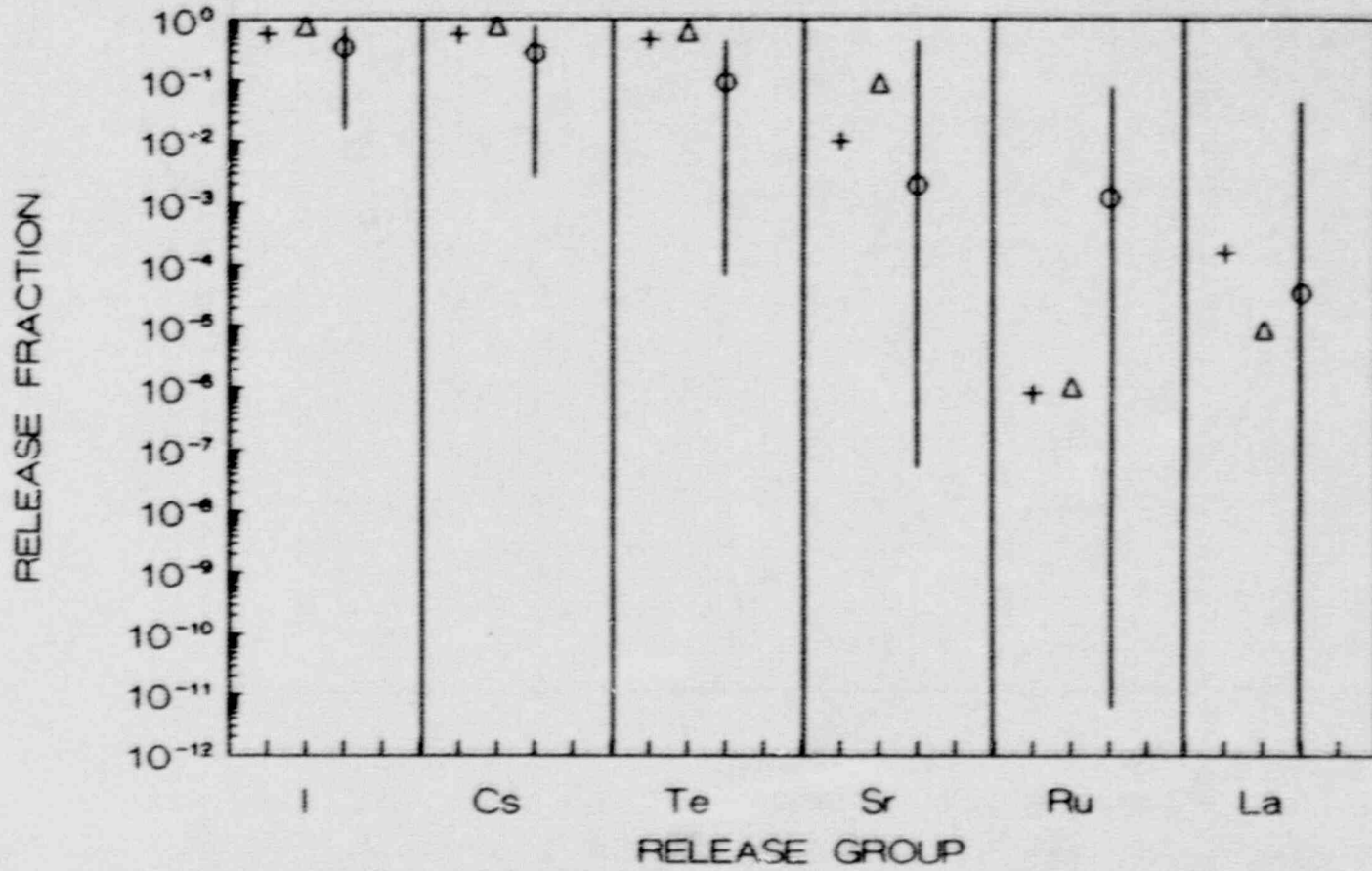


FIGURE 41.
COMPARISON OF SURSOR WITH STOP RESULTS
FOR V-wet

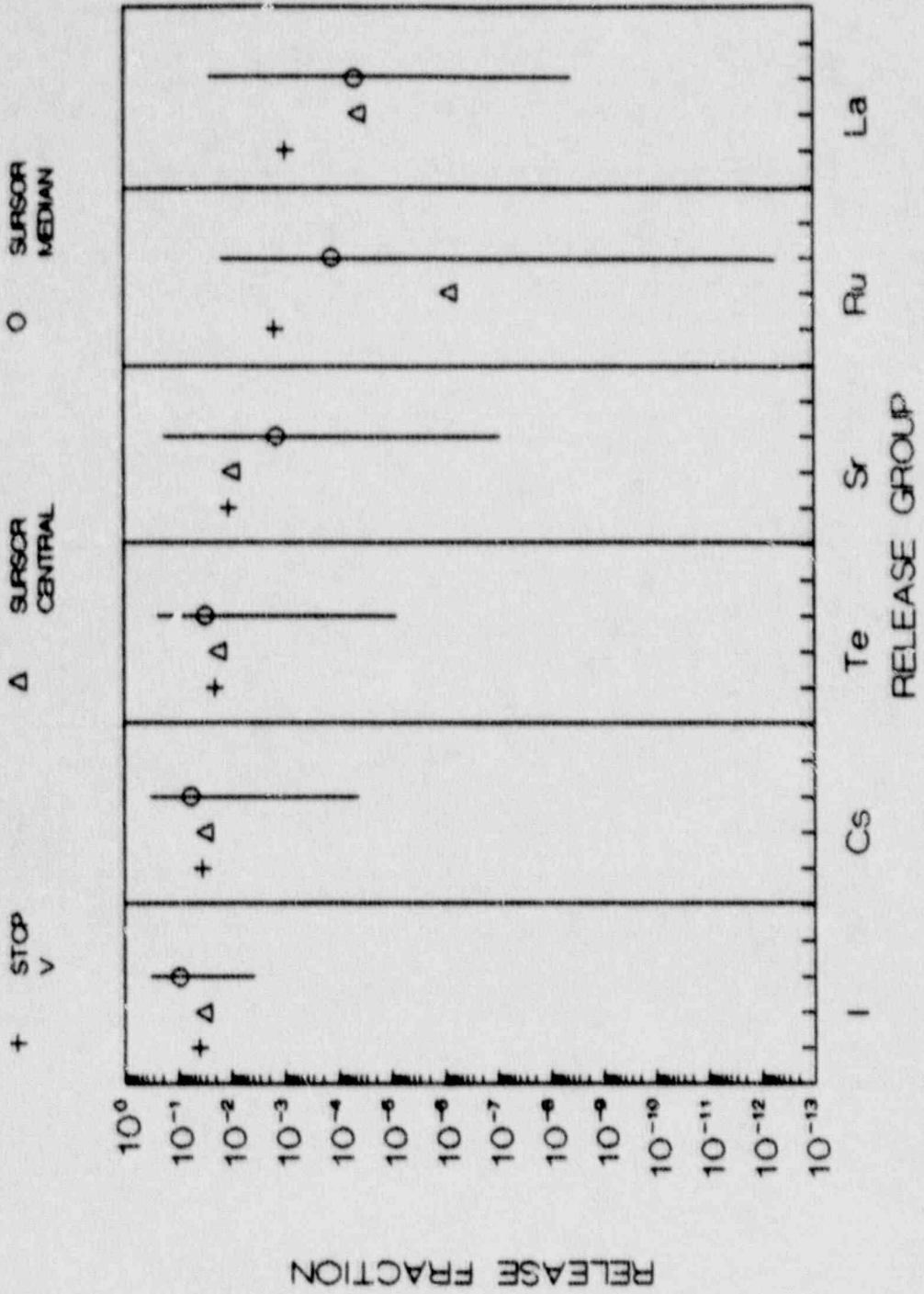


FIGURE 42.

COMPARISON OF SURSOR WITH STOP RESULTS
FOR V-dry

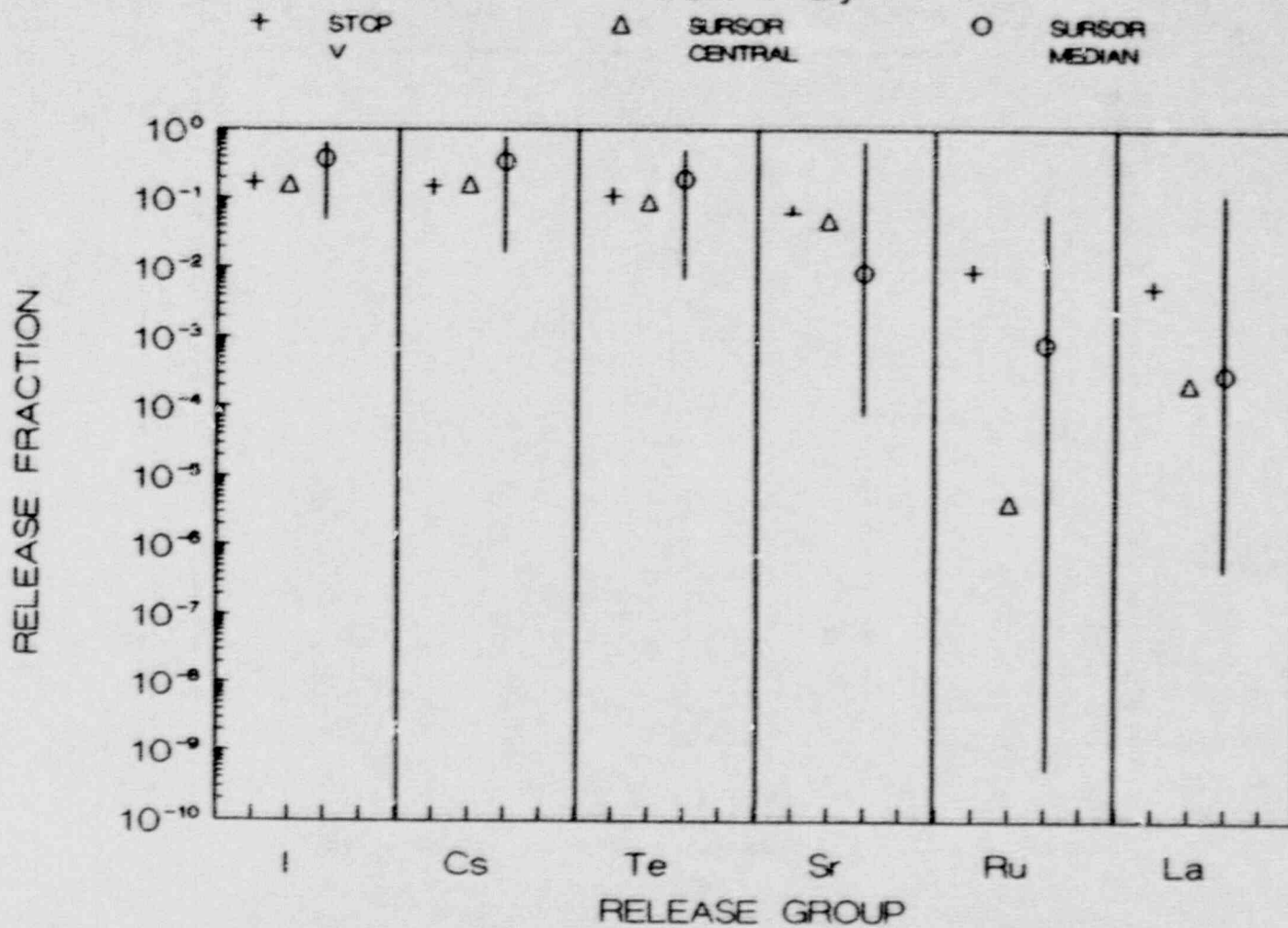


FIGURE 43.
 COMPARISON OF SURSOR WITH STOP RESULTS
 FOR AB-epsilon

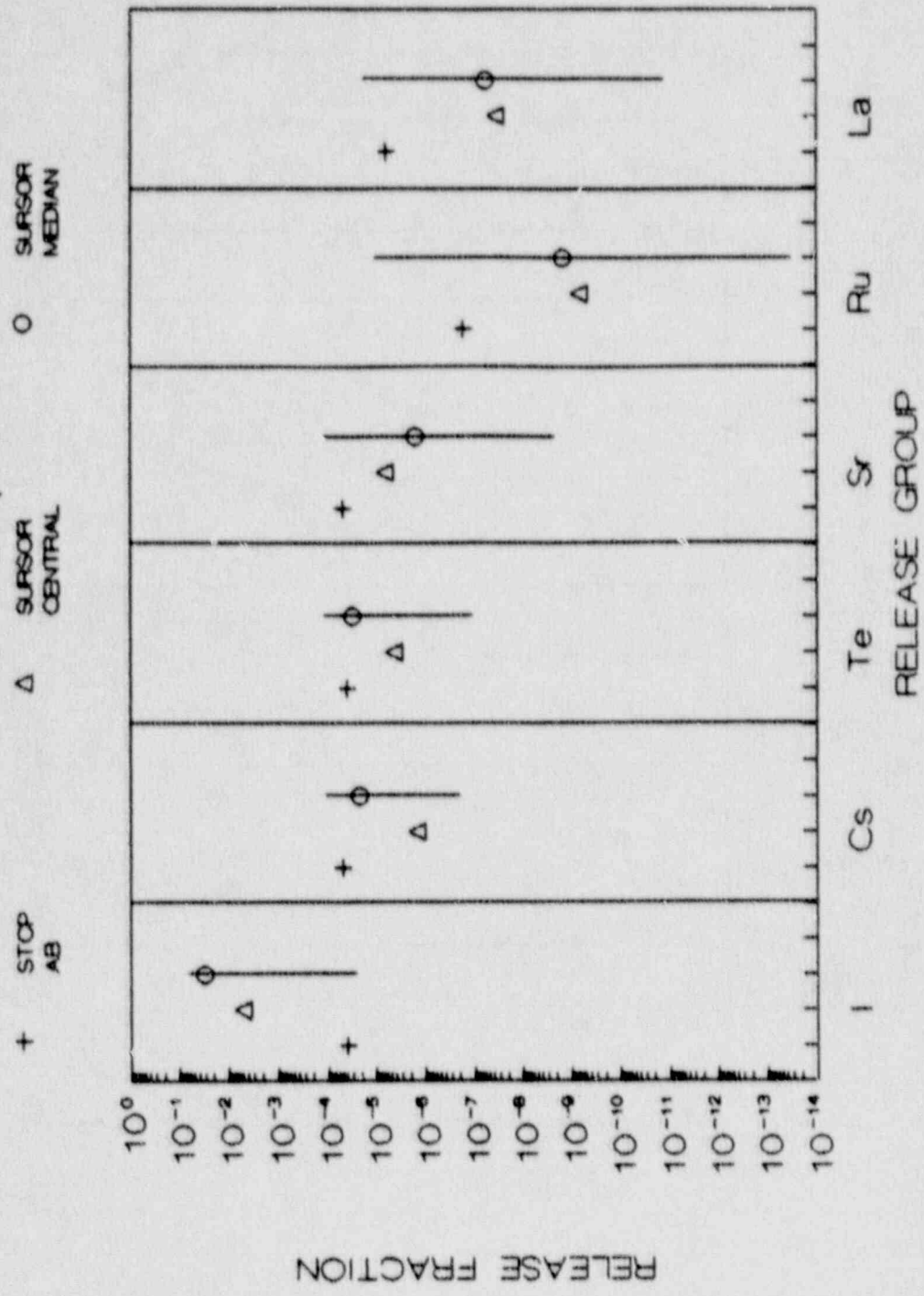


FIGURE 44.
 COMPARISON OF SURSOR WITH STOP RESULTS
 FOR AB-gamma

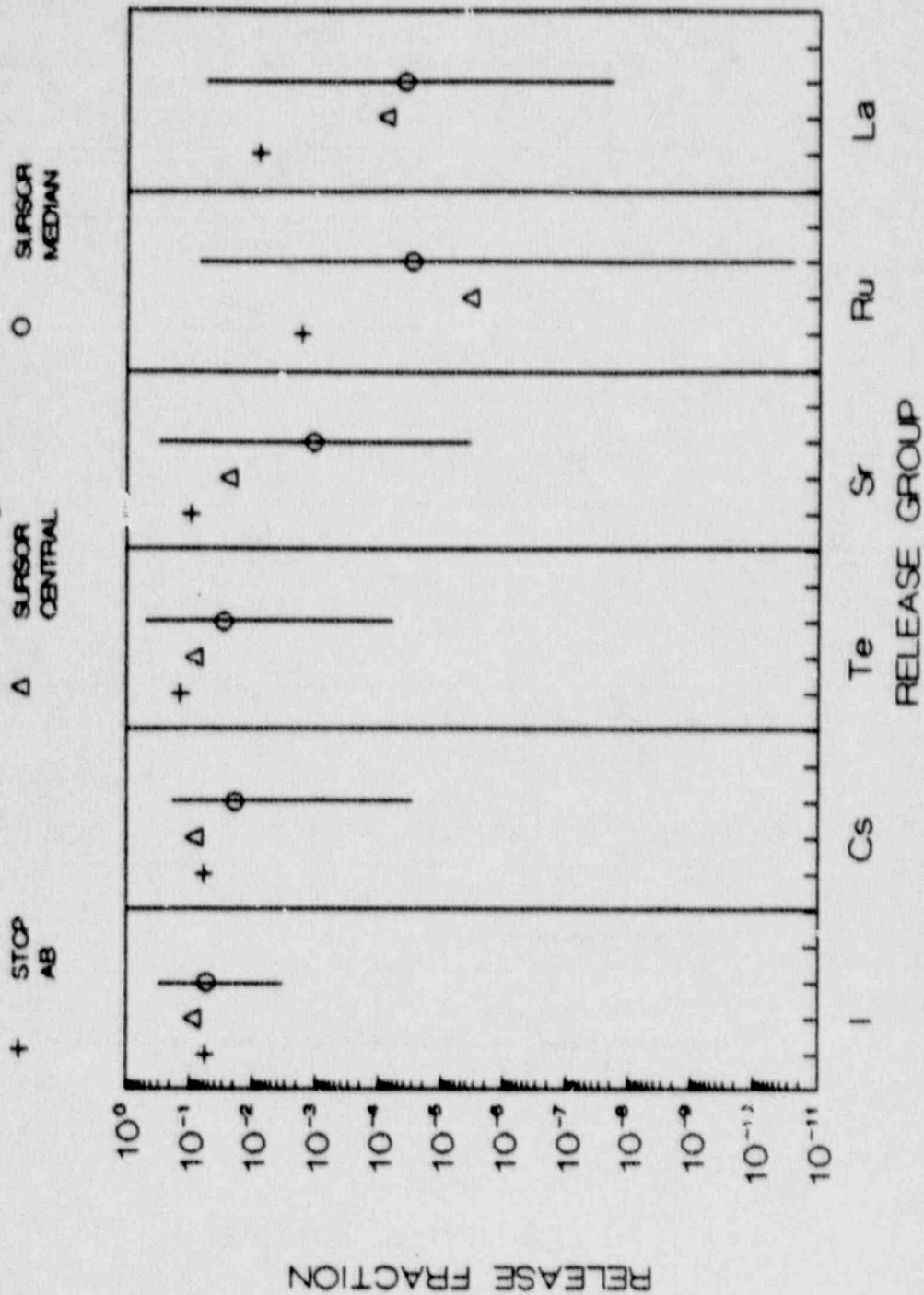


FIGURE 45.

COMPARISON OF SURSOR WITH STOP RESULTS FOR AB-beta

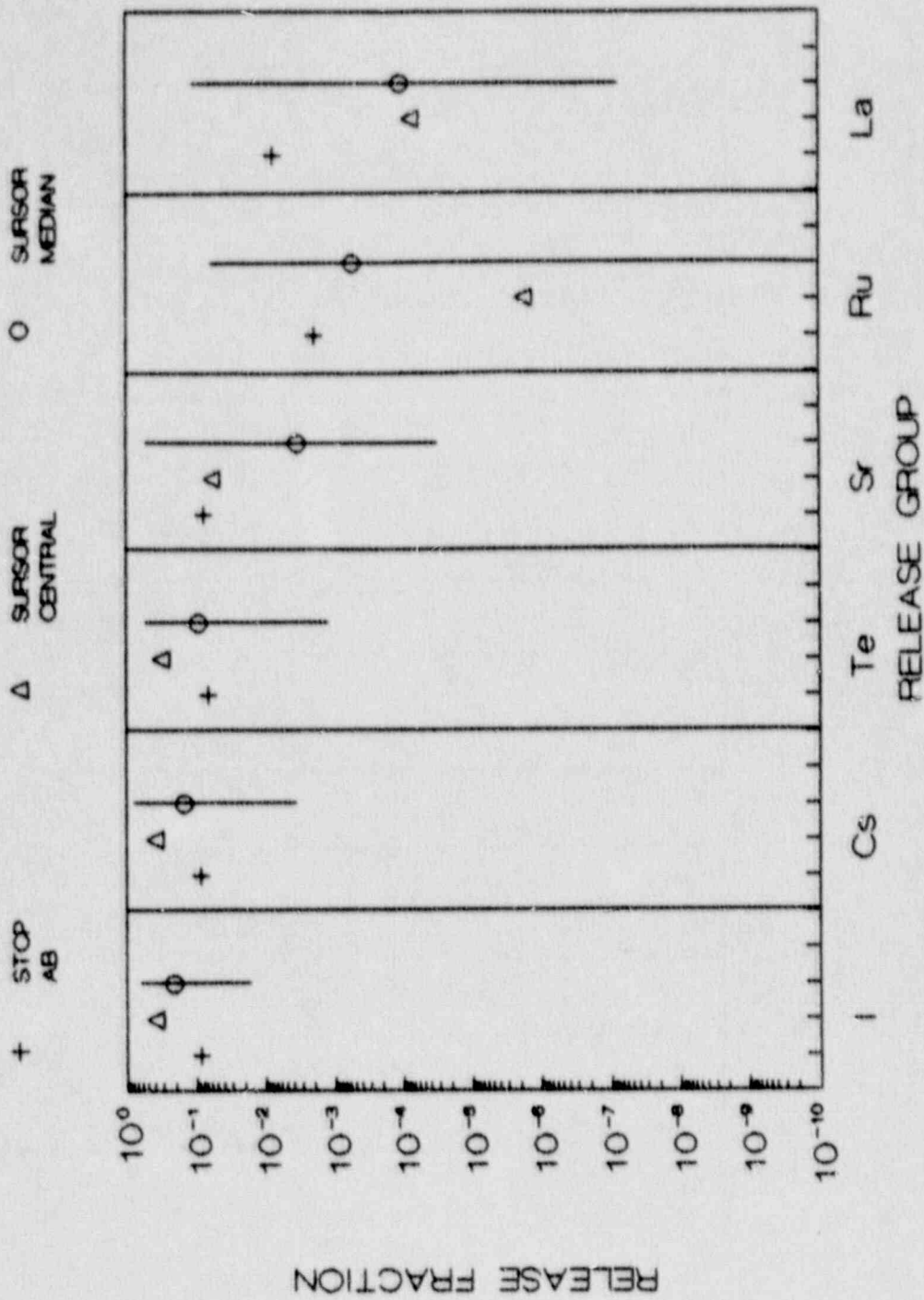


FIGURE 46.
 COMPARISON OF SURSOR WITH STCP RESULTS
 RESULTS FOR SGTR1

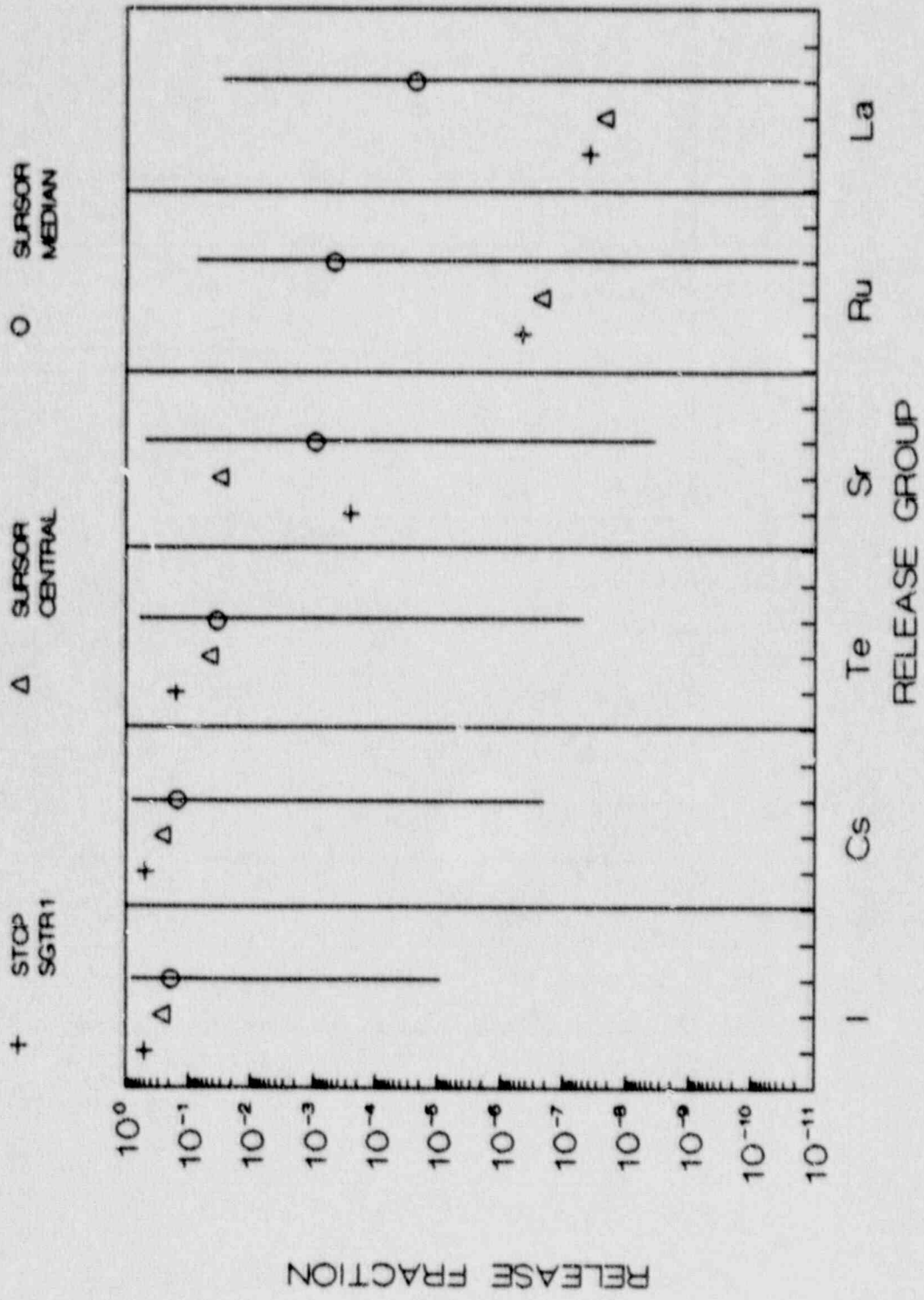


FIGURE 47.
 COMPARISON OF SURSOR WITH STCP RESULTS
 RESULTS FOR SGTR2

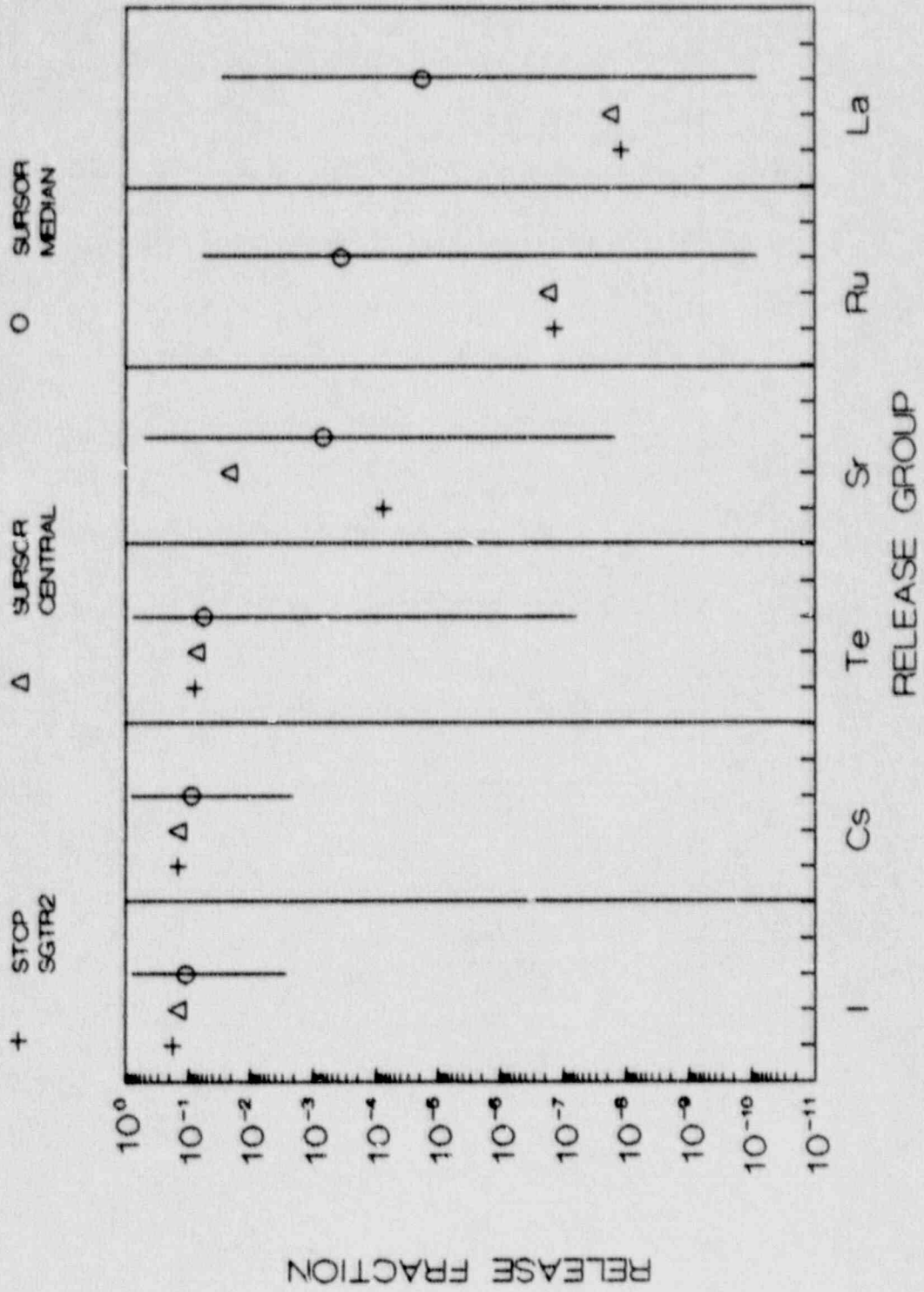
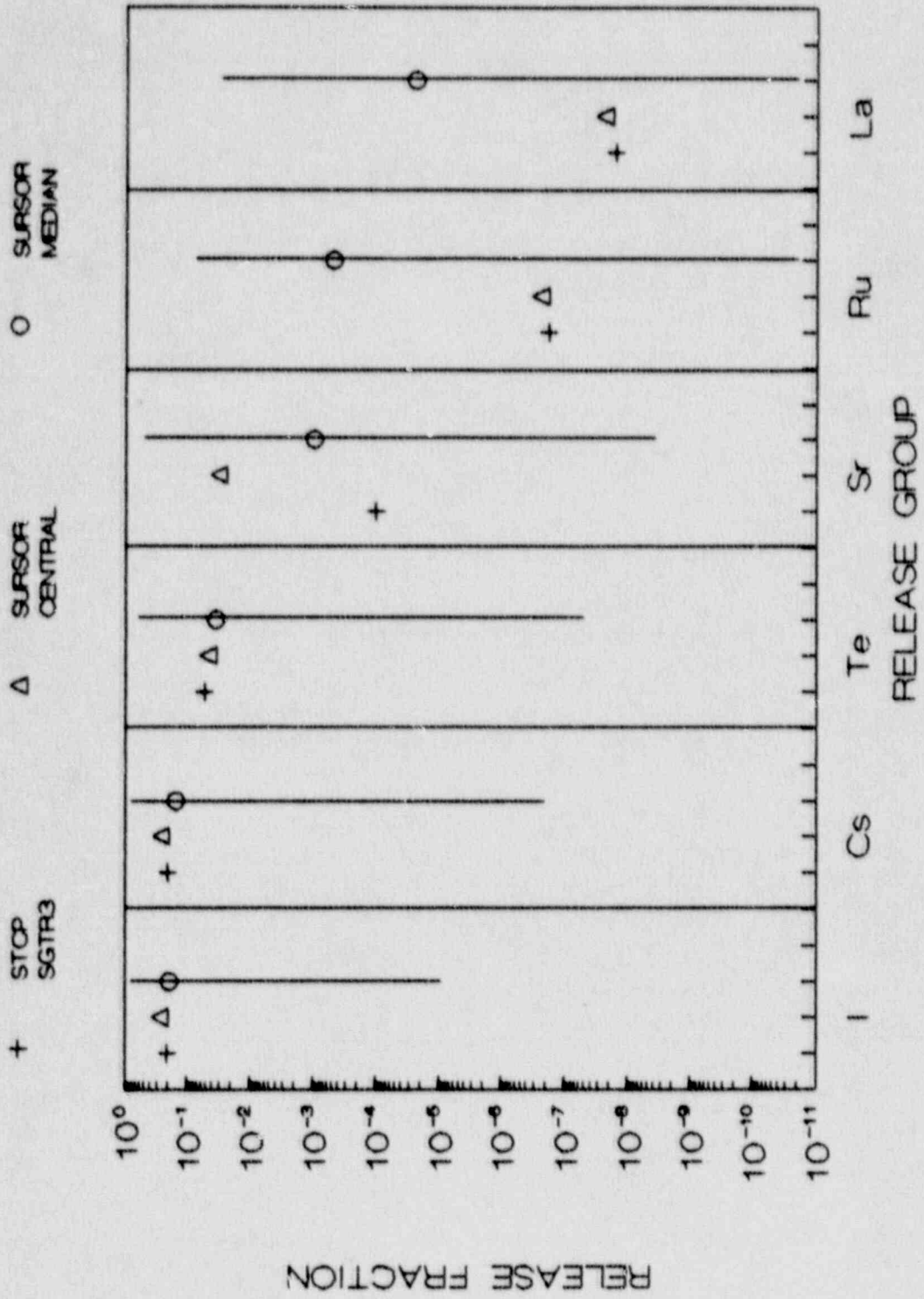


FIGURE 48.
 COMPARISON OF SURSOR WITH STOP RESULTS
 RESULTS FOR SGTR3



Results of SURSOR-STCP Comparison

The comparison of the SURSOR code predictions with available STCP results has provided a useful test of the ability of the parametric models to simulate the more detailed calculations. This is the interpolation mode of application of the parametric models. Some specific conclusions arising from these comparisons are given below.

For the most part the central estimate predictions of the SURSOR codes agree quite well with the applicable STCP results. This is true for the STCP calculations that were used in the derivation of the SURSOR parameters, as well as for the more limited number of STCP analyses that were not available or used for the derivation of these parameters. There are, however, some situations in which the agreement between the parametric models and the detailed analyses was not as good as could have been expected.

For cases in which the STCP calculated very low iodine releases, i.e., much less than 0.01 of the core inventory, the parametric models tended to predict higher releases for this species. The reasons for these differences are believed to be the following. The STCP assumes that iodine in the containment atmosphere exists as a cesium iodide aerosol which is continuously attenuated by natural deposition as well as engineered safety features, if applicable. The rate of attenuation of the airborne aerosols varies with the conditions existing in the containment. There is no imposed cutoff to aerosol deposition in the STCP, although it is generally believed that a small fraction of the available iodine could be converted to forms which would persist in the atmosphere for long periods of time. The XSOR codes take the latter into account and thus tend to predict a lower limit to iodine source terms. Similarly, the XSOR codes take into account the possibility that some of the iodine could be reevolved from the water in the containment, a factor not explicitly addressed by the STCP. (It may be noted that these factors are included in source term assessments by modifying the numerical results computed by the STCP.) A third factor that can lead to the prediction of higher iodine source terms by the parametric codes in comparison with the STCP is the release of iodine from the debris during core-concrete interactions. The STCP in its current formulation tends to predict essentially complete release of iodine from the core during the in-vessel phase of the accident, with nothing remaining for later release; the early release of iodine affords more opportunity for the available deposition mechanisms to act on the iodine. By keeping some of the iodine available for later release, SURSOR may release some fraction of the iodine when there is little opportunity for removal, at or near the time of containment failure, thus potentially increasing the overall environmental source term. A similar situation can exist with the calculation of cesium releases.

For certain of the accident scenarios considered there were also differences between the SURSOR predictions and the STCP results for the other fission product groups. The biggest differences appeared to be associated with situations in which several fission product attenuations were operative. The STCP explicitly considers the aerosol removal by each of the mechanisms, e.g., water over the debris as well as sprays; the overall effectiveness for aerosol attenuation of a series of processes is less than the linear combination of the

individual effects. The parametric models, on the other hand, assess the decontamination factors of each of the individual removal mechanisms, but apply only the largest one, since it is recognized that the overall effectiveness of a series of such mechanisms is not simply a linear combination of the individual effects. Thus, the parametric models in these situations tend to predict higher environmental source terms than the more detailed models.

The SURSOR predictions showed a pattern of higher ruthenium releases than did the STCP analyses, which were always very low. None of the other fission product groups displayed such a consistent pattern of difference between SURSOR and the STCP. The SURSOR uncertainty bands for ruthenium release were broader than for the other groups.

CONCLUSIONS

The comparisons of the SURSOR predictions with available STCP calculations discussed above, as well as the results with the other parametric codes discussed in the appendices, indicate that the several versions of the XSOR codes do a reasonable job of reproducing STCP results. The largest differences between the XSOR and STCP predictions appear for situations involving low releases to the environment. Some of the differences are due to the fact that the parametric codes attempt to address phenomena not explicitly considered by the STCP; others could be related to differences in the timing of the releases.

The uncertainty bands for environmental source terms generated by the parametric models, taking into account the input from the expert review panels, are extremely broad. These uncertainty bands are clearly much wider than those introduced by using the XSOR codes as surrogates for detailed STCP calculations.

The parametric models appear to be somewhat more successful in reproducing STCP results for the PWR's than for the BWR's. The complexities associated with the potential for suppression pool bypass in the BWR's make the predicted results more sensitive to the details of the timing of fission product release from the fuel relative to the times of vessel breach and containment failure.

The results of the present assessment indicate that while parametric models can be used as surrogates for detailed STCP calculations, such use requires knowledge of the timing of accident progression and related thermal hydraulic boundary conditions. This implies, as a minimum, the need for performing thermal hydraulic analyses of accident progression for the particular plant in question. The performance of selected complete source term analyses to benchmark the parametric models is clearly highly desirable.

APPENDIX A

COMPARISON OF SEQSOR AND STCP RESULTS

APPENDIX A

COMPARISON OF SEQSOR AND STCP RESULTS

The following discussion gives a comparison of the parametric code, SEQSOR, used for the Sequoyah ice condenser containment analyses. SEQSOR added the decontamination factor in the ice condenser to the list of uncertainties included in SURSOR. For the following comparisons the input parameters to SEQSOR were selected to match as closely as possible the accident sequences previously analyzed by the STCP.

Figures A-1 through A-13 compare SEQSOR predictions with available STCP results for the Sequoyah ice condenser PWR. In these comparisons two SEQSOR estimates are shown, the central and the median, as well as the ranges of the releases when uncertainties are considered. The SEQSOR central estimates are based on STCP results and would thus be expected to show reasonable agreement with the latter; the median and uncertainty estimates are based on the median results of the expert elicitations. The latter take into account uncertainties in the models as well as a variety of phenomena and data not included in the STCP.

Figure A-1 shows the comparison between the SEQSOR predictions and STCP results for TMLB-gamma, station blackout with early containment failure due to a hydrogen burn at vessel breach. As with a number of the cases discussed previously, the STCP results for this case tracked only three of the fission product species. For this case there is relatively little difference among the three sets of the results. The uncertainty ranges are extremely broad, particularly for the non-volatile species.

Figure A-2 compares the SEQSOR predictions with STCP results for TMLB-delta, station blackout with late containment overpressure failure. In this case the agreement between SEQSOR and STCP for the volatile species is not as good as in the previous case. The STCP does have explicit models for late iodine volatilization and the formation of organic iodides; the latter are taken into account by SEQSOR and lead to higher predicted release fractions. The uncertainty bands are typically large.

The comparison for TMLB-beta, station blackout with containment isolation failure, is presented in Figure A-3. The STCP calculation for this case explicitly tracked only three of the fission product groups. The SEQSOR median iodine results are higher than the other estimates due to the consideration of the formation of organic iodide and late iodine volatilization. The comparison for cesium and tellurium is quite reasonable.

SEQSOR predictions for the TML-gamma sequence are compared with STCP results in Figure A-4. In this sequence all makeup to the primary and secondary systems is lost, but the containment safety features are operating; containment failure takes place due to a hydrogen burn at vessel breach. The SEQSOR results for iodine release are higher than the STCP calculation due to

consideration of late iodine volatilization and formation of organic iodide. Cesium results are in good agreement; SEQSOR predicts higher releases of tellurium than did the STCP. The other species were not tracked in this particular STCP calculation.

Figure A-5 presents the comparison for the TML-delta sequence. In this case all makeup to the primary and secondary system is lost, but the containment safety features are operating; containment failure takes place due to the long term buildup of noncondensables. For this case the comparison between SEQSOR and the STCP is not very good. In the case of iodine the SEQSOR median result is dominated by the formation of organic iodide, which would not be subject to decontamination by any of the available mechanisms. As noted previously, the STCP does not model this phenomenon, although it is recognized as a real effect; typically a small fraction of the available iodine is assumed to be converted to volatile forms at the end of a STCP calculation. The differences in the predicted releases of cesium and tellurium are believed to be due to differences in the treatment of sprays, ice condensers, and water overlying the melt. The STCP explicitly considers aerosol removal by each of these processes; SEQSOR takes credit for only the highest of a series of decontamination factors. The other species were not tracked in this STCP calculation.

SEQSOR predictions for the S2HF-gamma sequence are compared with STCP results in Figure A-6. This scenario is initiated by a small break in the primary system and all safety systems function initially; however, due to the inadvertent closure of the drains between the upper and lower compartments of the containment, both the emergency core cooling and containment spray systems fail upon switchover to the recirculation phase of operation. Containment failure is due to a hydrogen burn at the time of vessel breach. The SEQSOR results for iodine and cesium are above those of the STCP. This appears due to the fact that the STCP releases these species largely in-vessel while the containment is intact, whereas SEQSOR retains some of these species for release ex-vessel, after the containment has failed. The tellurium and strontium releases are in reasonable agreement, those for ruthenium and lanthanum show more scatter.

Figure A-7 presents the results for the S3HF1 sequence. The initiating event in this case is a pump seal failure; the engineered safety features function initially, but both the emergency core cooling and containment spray systems fail on switchover to recirculation. The containment fails due to a hydrogen burn at about the time of reactor vessel failure. Since the bottom of the reactor vessel would be expected to be submerged in this case, both the release at the time of vessel failure as well as the subsequent release during concrete attack are scrubbed by the water. The agreement between SEQSOR and the STCP is quite good, except for the median estimate for ruthenium. The uncertainty bands are typically large.

The results for the S3HF3 sequence are illustrated in Figure A-8. This case is very similar to the preceding one, except that the water in the reactor cavity is limited to that injected from the accumulators. Again, the agreement is quite good with the exception of the SEQSOR median estimate for ruthenium.

The STCP results for an accident-induced steam generator tube rupture event are compared with SEQSOR predictions in Figure A-9. For purpose of analysis the initiating event was assumed to be loss of makeup to both the primary and secondary systems. The induced steam generator tube rupture was assumed to take place at the time of initial fuel slumping out of the core region. The secondary side safety/relief valves were assumed to open as required to maintain pressure and reclose as the pressure dropped below their setpoint. The analyses in this case were limited to the in-vessel phase of the accident. The agreement between the STCP results and SEQSOR predictions is seen to be quite good for the more volatile fission product groups. The SEQSOR median estimates for the ruthenium and lanthanum releases are well above the STCP results and the corresponding SEQSOR central estimates. The higher in-vessel releases for these species reflect the input from the expert panels.

The results for TBA, station blackout with an accident induced hot leg rupture, are illustrated in Figure A-10. This is a complex scenario, with initial core melting taking place at high primary system pressure, quenching of the melt by accumulator water following the induced hot leg rupture and depressurization, and eventual remelting at low pressure. Containment failure was postulated to take place due to a hydrogen burn shortly after the induced hot leg rupture. The SEQSOR predictions for iodine and cesium are above those of the STCP due to the assignment of some fraction of these releases to the ex-vessel stage of the accident. Tellurium, strontium, and lanthanum releases are in reasonable agreement. The median estimate for ruthenium release is well above the STCP result, reflecting the expert panel views. Figure A-11 shows the results for a variation of this scenario in which the ice condenser fission product removal capability was degraded. The results are comparable to the preceding.

Figure A-12 gives the comparison for S3B-gamma, a station blackout accompanied by pump seal failure. Containment failure in this case was postulated to be the result of a localized hydrogen detonation in the upper plenum of the ice condenser, occurring at about the time of fuel slump. Concrete attack by the core debris was assumed to be delayed until after the water in the cavity had been evaporated. The STCP results for iodine and cesium are well above the SEQSOR estimates. This is due to the fact that STCP tends to reflect early complete release of these species, whereas SEQSOR releases them over a longer time. The other species are in reasonable agreement.

The results for the S3HF-delta sequence are presented in Figure A-13. The initiating event in this case is a pump seal failure, the emergency core cooling and containment systems operate in the injection mode but fail on switchover to recirculation. The air return fans and igniters are operable. Containment failure takes place by long term overpressurization and is calculated to occur after all the ice has melted. Concrete attack in this case is delayed until all the water in an initially filled cavity has been boiled off by the core debris. The SEQSOR results for the volatile species are above those of the STCP, due to consideration of late revolatization. The results for the nonvolatiles are in reasonable agreement.

Figure A-14 gives the comparison between SEQSOR and the STCP for the ACD sequence. This is a large break loss of coolant accident with failure of both the emergency core cooling and containment spray systems; the air return fans and the hydrogen igniters are operable. Containment failure in this case takes place due to the long term buildup of noncondensables. The STCP calculated iodine and cesium release fractions for this case are below the range of the figure. In the STCP analysis these species are released early in the sequence and with the operation of the air return fans experience multiple passes through the ice condenser, with some attenuation during each pass. The SEQSOR results take note of the possibility that some of the iodine may be in the form of organic iodides which would not be attenuated by the ice condenser; also SEQSOR considers late revolatilization of cesium and iodine from the primary system. The results for the other species show considerable scatter, but fall well within the uncertainty ranges as given by SEQSOR.

The comparison for TB-gamma, station blackout with pump seal failure and containment failure due to a hydrogen burn, is presented in Figure A-15. The agreement among the various results is quite reasonable. The uncertainty bands are typically large.

The SEQSOR predictions showed a pattern of higher ruthenium releases than were calculated by the STCP. None of the other fission product groups appeared to display consistent patterns of difference between SEQSOR and the STCP.

FIGURE A-1

COMPARISON OF SEQSOR WITH
STCP RESULTS FOR TMLB-gamma

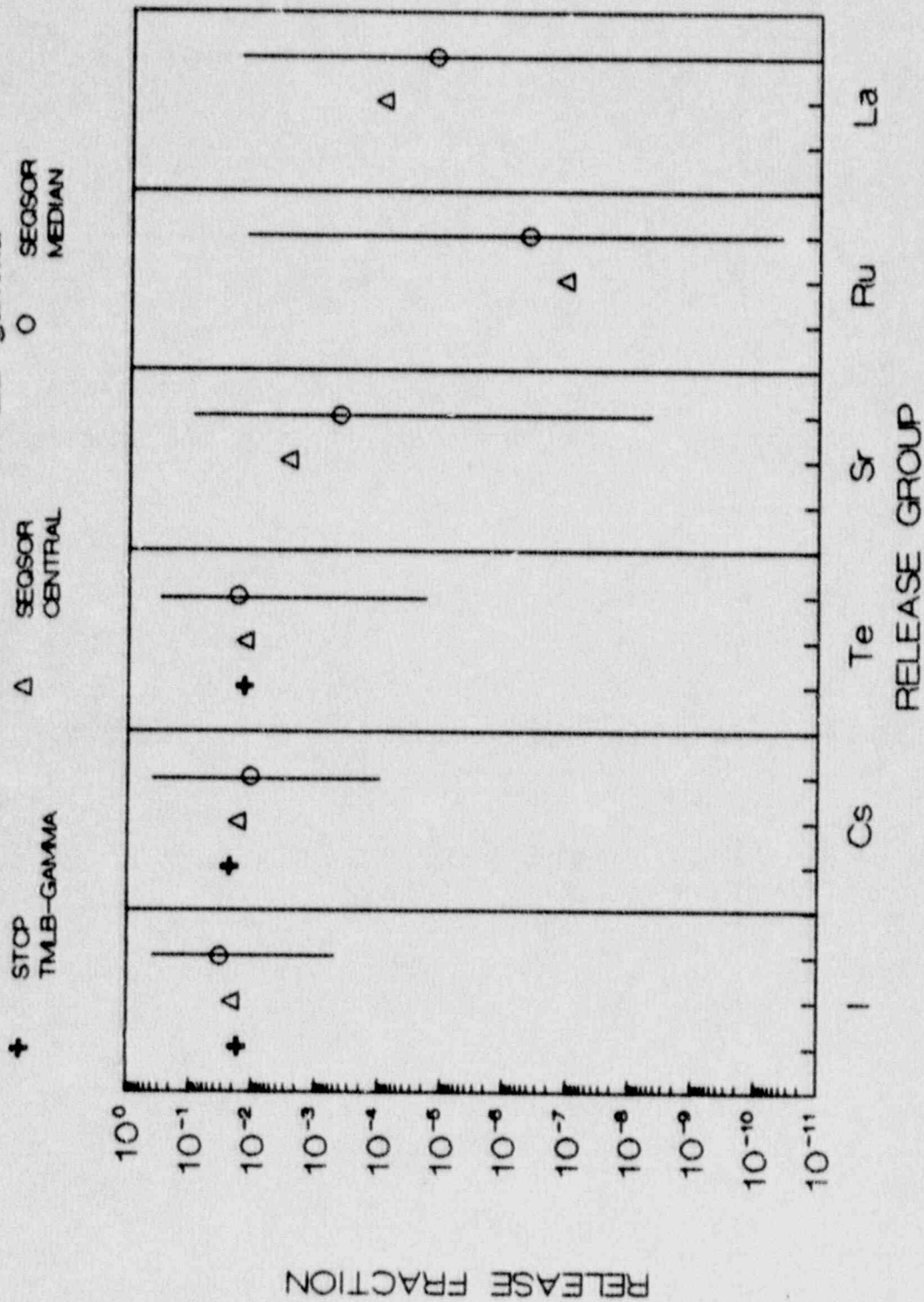
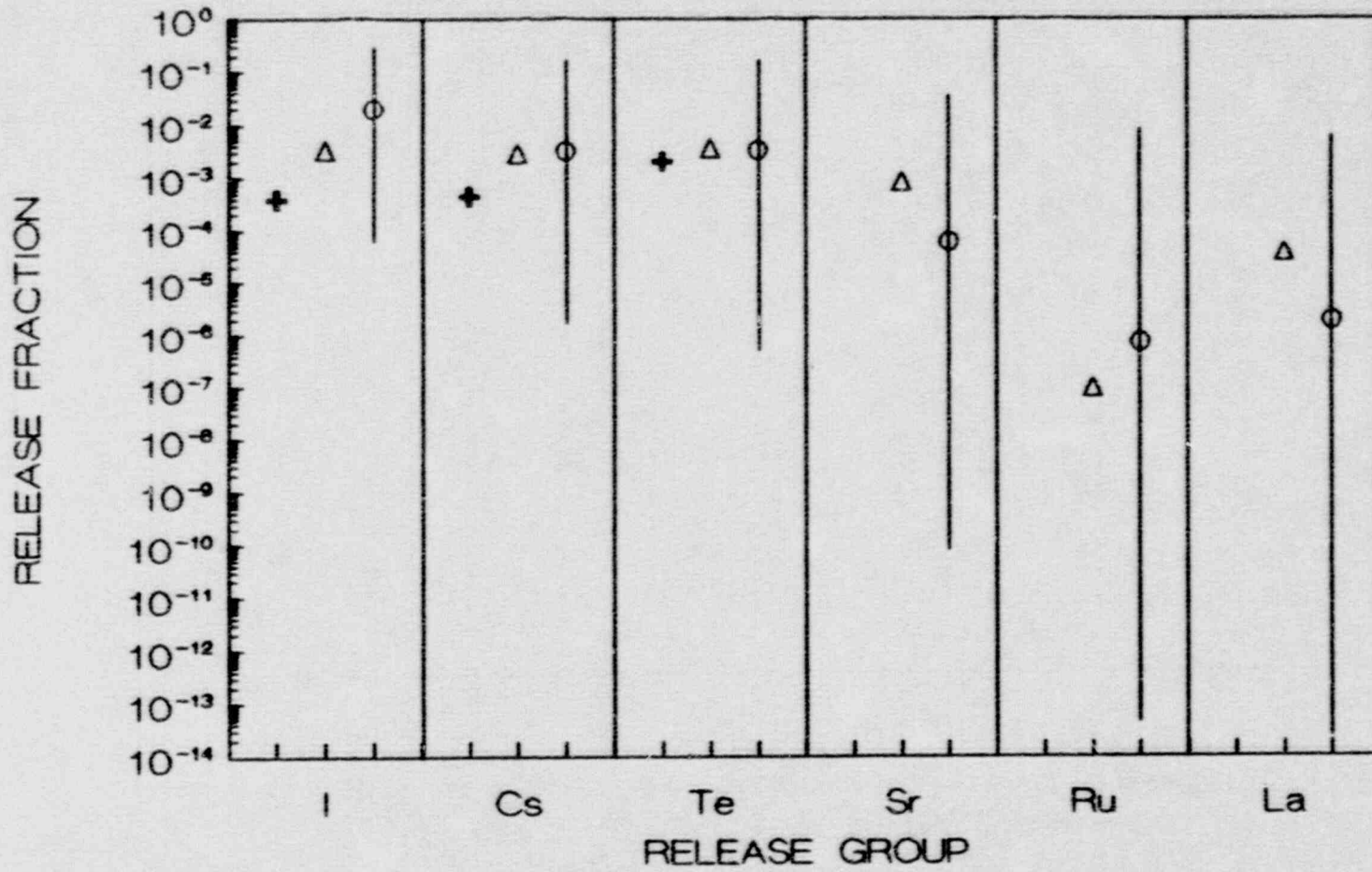


FIGURE A-2

COMPARISON OF SEQSOR WITH
STCP RESULTS FOR TMLB-delta

+ STOP TMLB-DELTA Δ SEQSOR CENTRAL ○ SEQSOR MEDIAN



A-6

FIGURE A-3
 COMPARISON OF SEQSOR WITH
 STCP RESULTS FOR TMLB-beta

+ STOP TMLB-BETA Δ SEQSOR CENTRAL ○ SEQSOR MEDIAN

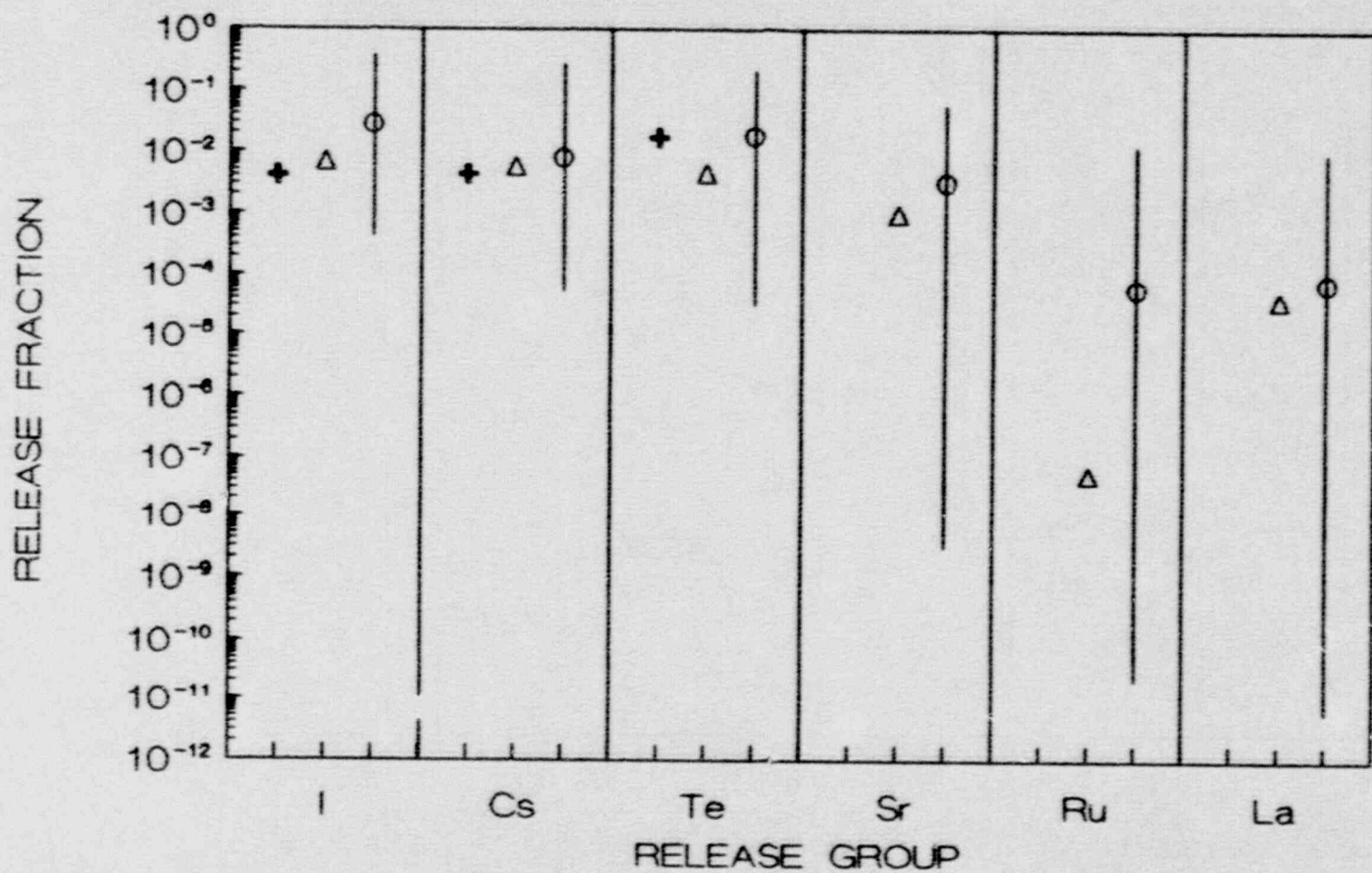


FIGURE A-4
 COMPARISON OF SEQSOR WITH
 STOP RESULTS FOR TML-gamma

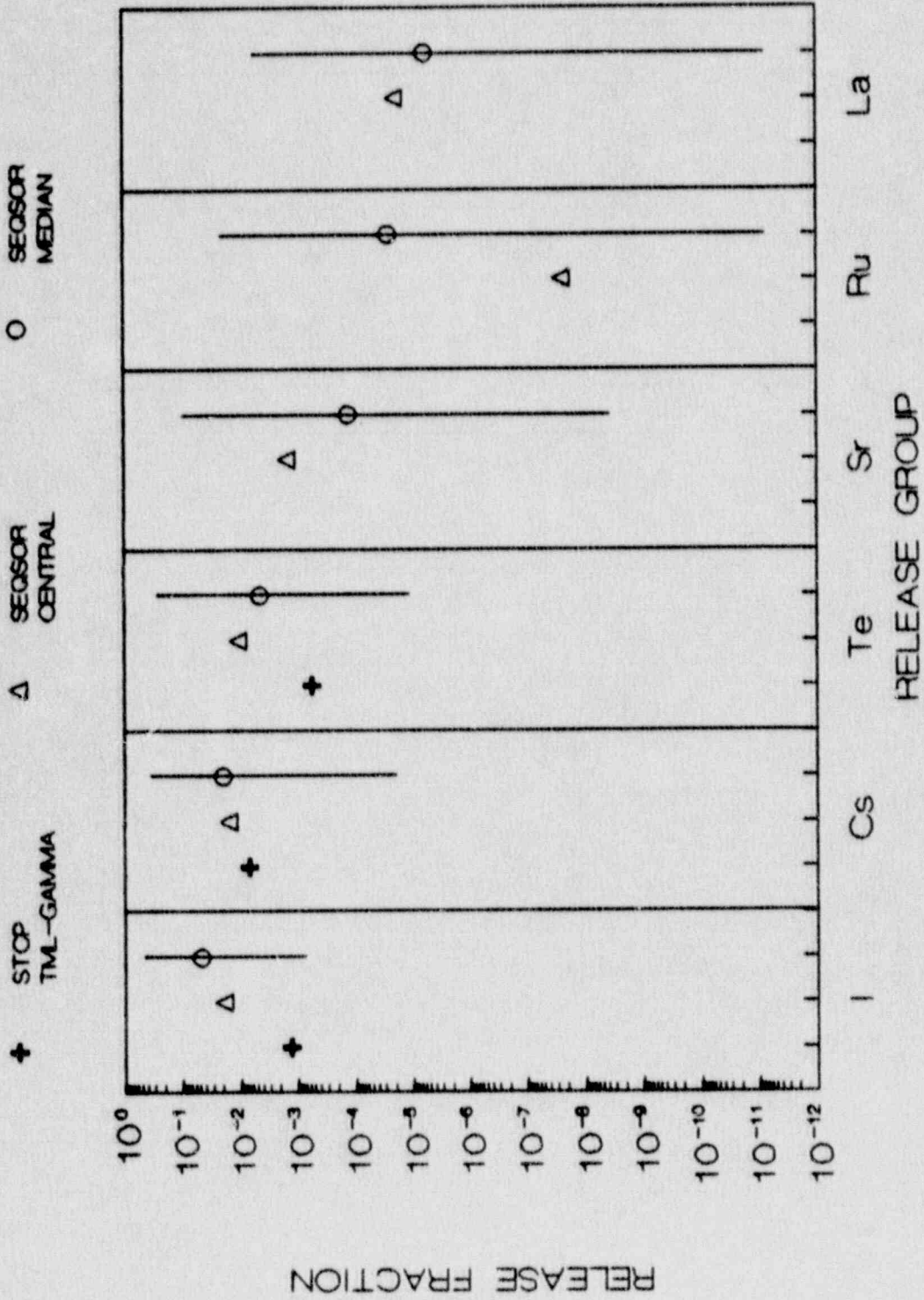


FIGURE A-5

COMPARISON OF SEQSOR WITH
STOP RESULTS FOR TML-delta

+ STOP TML-DELTA Δ SEQSOR CENTRAL ○ SEQSOR MEDIAN

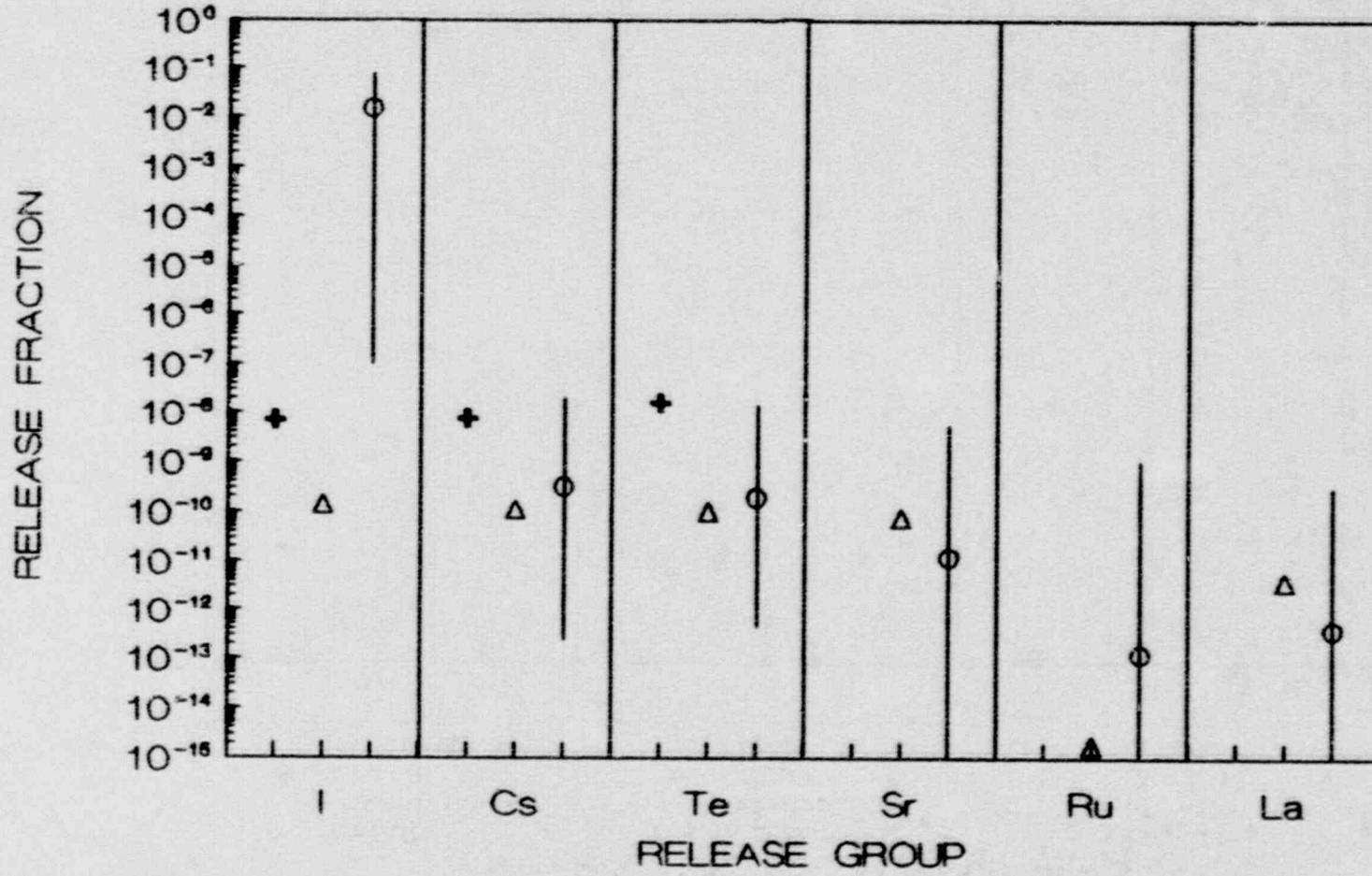


FIGURE A-6
 COMPARISON OF SEQSOR WITH
 STCP RESULTS S2HF-gamma

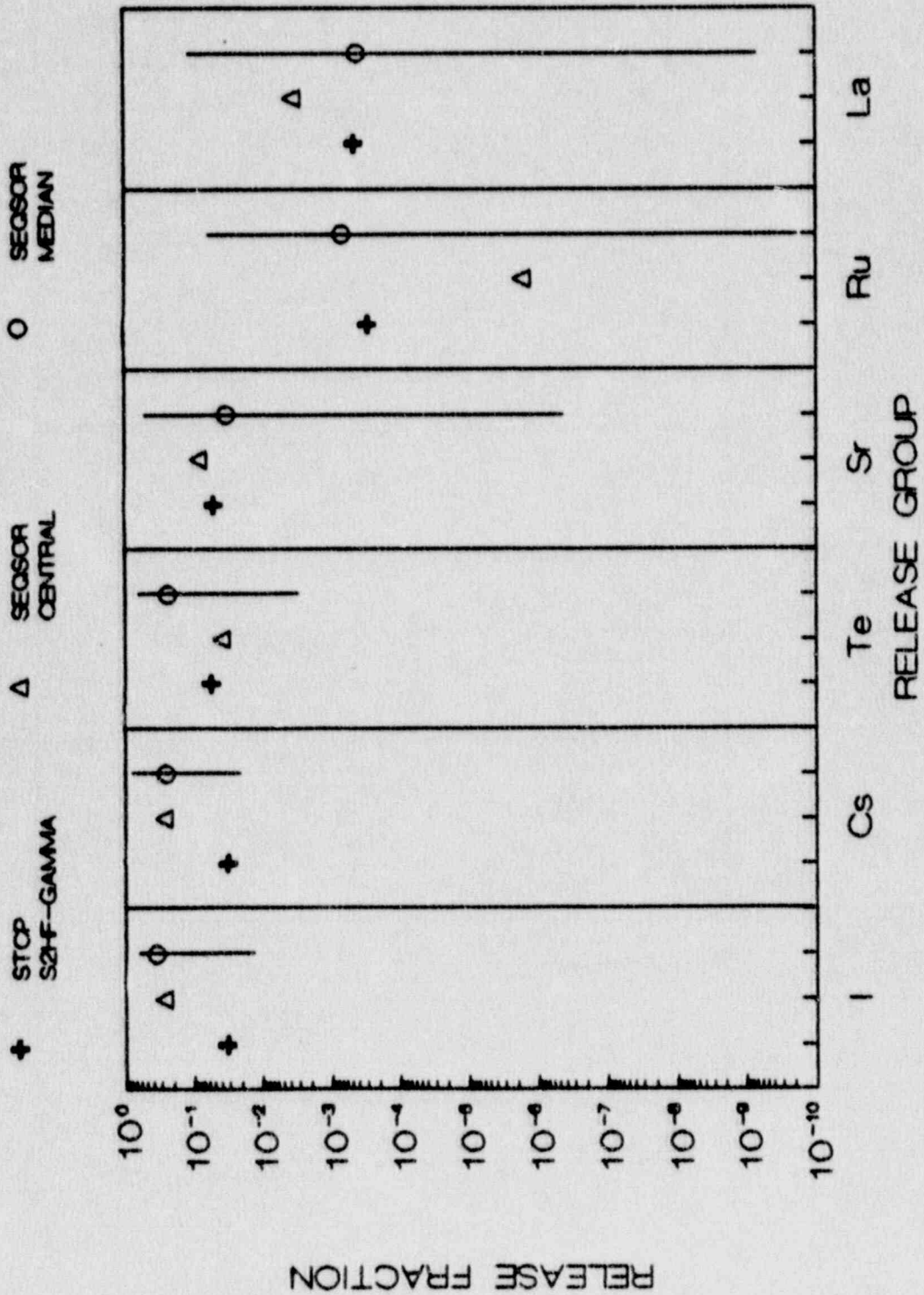
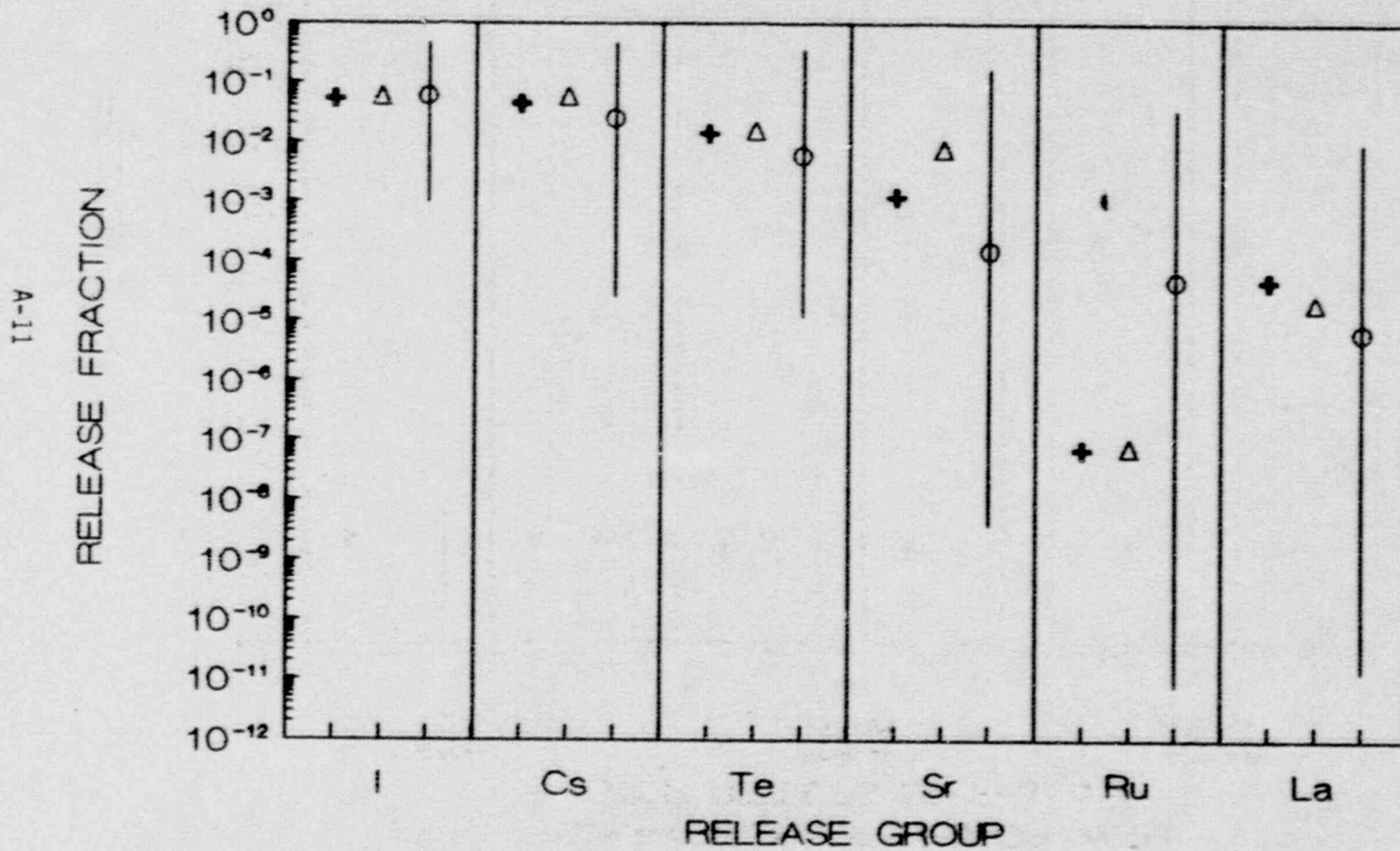


FIGURE A-7
 COMPARISON OF SEQSOR WITH
 STCP RESULTS FOR S3HF1

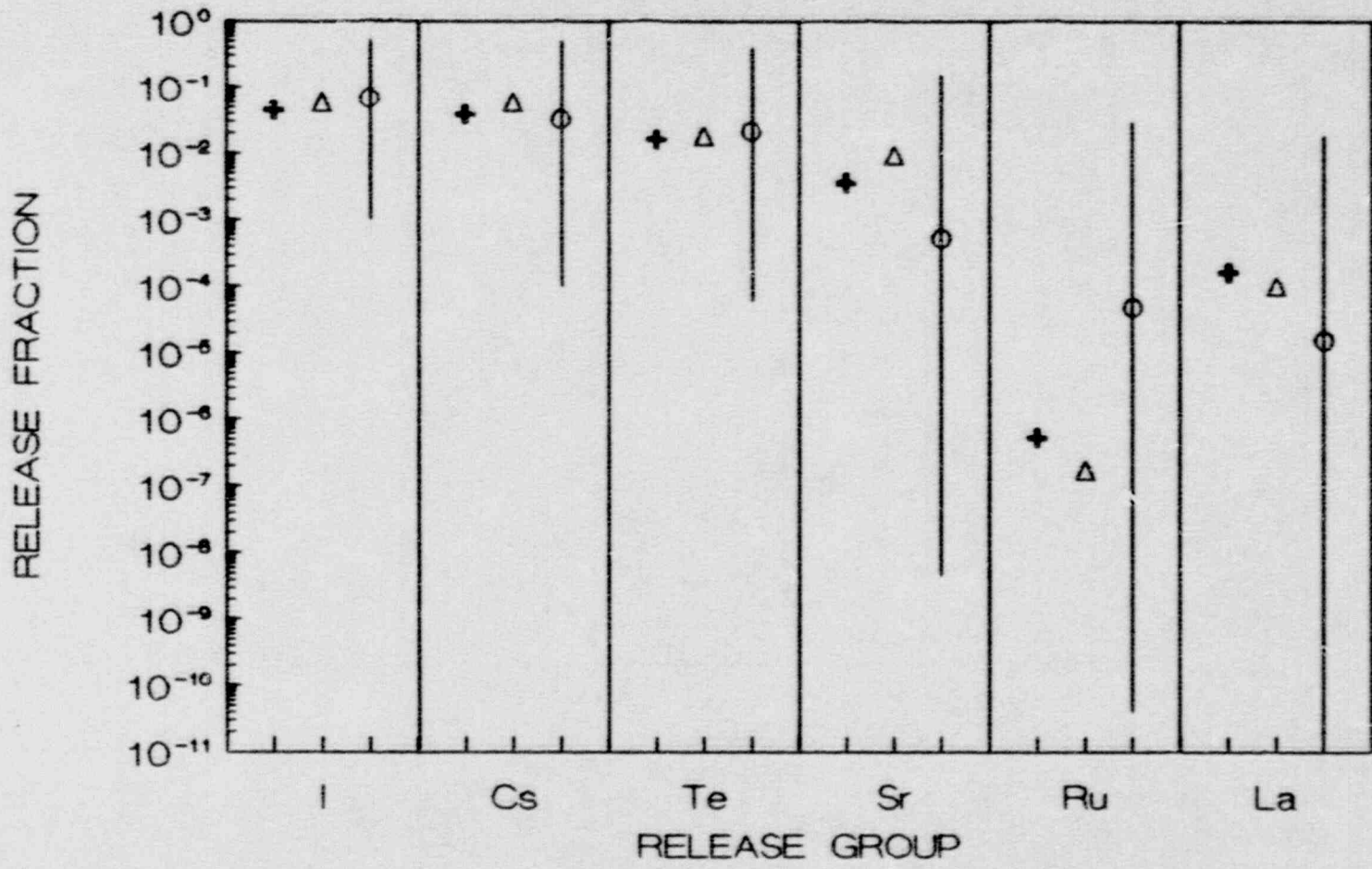
+ STCP
 S3HF1
 Δ SEQSOR
 CENTRAL
 ○ SEQSOR
 MEDIAN



A-11

FIGURE A-8
 COMPARISON OF SEQSOR WITH
 STOP RESULTS FOR S3H-F3

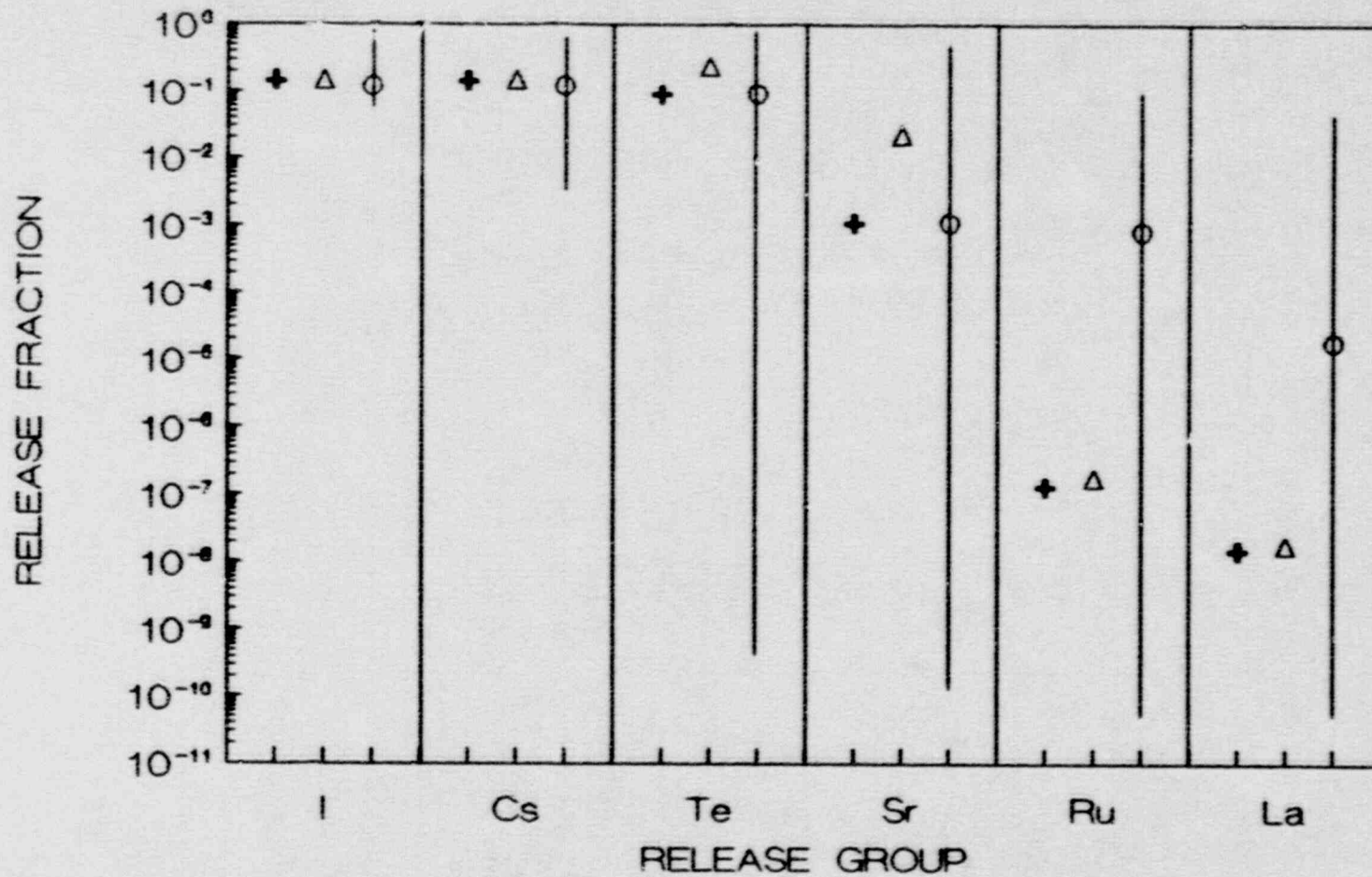
+ STOP S3H-F3 Δ SEQSOR CENTRAL ○ SEQSOR MEDIAN



A-12

FIGURE A-9
 COMPARISON OF SEQSOR WITH
 STCP RESULTS FOR TMLU-SGTR

+ STOP SGTR Δ SEQSOR CENTRAL ○ SEQSOR MEDIAN



A-13

FIGURE A-10
 COMPARISON OF SEQSOR WITH
 STOP RESULTS FOR TBA

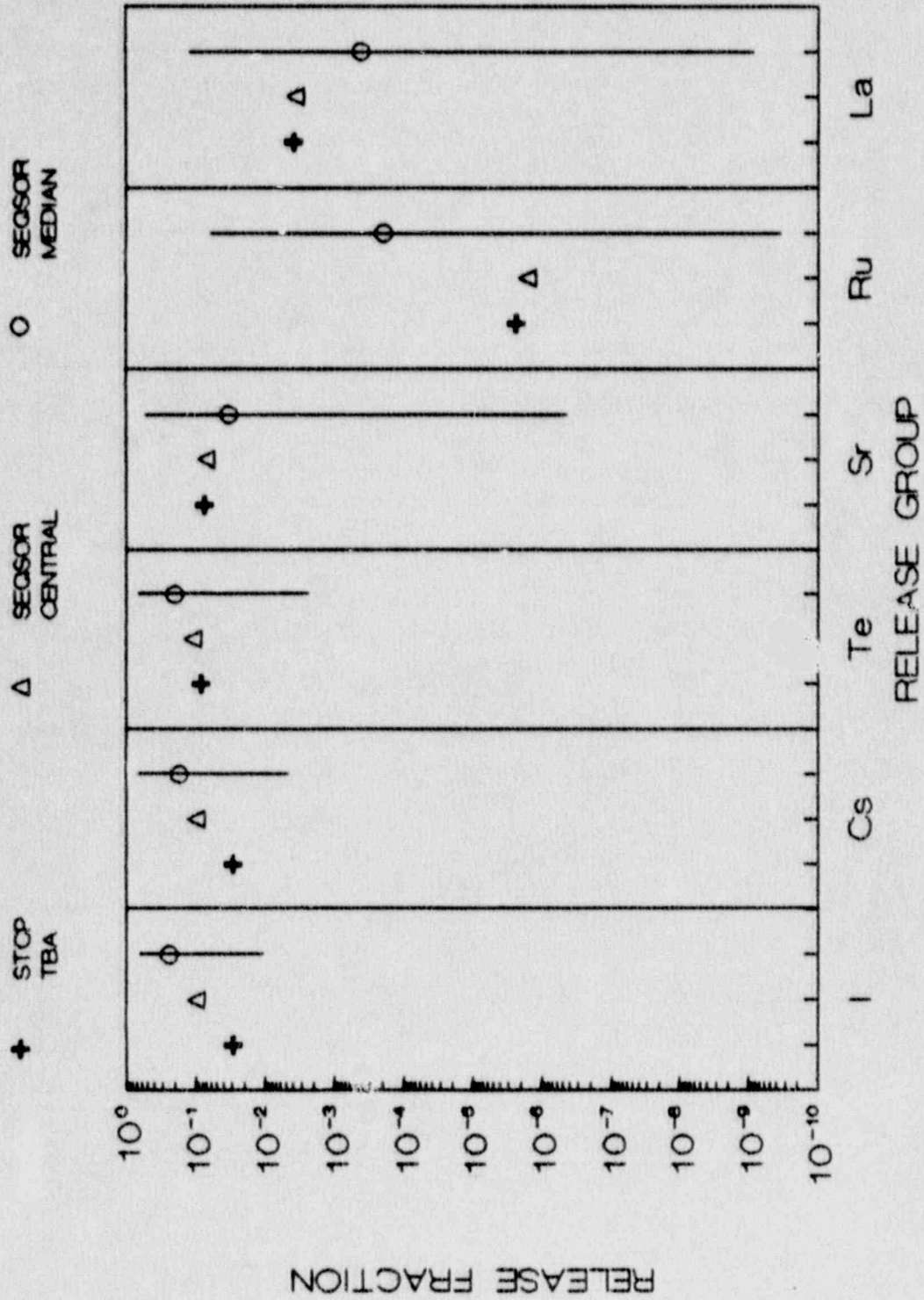
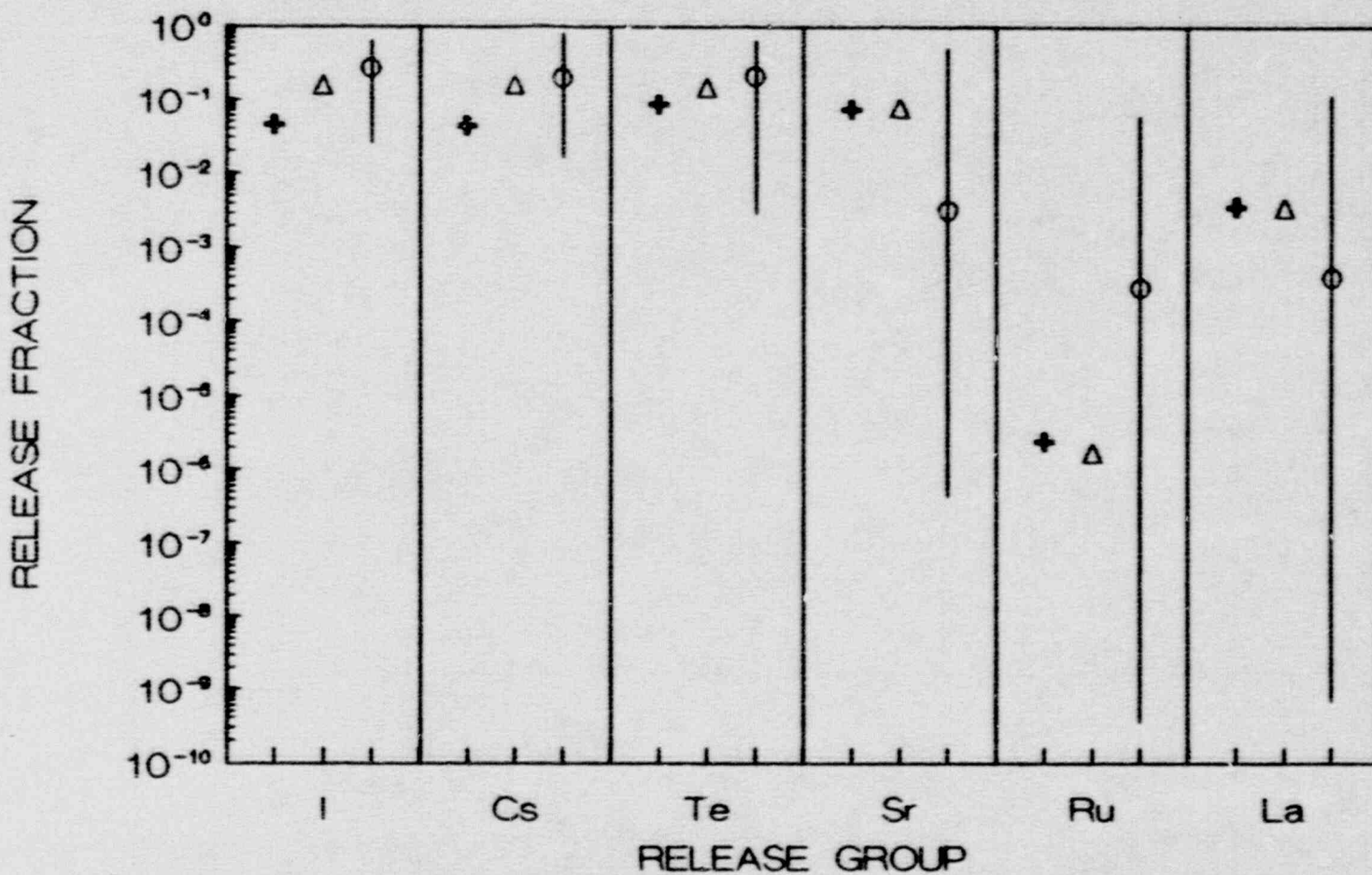


FIGURE A-11

COMPARISON OF SEQSOR WITH
STCP RESULTS FOR TBA 1

+ STOP TBA 1 Δ SEQSOR CENTRAL ○ SEQSOR MEDIAN



A-15

FIGURE A-12

COMPARISON OF SEQSOR WITH
STOP RESULTS FOR S3B-gamma

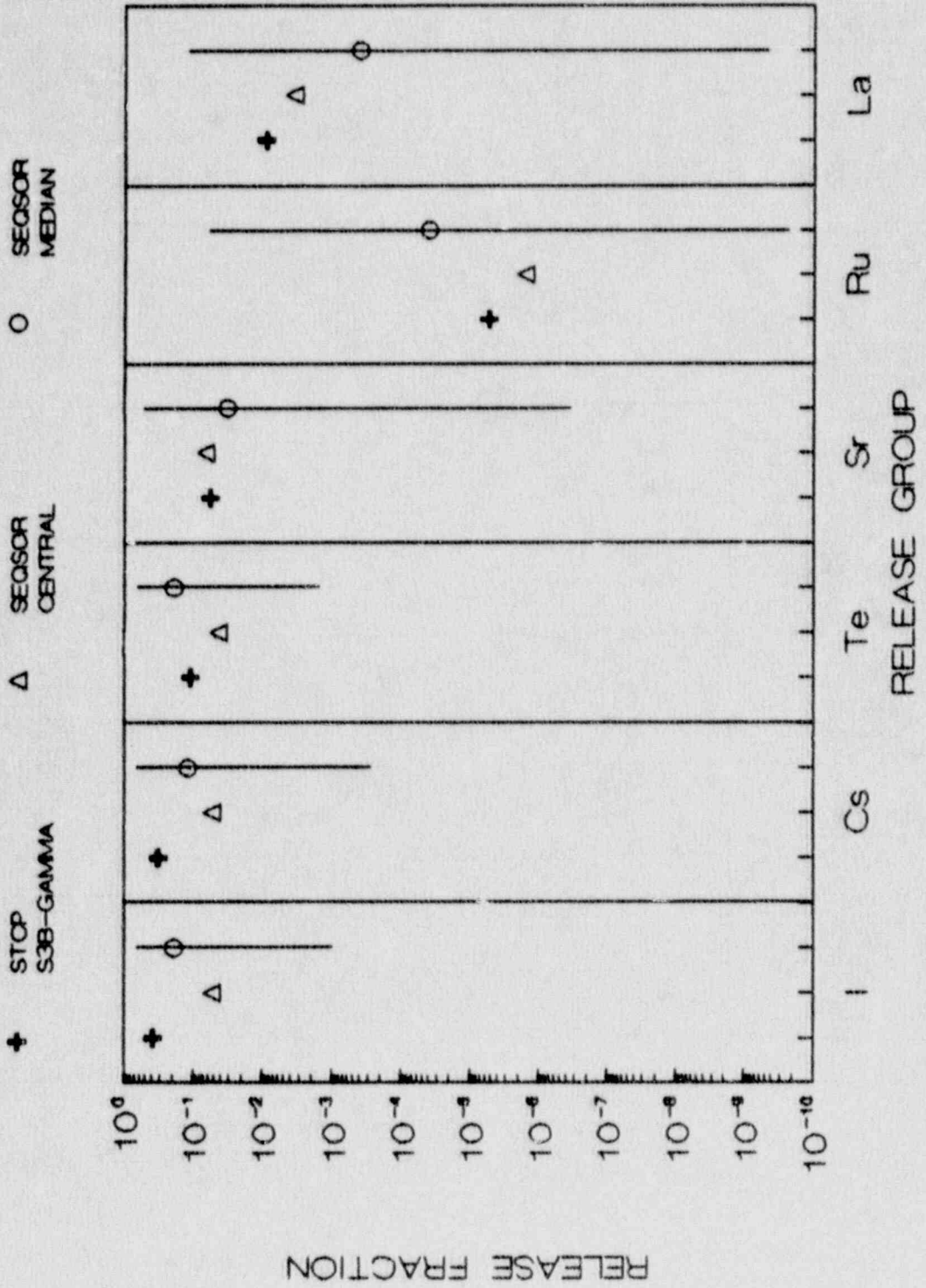


FIGURE A-13
 COMPARISON OF SEQSOR WITH
 STCP RESULTS FOR S3HF-delta

+ S3HF DELTA Δ SEQSOR CENTRAL ○ SEQSOR MEDIAN

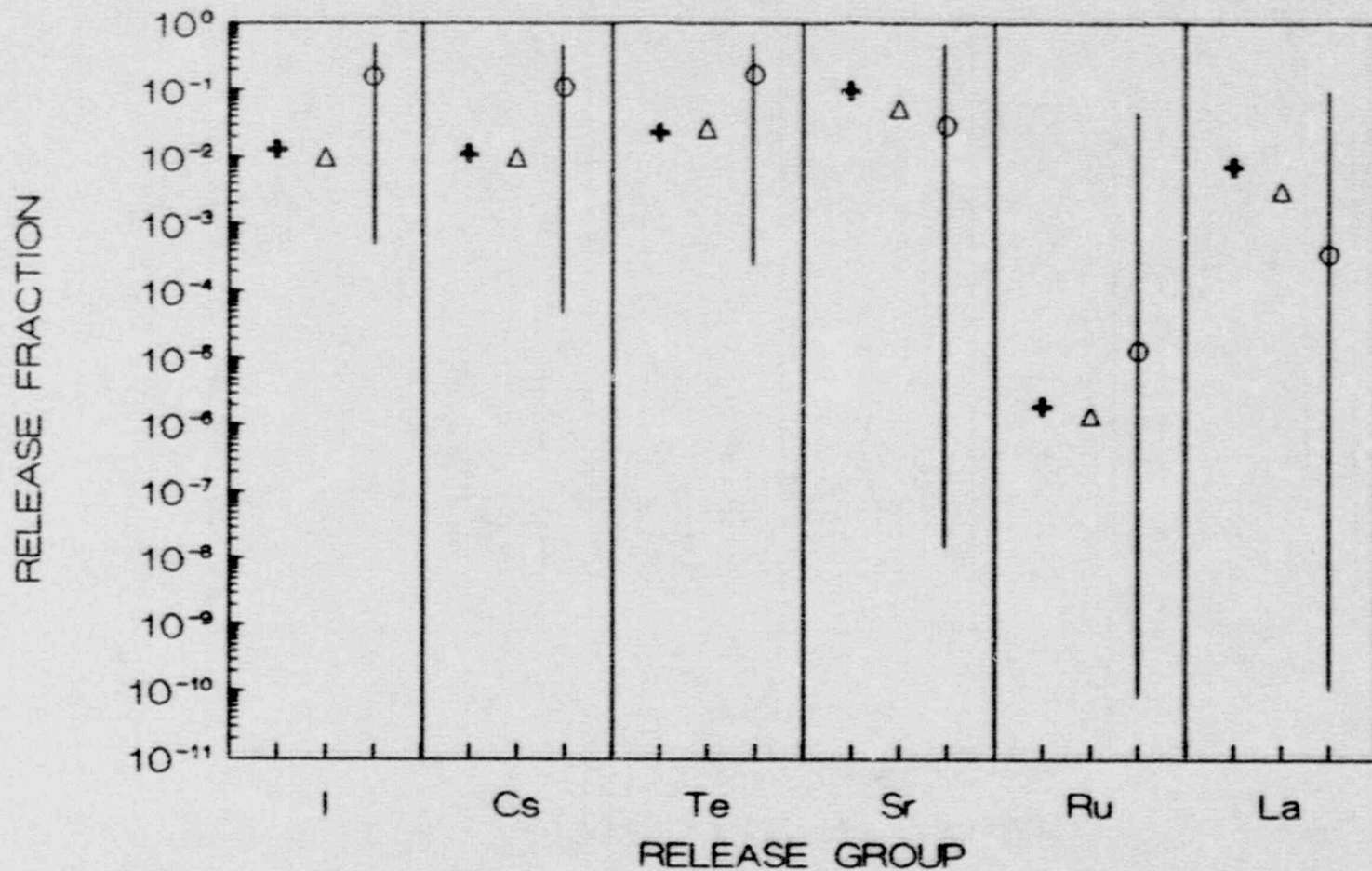
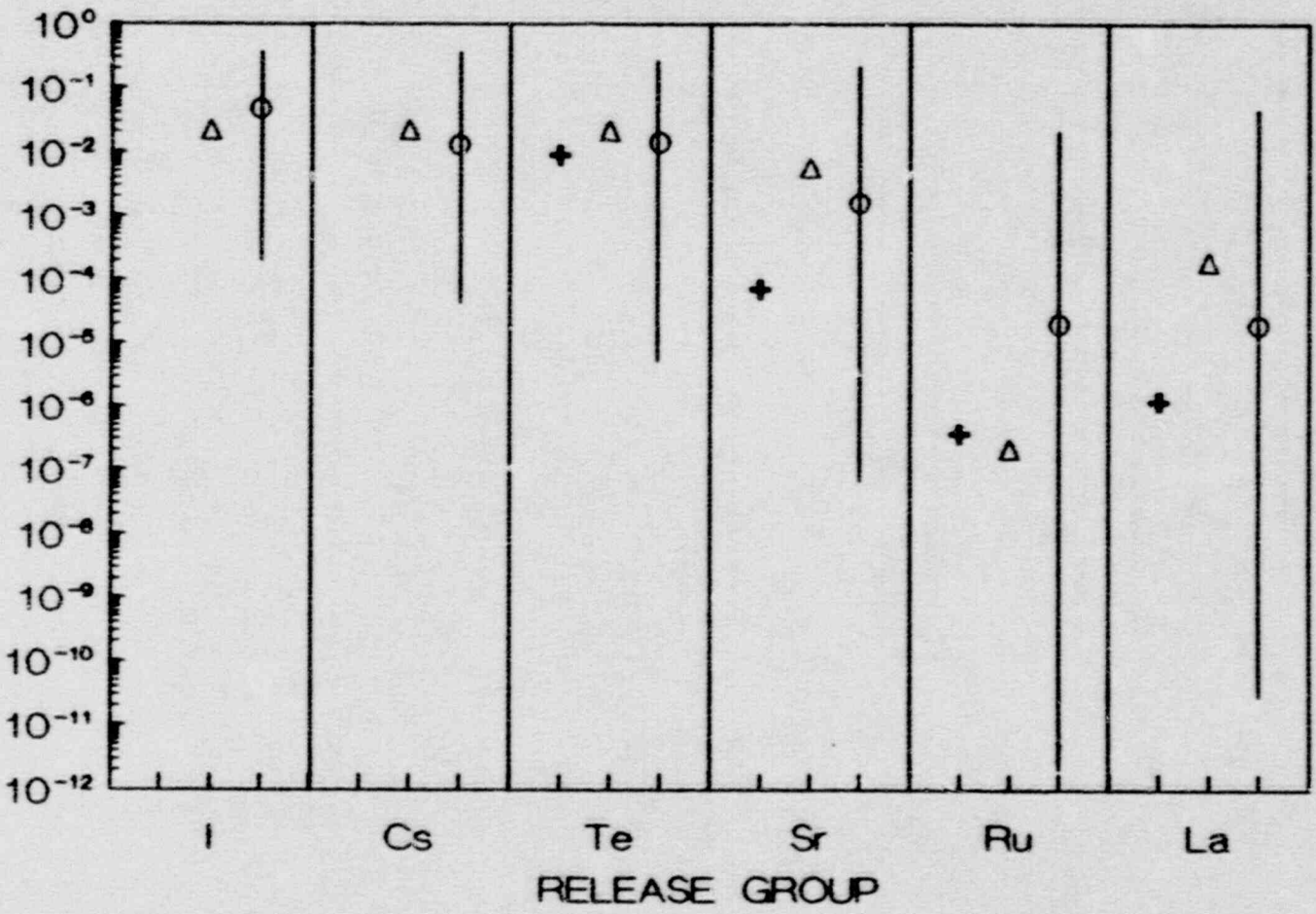


FIGURE A-14
 COMPARISON OF SEQSOR WITH
 STOP RESULTS FOR ACD

+ STOP ACD Δ SEQSOR CENTRAL ○ SEQSOR MEDIAN

RELEASE FRACTION

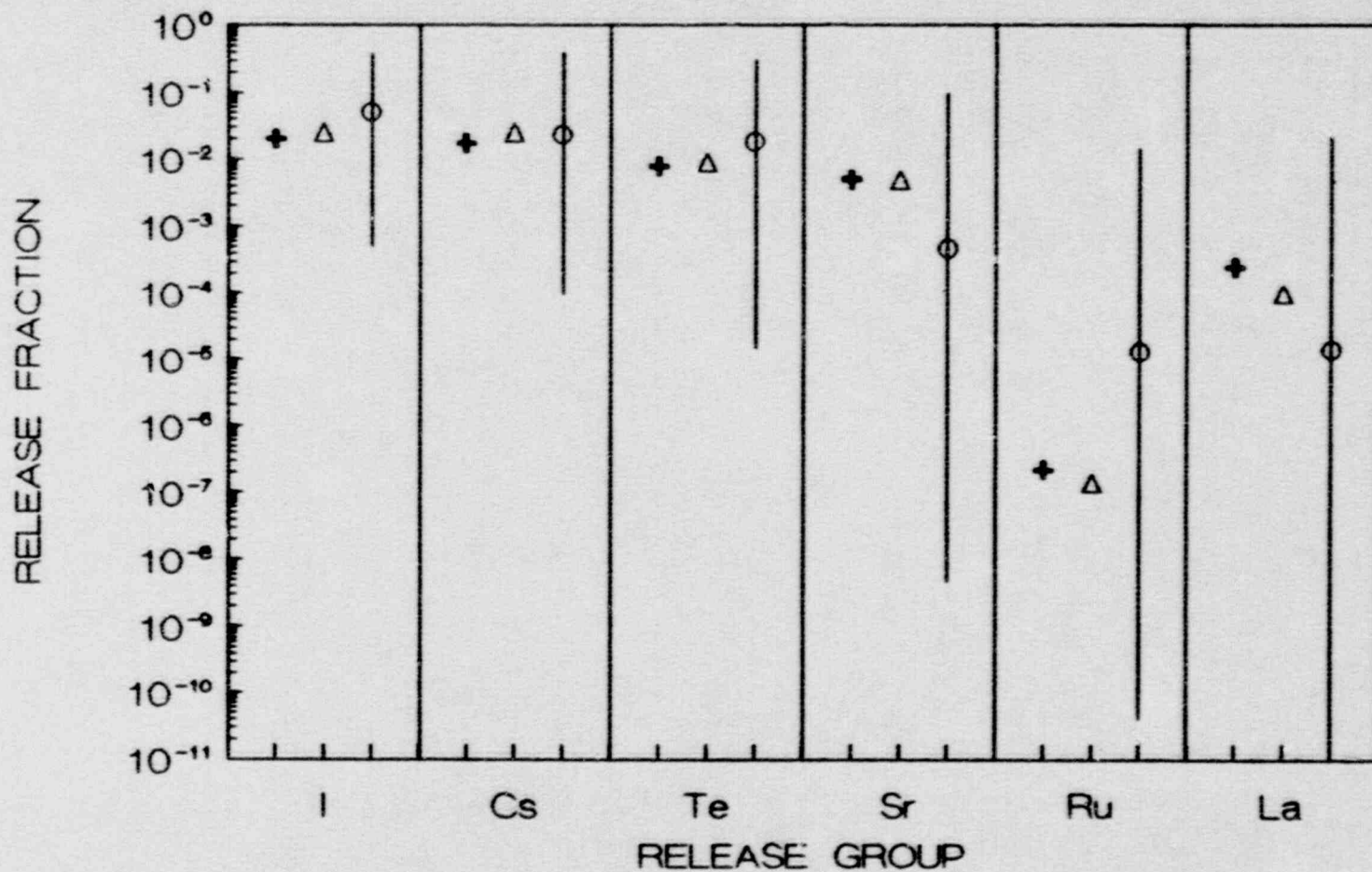


A-18

FIGURE A-5

COMPARISON OF SEQSOR WITH
STCP RESULTS FOR TB-gamma

+ STOP TB-GAMMA Δ SEQSOR CENTRAL ○ SEQSOR MEDIAN



APPENDIX B

COMPARISON OF PBSOR AND STCP RESULTS

APPENDIX B

COMPARISON OF PBSOR AND STCP RESULTS

This appendix present comparisons of PBSOR, used for the Peach Bottom BWR analyses, with available STCP results. The PBSOR formulation did not permit a convenient generation of central estimates, as had been done with the other versions. Thus the discussion below will compare the STCP calculations with the PBSOR median estimates as well as uncertainty ranges. The PBSOR median and uncertainty estimates are based on the input from the expert panels and address uncertainties in the models as well as a variety of phenomena not included in the STCP. The specific issues considered in the PBSOR uncertainty analyses include:

- In-vessel release of fission products from the fuel,
- Fission product release from the primary system prior to vessel breach,
- Revolatization of deposited iodine, cesium, and tellurium after vessel breach,
- Fission product release from the fuel during concrete attack,
- Fission product release from the containment prior to vessel breach,
- Fission product release from the containment after vessel breach,
- Late iodine revolatization from the suppression pool,
- Late iodine revolatization from the water on the drywell floor,
- Reactor building decontamination factors,
- Fission product release from the fuel due to direct containment heating,
- Suppression pool decontamination factors for releases through the T-quenchers,
- Suppression pool decontamination factors for releases through the downcomers,
- Decontamination factors due to the water on the drywell floor,
- Drywell spray decontamination factors for in-vessel releases,

- Drywell spray decontamination factors for ex-vessel releases, and
- Fission product release due to ex-vessel steam explosions.

Figure B-1 gives the comparison of the PBSOR estimates with STCP results for TC1; this is a ATWS scenario in which the containment fails prior to core melt as a result of excessive steam generation by the core and leads to failure of the emergency core cooling system. The PBSOR median estimates for iodine and cesium are seen to be somewhat above the STCP results, but the agreement is reasonable. The STCP results for tellurium, strontium, and lanthanum lie very near the upper range of the PBSOR estimates. The STCP results for these species were dominated by high corium-concrete interaction releases; the PBSOR results, reflecting the input from the expert panels, indicate these results to be conservative.

Figure B-2 shows the comparison for an ATWS sequence in which the emergency core cooling systems fail prior to containment failure, core melting takes place at high primary system pressure, and containment fails in the drywell following reactor vessel breach. In this case, also, the STCP results for strontium and lanthanum lie near the upper range of the PBSOR estimates.

Figure B-3 is for an ATWS scenario in which containment failure is precluded by venting through the suppression pool. The agreement between PBSOR and STCP is better for this case than the previous ones.

The PBSOR results for a station blackout are compared with STCP results in Figure B-4. In this sequence all AC power is lost, but the steam driven emergency core cooling systems operate until the station batteries are depleted; after that the coolant boils off and the core melts under a high primary system pressure. Containment fails in the drywell during concrete attack; thus at least some of the ex-vessel releases bypass the suppression pool. The results for iodine and cesium are in good agreement. The STCP results for tellurium, strontium, and lanthanum releases are seen to lie near the upper range of the PBSOR estimates. For this scenario the source terms would be sensitive to the specific timing of containment failure relative to the progression of concrete attack. In the STCP analyses for this scenario containment failure was predicted after vessel breach, but coincided with the timing of vigorous attack of the concrete by the core debris.

The PBSOR estimates in Figure B-4 were based on containment failure taking place some time after vessel breach. Figure B-5 compares the same STCP results with a PBSOR run in which containment failure is assumed to take place near the time of vessel breach. The comparison for the iodine and cesium releases is not as favorable in this case, since some of the PBSOR releases now bypass the suppression pool. The results for the less volatile species compare more favorably. These comparisons illustrate the sensitivity of the source term predictions to the timing of containment failure relative to suppression pool bypass.

Figure B-6 shows the results for the same initiating station blackout event as the preceding, but assumes containment failure in the drywell at the time of reactor vessel breach both in the STCP and PBSOR analyses. The

predicted releases are higher than the previous case, with some of the STCP results near the upper range of PBSOR estimates.

Figure B-7 presents the results for a station blackout with no active engineered safety systems; in this case the containment failure was assumed to take place in the wetwell due to long term pressurization. The comparison between PBSOR and STCP results for this case is much more favorable.

The results for the S2E sequence, a small break in the primary system with complete failure of makeup to the primary system, are given in Figure B-8. Containment failure was assumed to take place in the drywell due to buildup of noncondensables. In the STCP calculation for this case the containment was predicted to fail during the time of vigorous corium-concrete interaction, thus leading to the relatively high releases. Figure B-9 compares the same STCP results with a PBSOR calculation assuming early containment failure, rather than late failure as assumed in the foregoing. With the redefined containment failure time the agreement between PBSOR and STCP is much more favorable. This is an illustration of the sensitivity of source term results to the specific timing of containment failure relative to ongoing physical processes.

Figure B-10 shows the results for AE, a large pipe break with complete failure of the emergency core cooling system, and drywell failure during concrete attack. The iodine, cesium, and rubidium results are in good agreement. As in some previous cases, the STCP results for tellurium, strontium, and lanthanum lie near the upper range of the PBSOR estimates. These predictions are sensitive to the specific timing of containment failure relative to progression of concrete attack.

The PBSOR predictions for a number of the cases discussed above gave iodine and cesium releases higher than those obtained with the STCP. These differences can be attributed to the timing of the releases of these species from the fuel. The STCP tends to predict early releases of iodine and cesium during the in-vessel phase of the accident; during this phase the fission products are passed to the suppression pool and undergo effective scrubbing. PBSOR, on the other hand, retains a fraction of these species for release during the ex-vessel phase; the containment may be failed at that time, and the decontamination factors for flow through the downcomers are not as high as those through the T-quenchers.

The strontium and lanthanum releases predicted by PBSOR were in a number of cases significantly lower than those calculated by the STCP. In the STCP analyses containment failure was found to coincide closely with vigorous concrete attack, when the releases of these species were high. The PBSOR median release fractions for these species were generally lower than given by the STCP.

FIGURE B-1
 COMPARISON OF PBSOR
 WITH STOP RESULTS FOR TC1

+ STOP
 TC1

Δ PBSOR
 MED

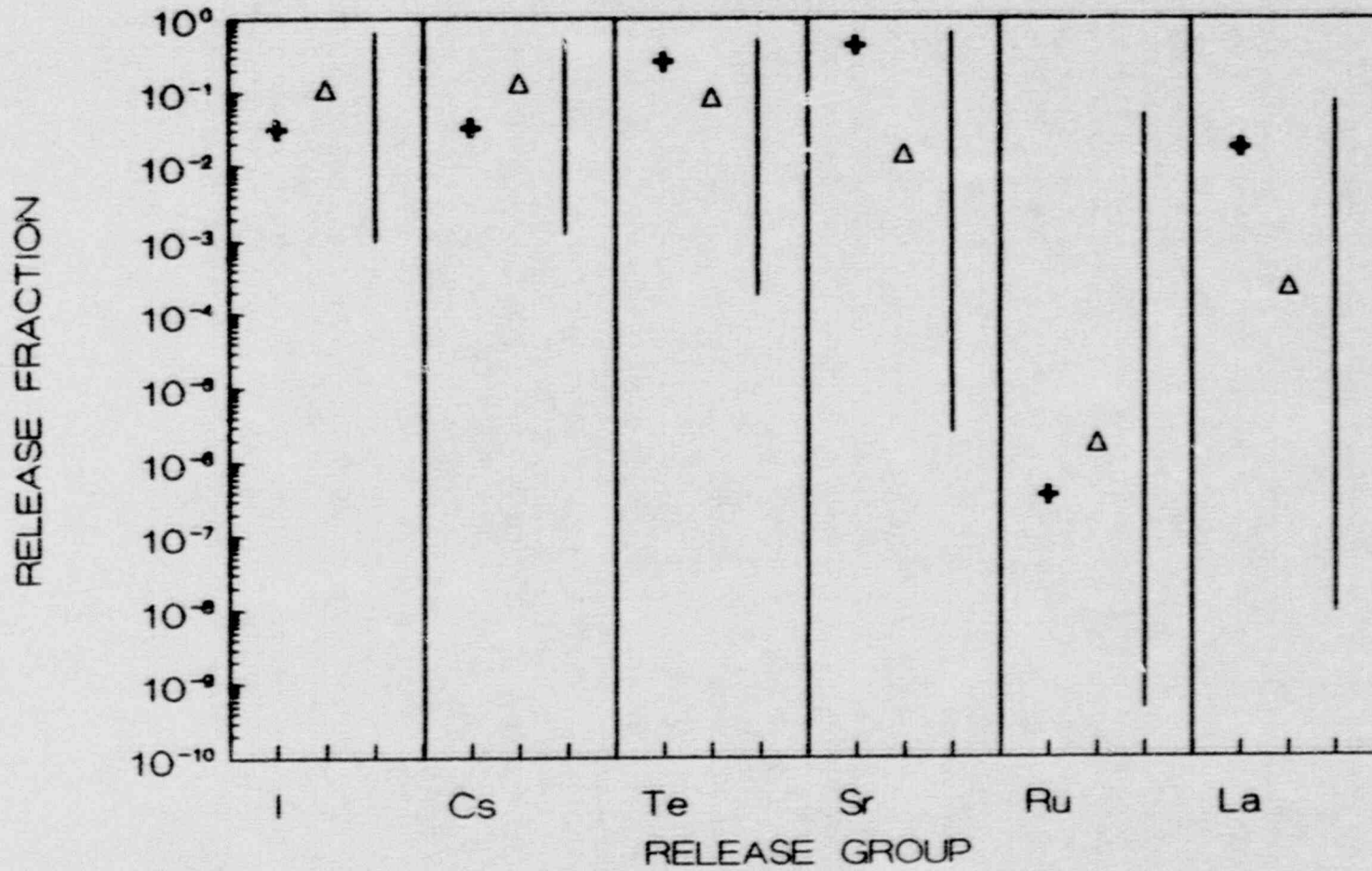


FIGURE B-2
 COMPARISON OF PBSOR
 WITH STOP RESULTS FOR TC2

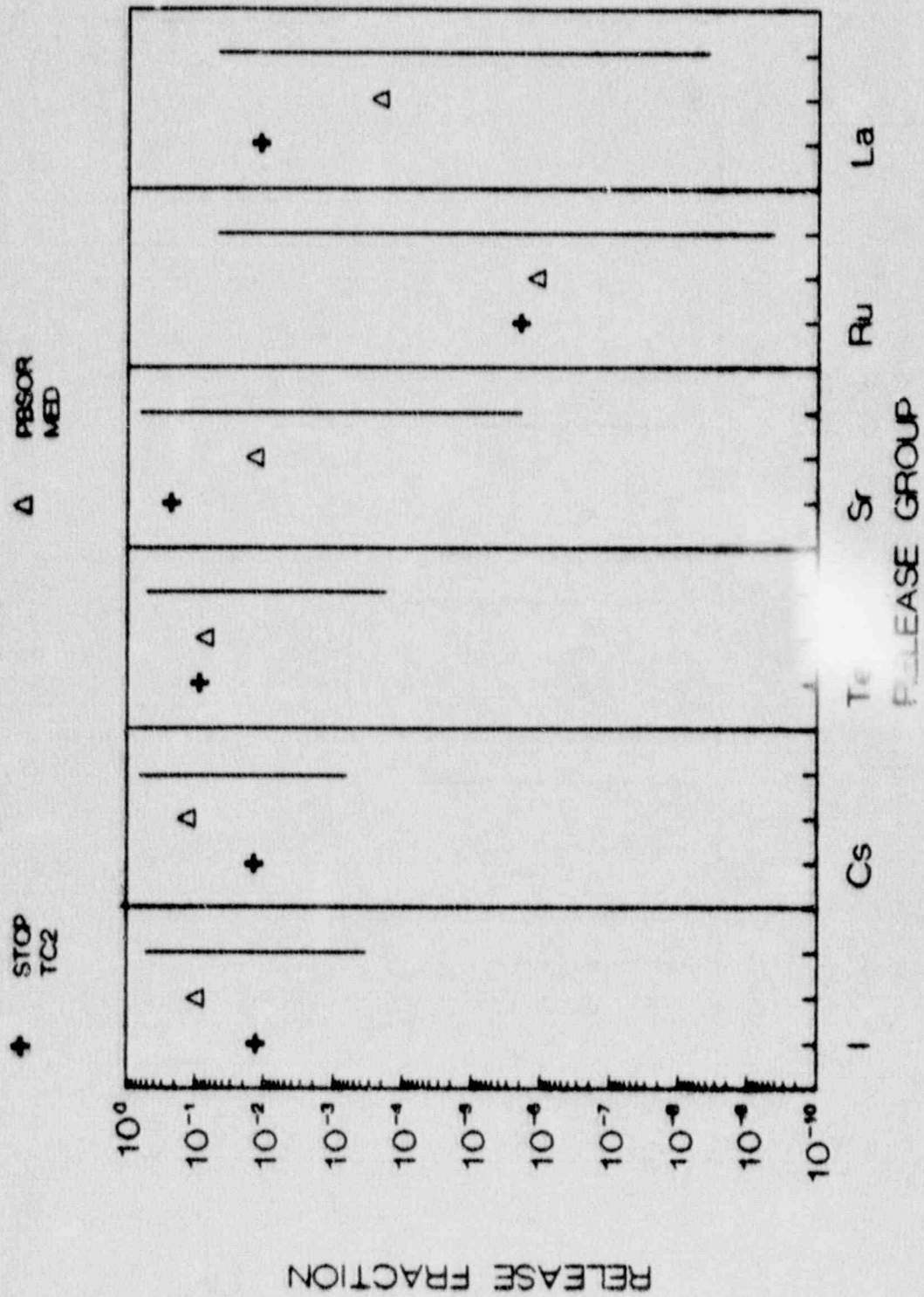


FIGURE B-3
 COMPARISON OF PBSOR
 WITH STCP RESULTS FOR TC3

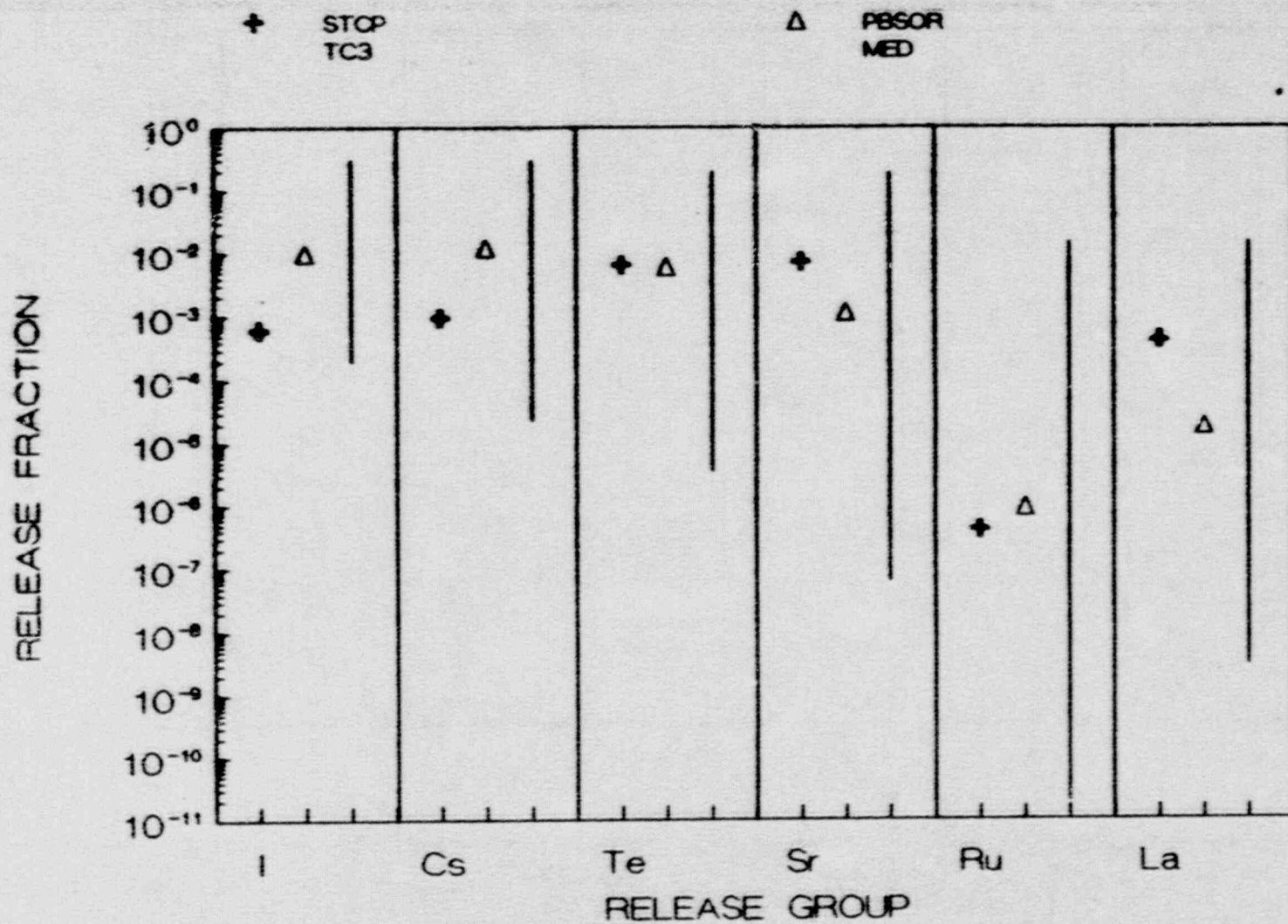


FIGURE B-4
 COMPARISON OF PBSOR
 WITH STOP RESULTS FOR TB1

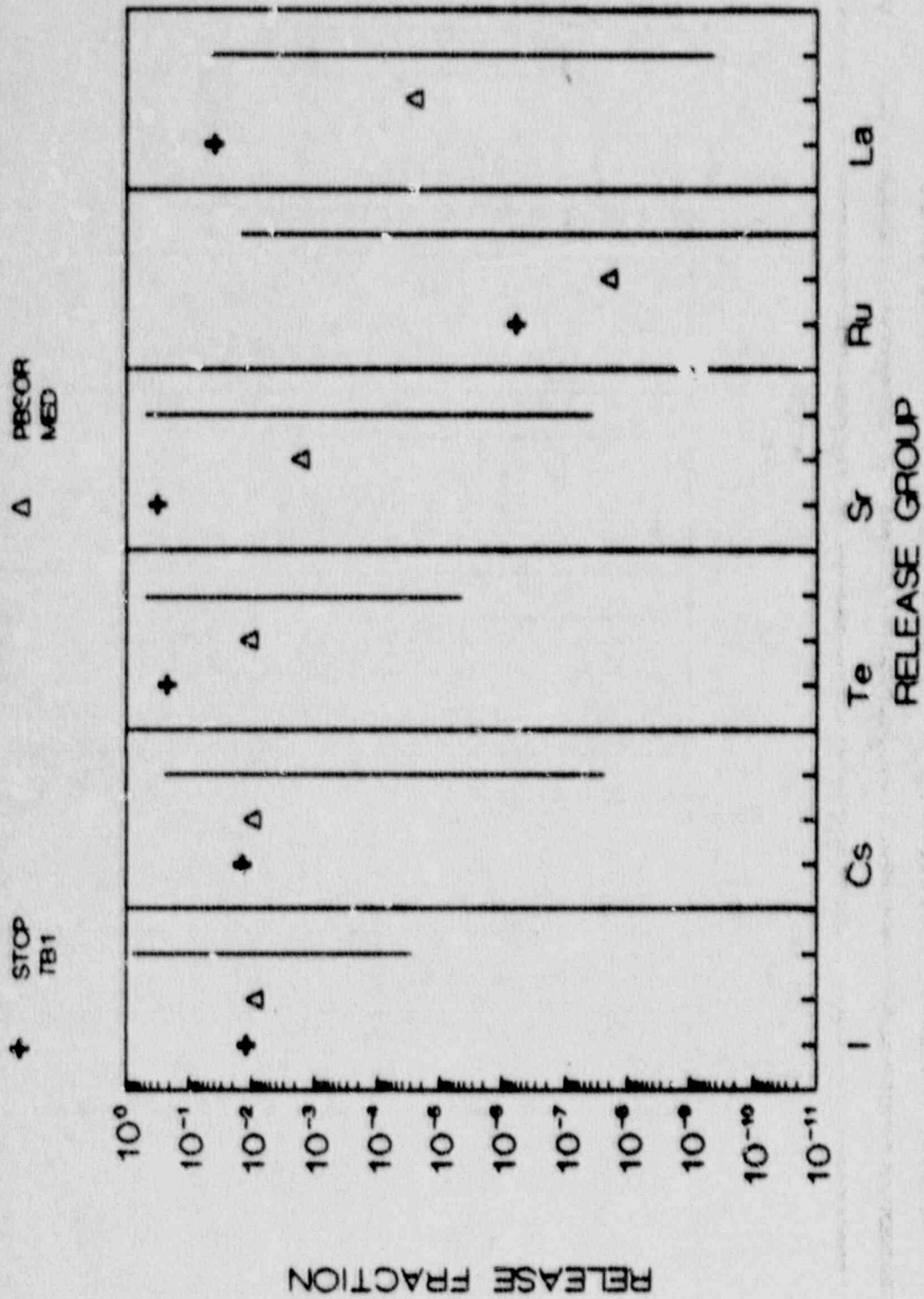


FIGURE B-5
 COMPARISON OF PBSOR
 WITH STOP RESULTS FOR TB1*

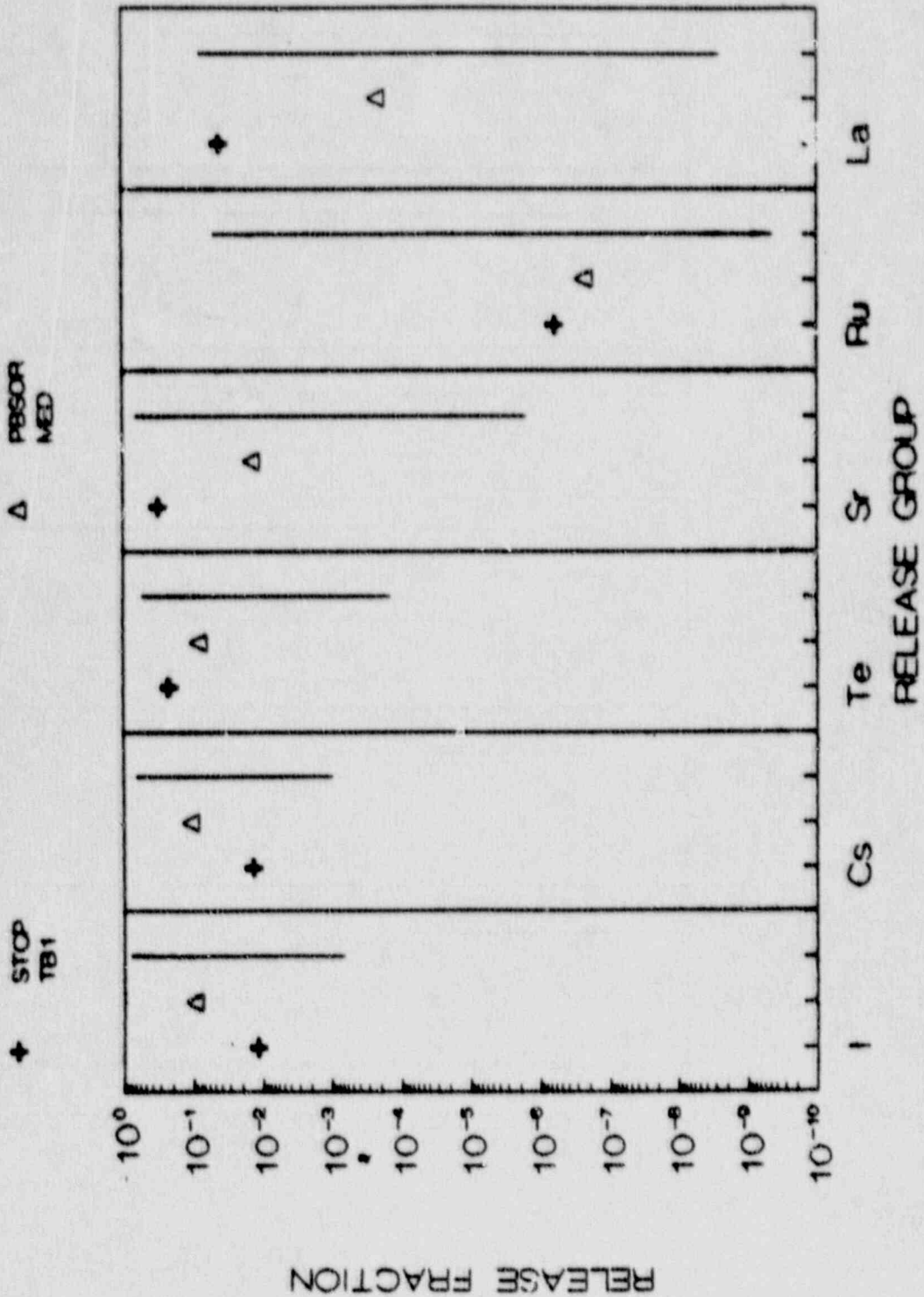


FIGURE B-6
 COMPARISON OF PBSOR
 WITH STOP RESULTS FOR TB2

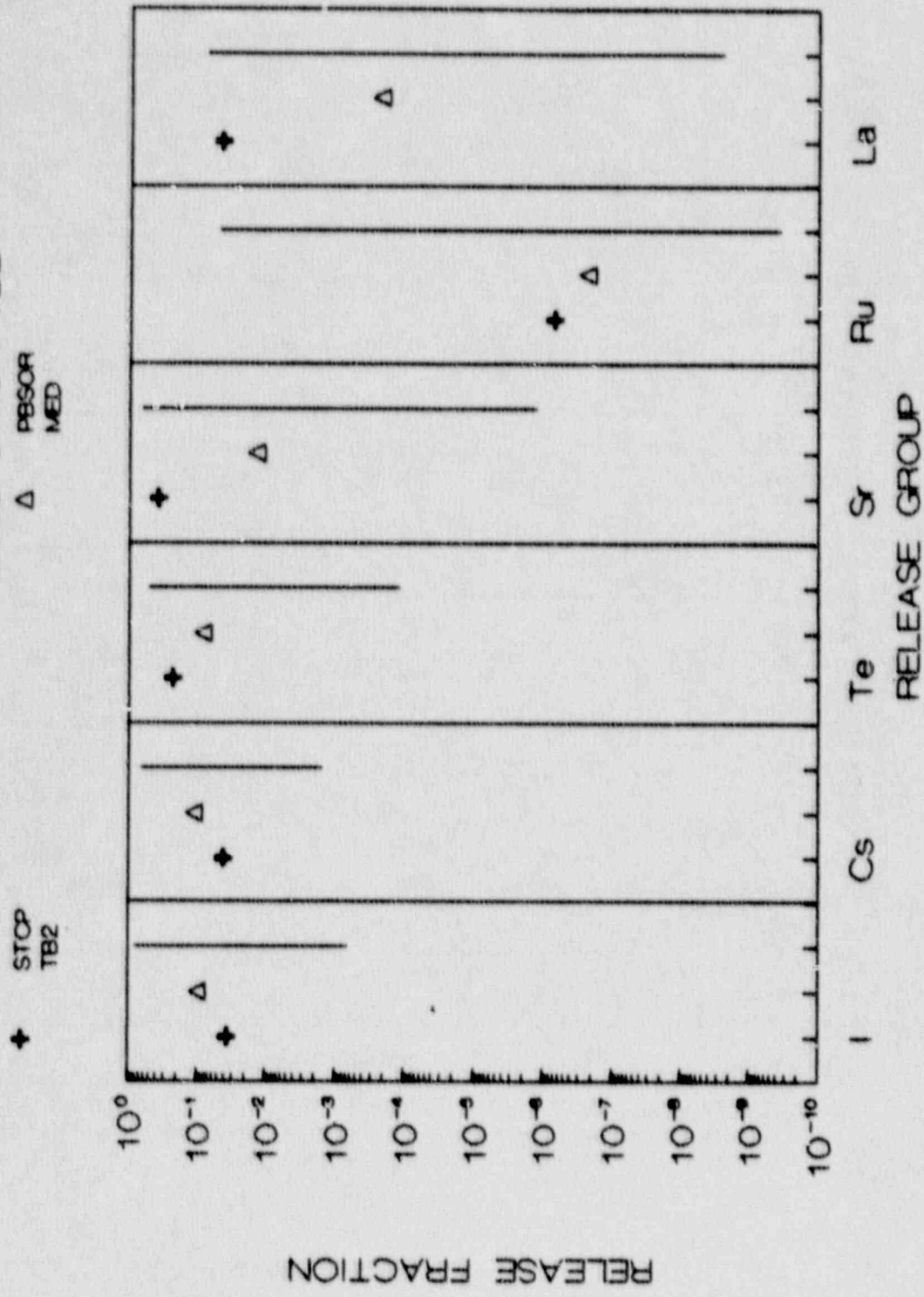


FIGURE B-7
 COMPARISON OF PBSOR
 WITH STOP RESULTS FOR TBUX

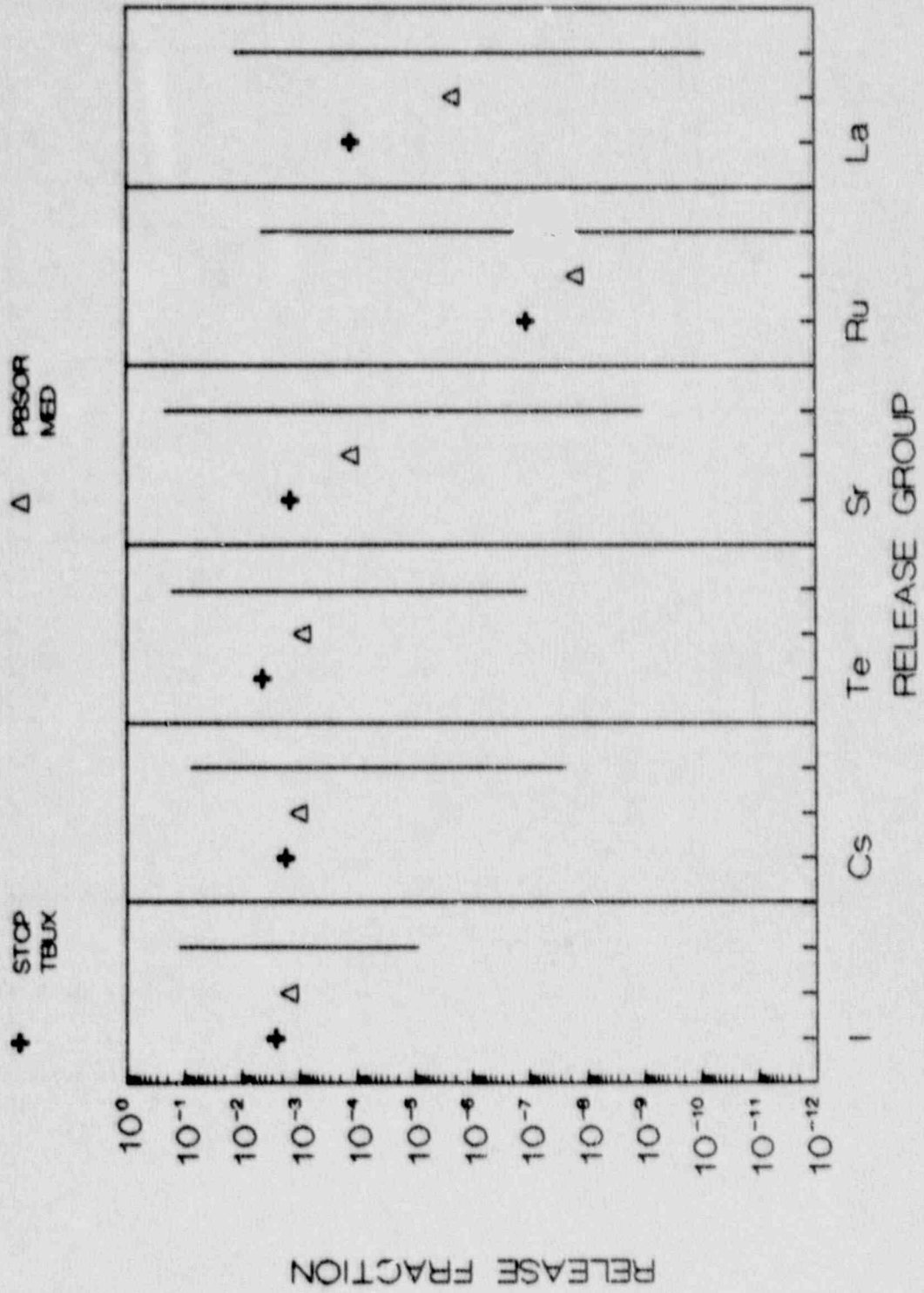


FIGURE B-8
 COMPARISON OF PBSOR
 WITH STCP RESULTS FOR S2E

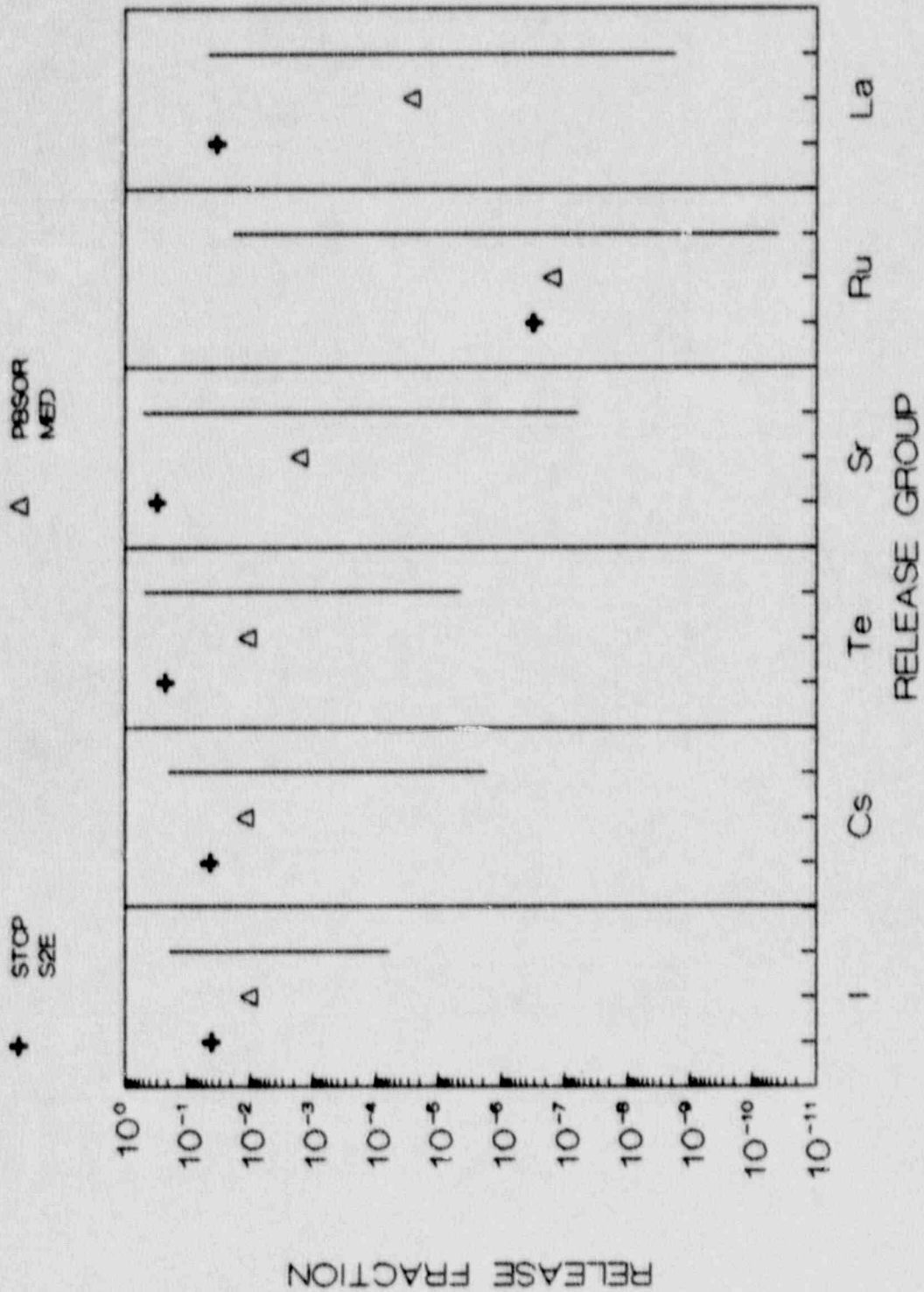


FIGURE B-9
 COMPARISON OF PBSOR
 WITH STOP RESULTS FOR S2E'

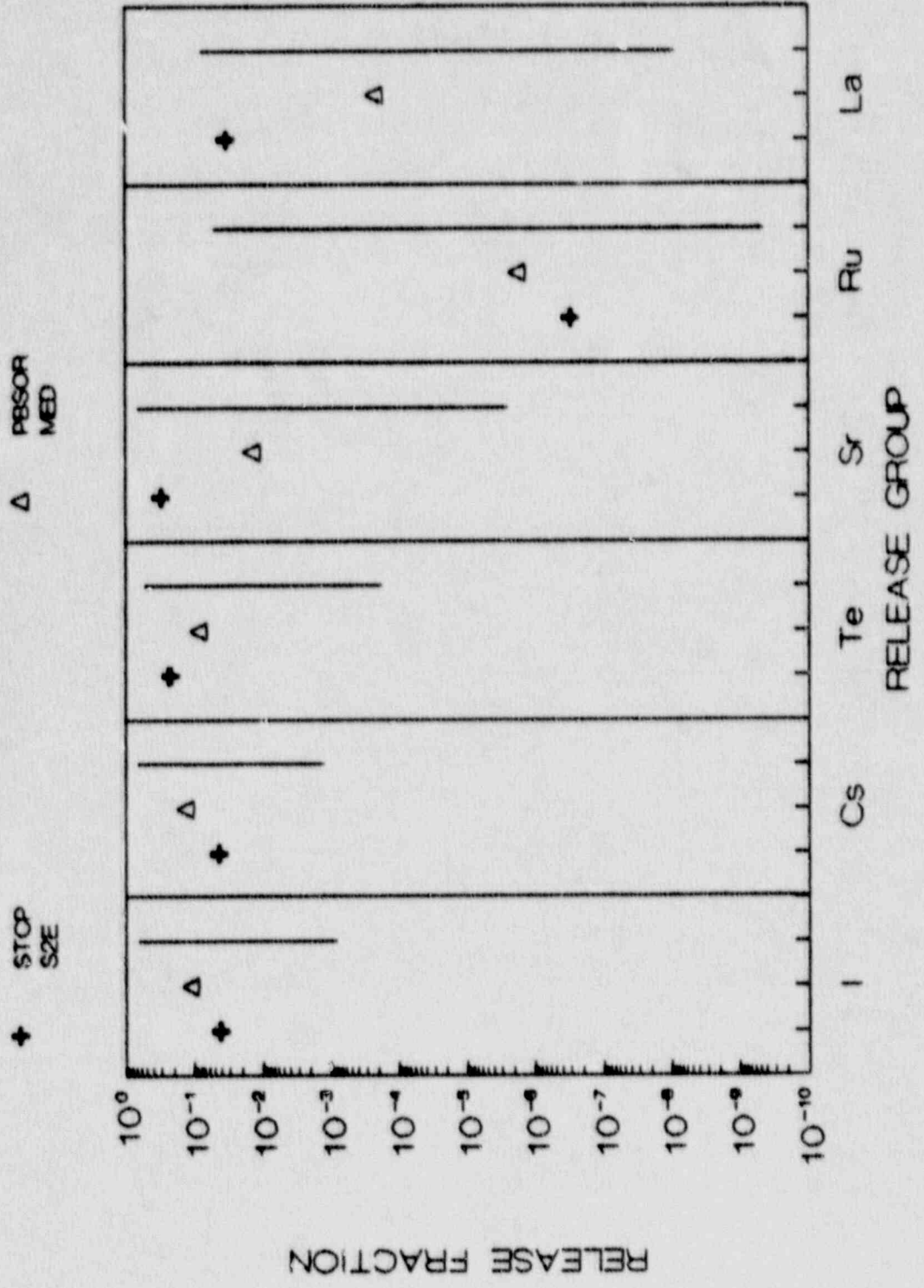
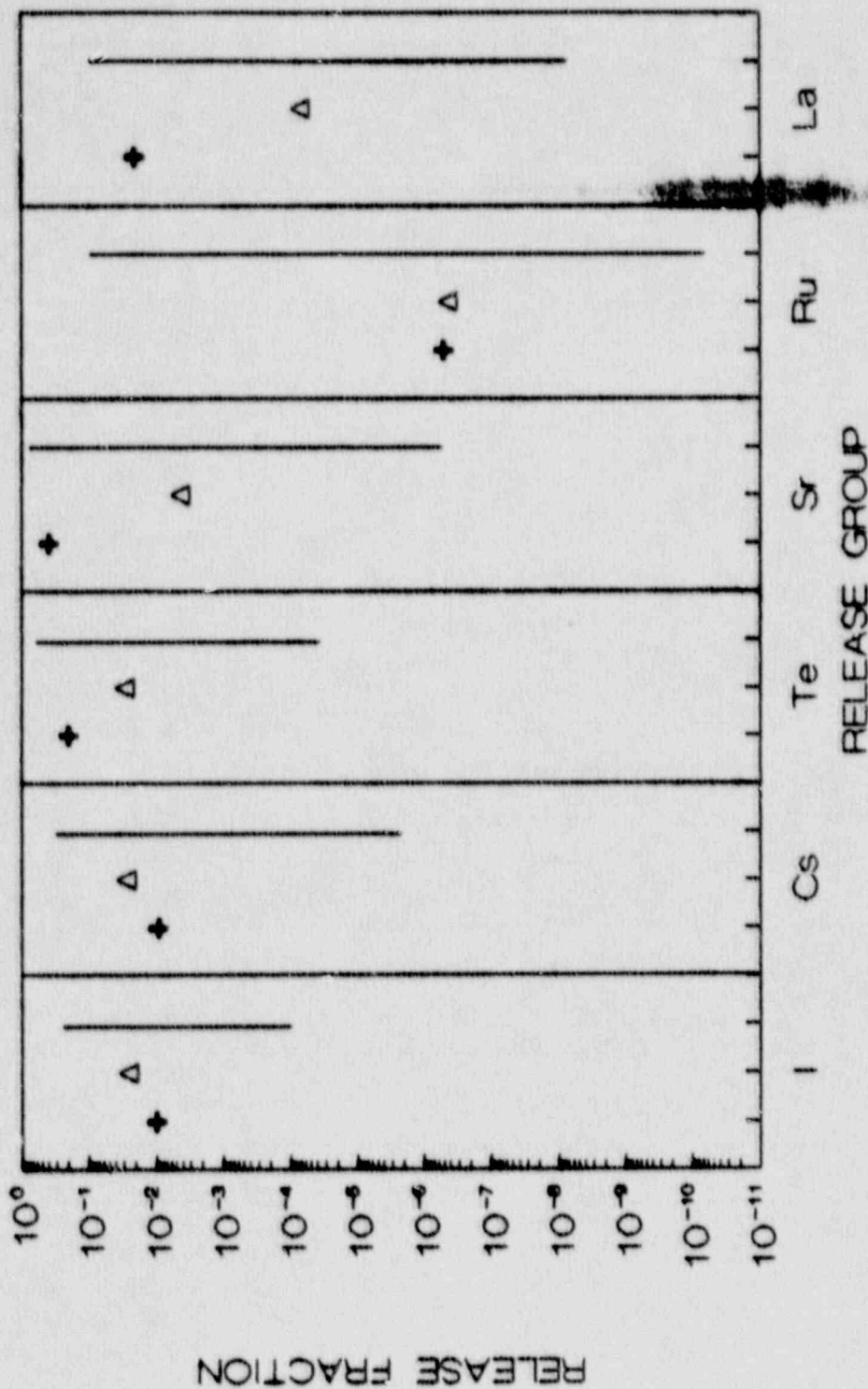


FIGURE B-10
 COMPARISON OF PBSOR
 WITH STOP RESULTS FOR AE



APPENDIX C

COMPARISON OF GGSOR AND STCP RESULTS

APPENDIX C

COMPARISON OF GGSOR AND STCP RESULTS

This appendix presents the comparison between GGSOR, used for the Grand Gulf BWR analyses, and available STCP calculations. The GGSOR formulation did not permit a convenient generation of central estimates; thus the discussion below will compare the STCP results with GGSOR median estimates as well as uncertainty ranges. The GGSOR median and uncertainty estimates are based on the input from the expert panels and take into account model uncertainties as well as a variety of phenomena not considered in the STCP. The specific issues addressed in the GGSOR uncertainty analyses include:

- In-vessel fission product release,
- Release of fission products from the primary system prior to vessel breach,
- Revolatilization of deposited iodine, cesium, and tellurium after vessel breach,
- Fission product release from the fuel during concrete attack,
- Fission product release from the containment prior to vessel breach,
- Fission product release from the containment after vessel breach,
- Revolatilization of iodine from the suppression pool,
- Revolatilization of iodine from the water in the drywell,
- Release of fission products from the fuel due to direct containment heating,
- Decontamination factors for flow through the T-quenchers,
- Decontamination factors for flow through the downcomers,
- Decontamination factors due to the water on the drywell floor,
- Spray decontamination factors for in-vessel releases,
- Spray decontamination factors for ex-vessel releases, and
- Fission product release due to ex-vessel steam explosions.

Figure C-1 shows the comparison for a station blackout in which steam driven emergency core cooling systems function until battery depletion, then

core cooling stops, the core overheats with the primary system at high pressure, and containment failure takes place late due to overpressurization. The GGSOR results for iodine are seen to be well above those of the STCP. This is due to late iodine evolution from the suppression pool and the fact that in GGSOR some of the iodine is released from the fuel during concrete attack; STCP generally predicts complete iodine release in-vessel, with transport to the suppression pool. The latter factor is also apparently the reason for the difference in the cesium results. The other species are in good agreement.

Figure C-2 shows the results for the same initiating event as previous, but with early containment failure. The GGSOR results for iodine and cesium are higher than the STCP calculations because, as noted above, in GGSOR some of their release takes place during concrete attack; in this case in a failed containment. The STCP results for strontium and lanthanum are near the upper range of GGSOR estimates. The expert panels reflected lower releases of the nonvolatile species during concrete attack than are reflected in the STCP modeling.

Figure C-3 shows the results for an early station blackout with no safety systems functioning, and containment failure at the time of vessel breach. The iodine results from GGSOR are higher than those of the STCP for the reasons previously noted. The other results in this case are in more reasonable agreement.

Figure C-4 shows the results for a station blackout in which electric power is restored after core melting, the actuation of the containment sprays leads to a hydrogen burn and subsequent containment failure. Again, the GGSOR iodine result is higher than the STCP calculation, reflecting consideration of iodine revolatilization. The other species are in reasonable agreement.

Figure C-5 gives the results for an ATWS scenario in which containment failure precedes core melting, due to excessive steaming to the suppression pool, and the primary system is depressurized. The GGSOR results for iodine, cesium, and tellurium are well above those of the STCP. In the STCP essentially all of the iodine and cesium are released in-vessel, prior to pool bypass taking place; in GGSOR a significant fraction of these releases takes place ex-vessel, when suppression pool bypass has increased.

Figure C-6 gives the results for an ATWS scenario in which containment failure precedes core melting, but where the primary system remains at high pressure. The STCP results for this case were obtained with an early version in which only three of the fission product species were explicitly tracked. Also, in these early STCP calculations, suppression pool bypass was not considered. Thus the STCP results are significantly below those of GGSOR.

Figure C-7 gives the results for a scenario in which containment heat removal is lost and containment fails prior to core melting. The STCP results are from an early version with only three of the fission product groups explicitly tracked. In this early STCP calculation suppression pool bypass was not considered. In the STCP calculation all the cesium and iodine are released in-vessel and transported to the suppression pool to be scrubbed; in GGSOR

some of the releases of these species take place ex-vessel when pool scrubbing is not as effective, and when some pool bypass may take place. Thus the large differences in the two sets of results.

Figure C-8 shows the results for a scenario in which all makeup to the primary system is lost, the primary system is depressurized, and containment failure takes place late in the sequence. The STCP results are from an early version with only three of the species tracked, and without consideration of suppression pool bypass. The previously noted differences in modeling would apply in this case also.

The GGSOR predictions for iodine and cesium releases were generally higher than the corresponding STCP calculations. The reasons for these differences are the same as for PBSOR, and relate to the timing of the release of these species from the fuel relative to the timing of vessel breach.

FIGURE C-1.
COMPARISON OF GGSOR
WITH STCP RESULTS FOR TB1

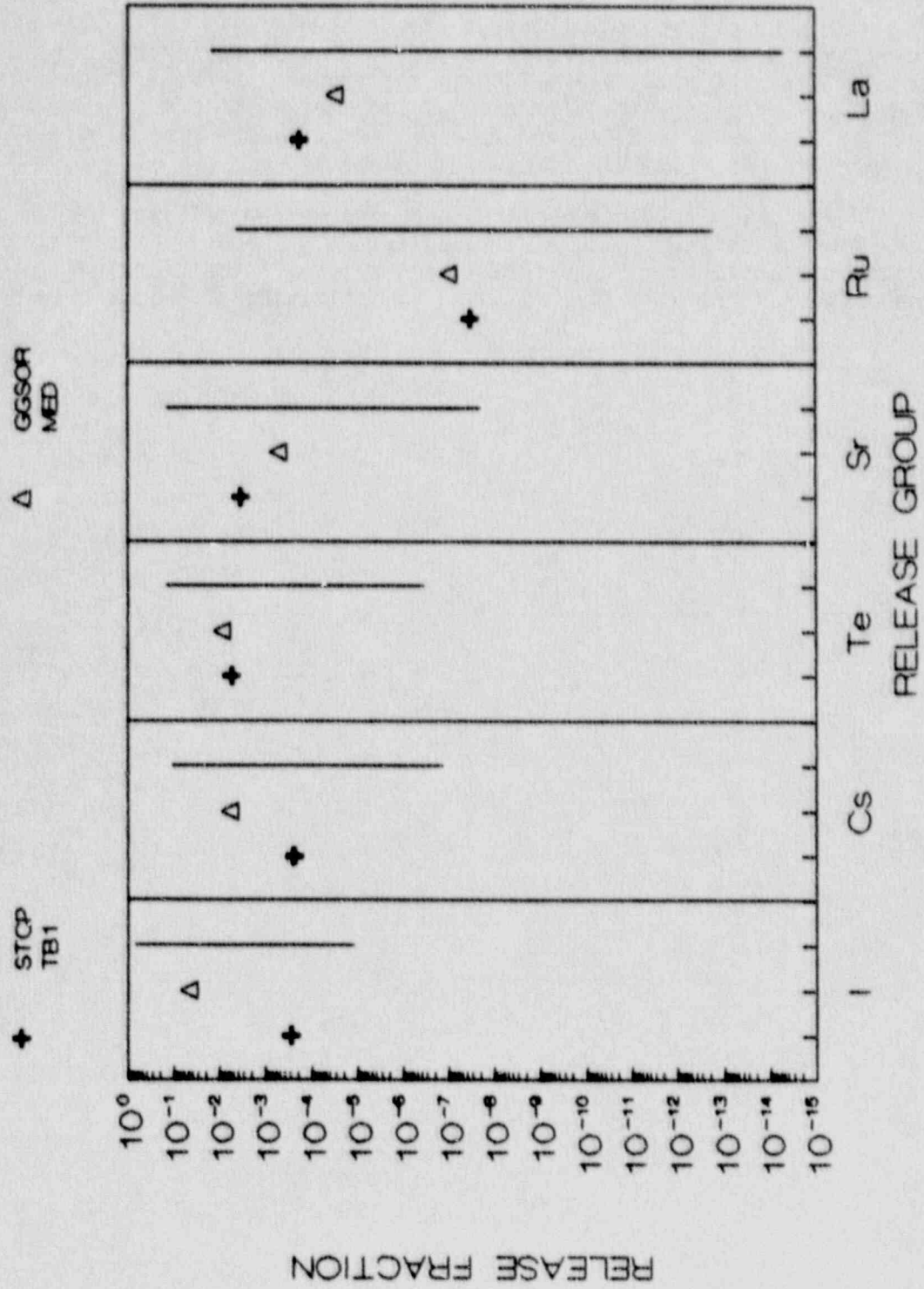
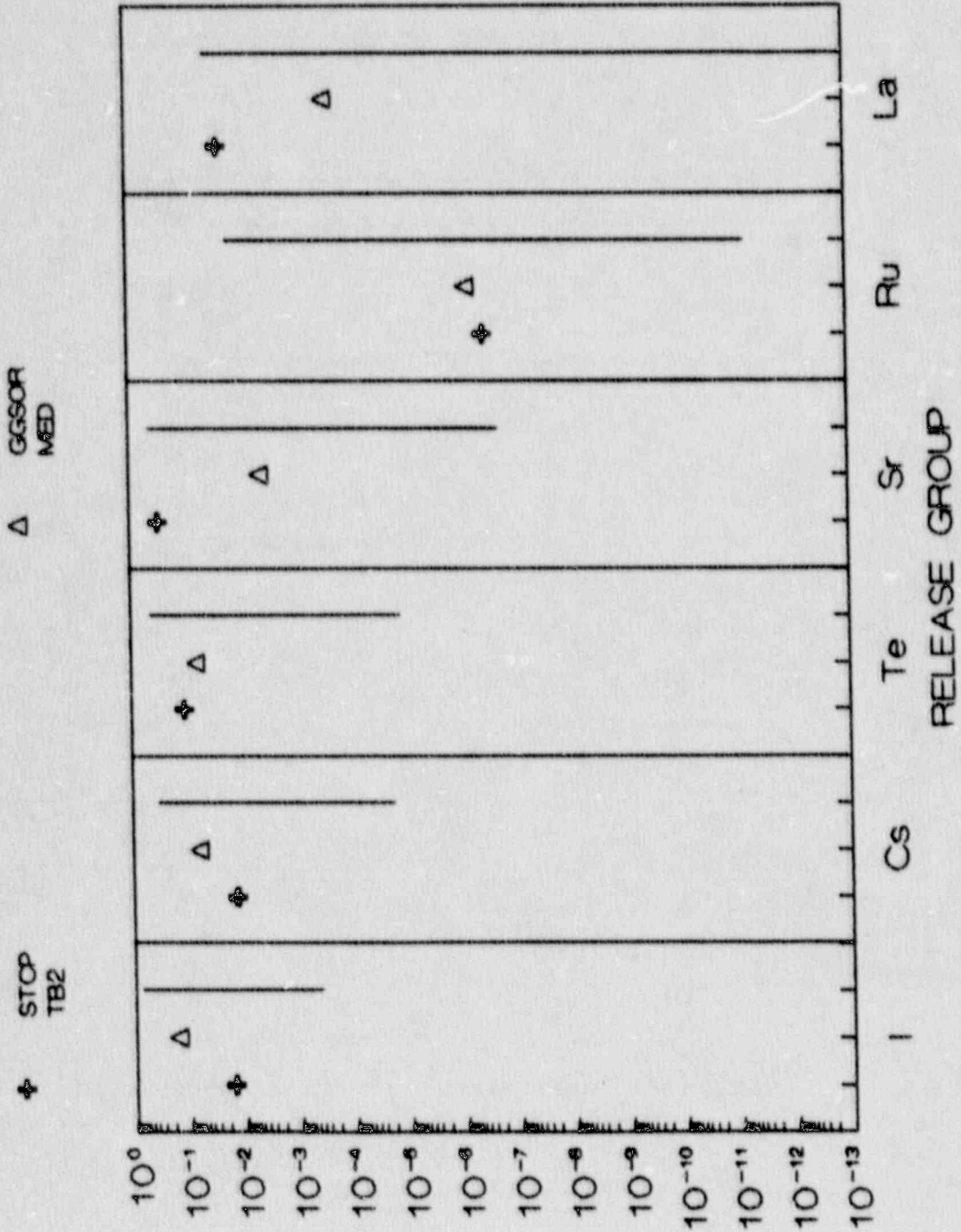


FIGURE C-2
 COMPARISON OF GGSOR
 WITH STOP RESULTS FOR TB2



RELEASE FRACTION

FIGURE C-3
 COMPARISON OF GGSOR
 WITH STOP RESULTS FOR TBS

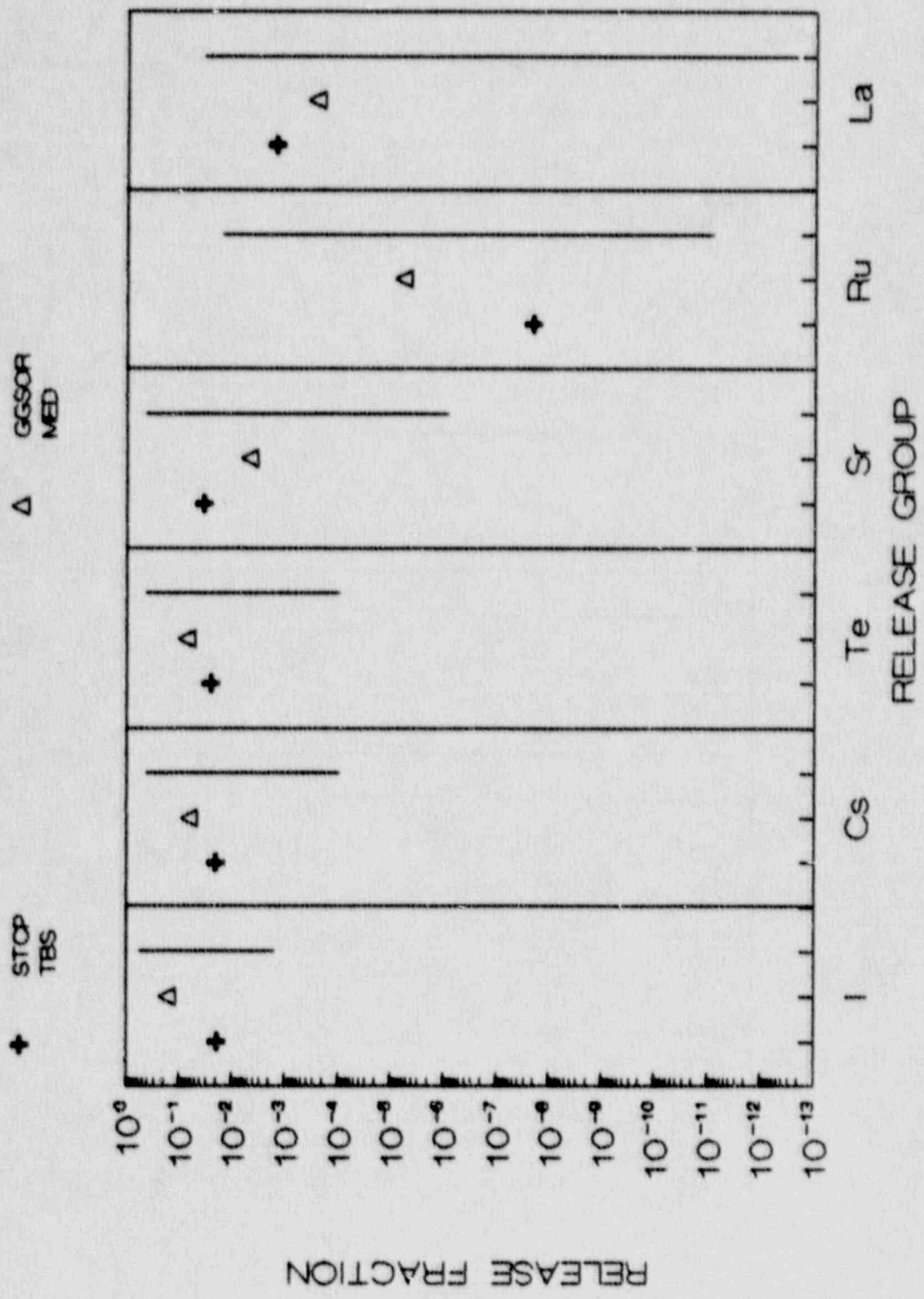


FIGURE C-4
 COMPARISON OF GGSOR
 WITH STOP RESULTS FOR TBR

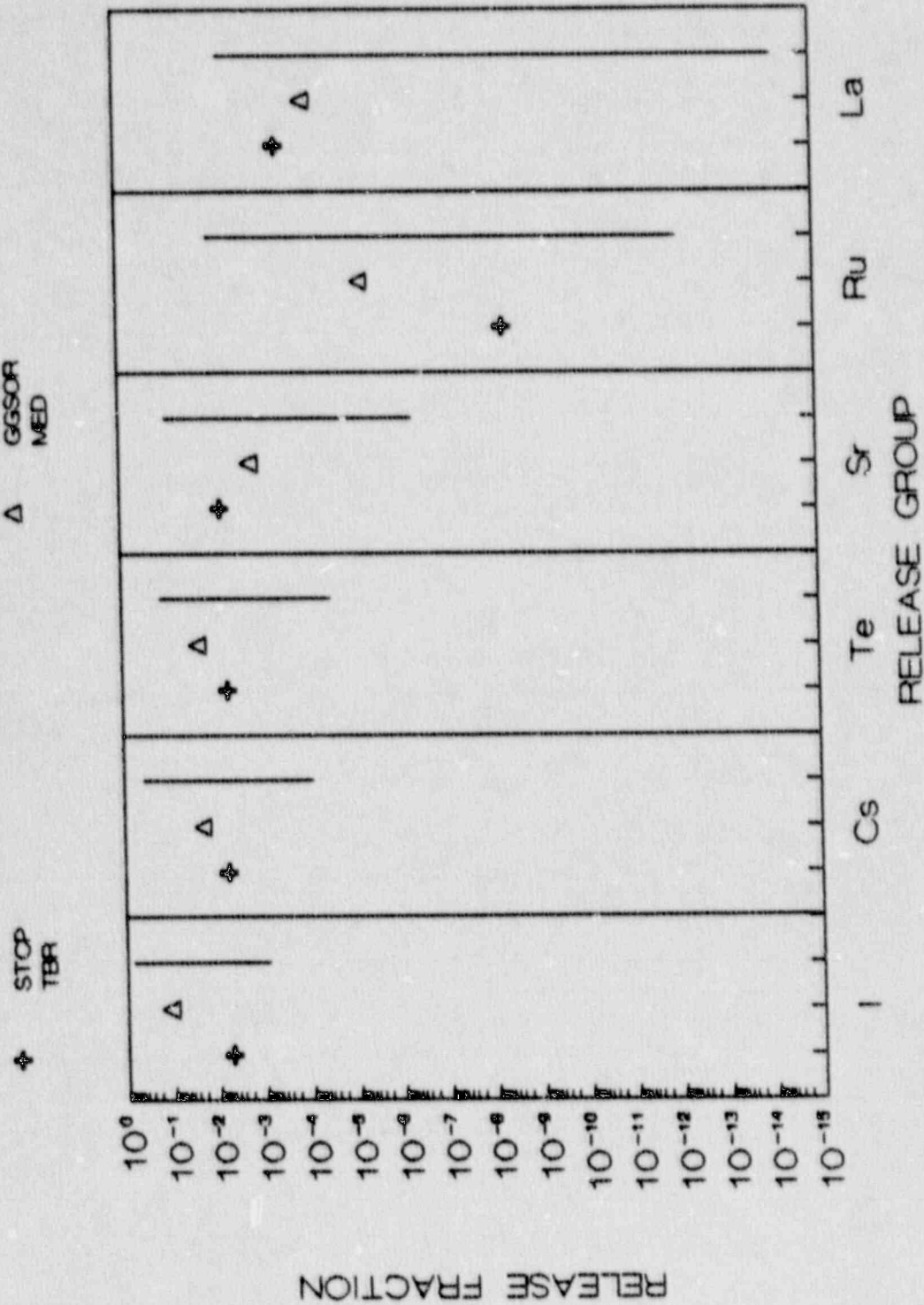


FIGURE C-5
COMPARISON OF GGSOR
WITH STOP RESULTS FOR TC

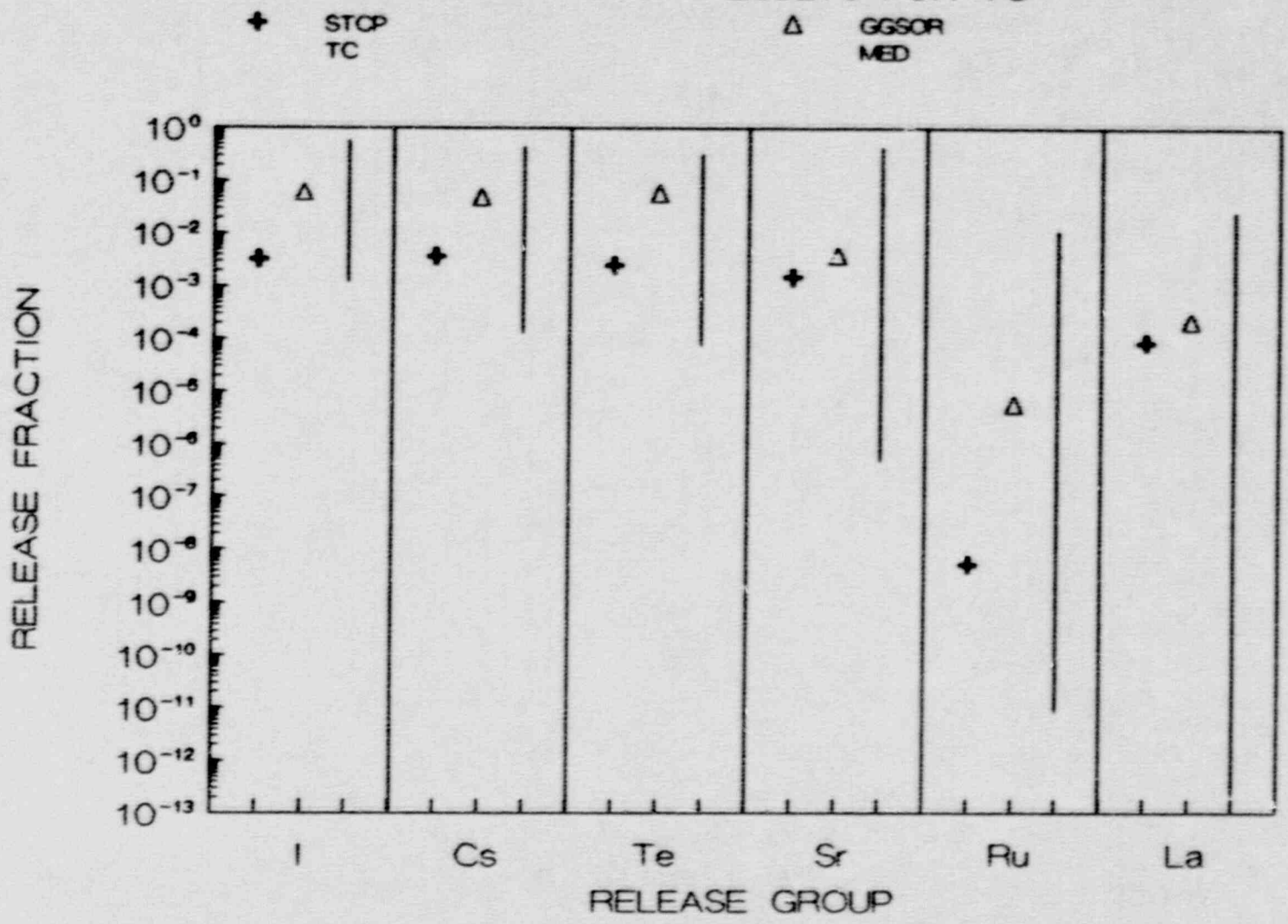


FIGURE C-6
 COMPARISON OF GGSOR
 WITH STOP RESULTS FOR TC1

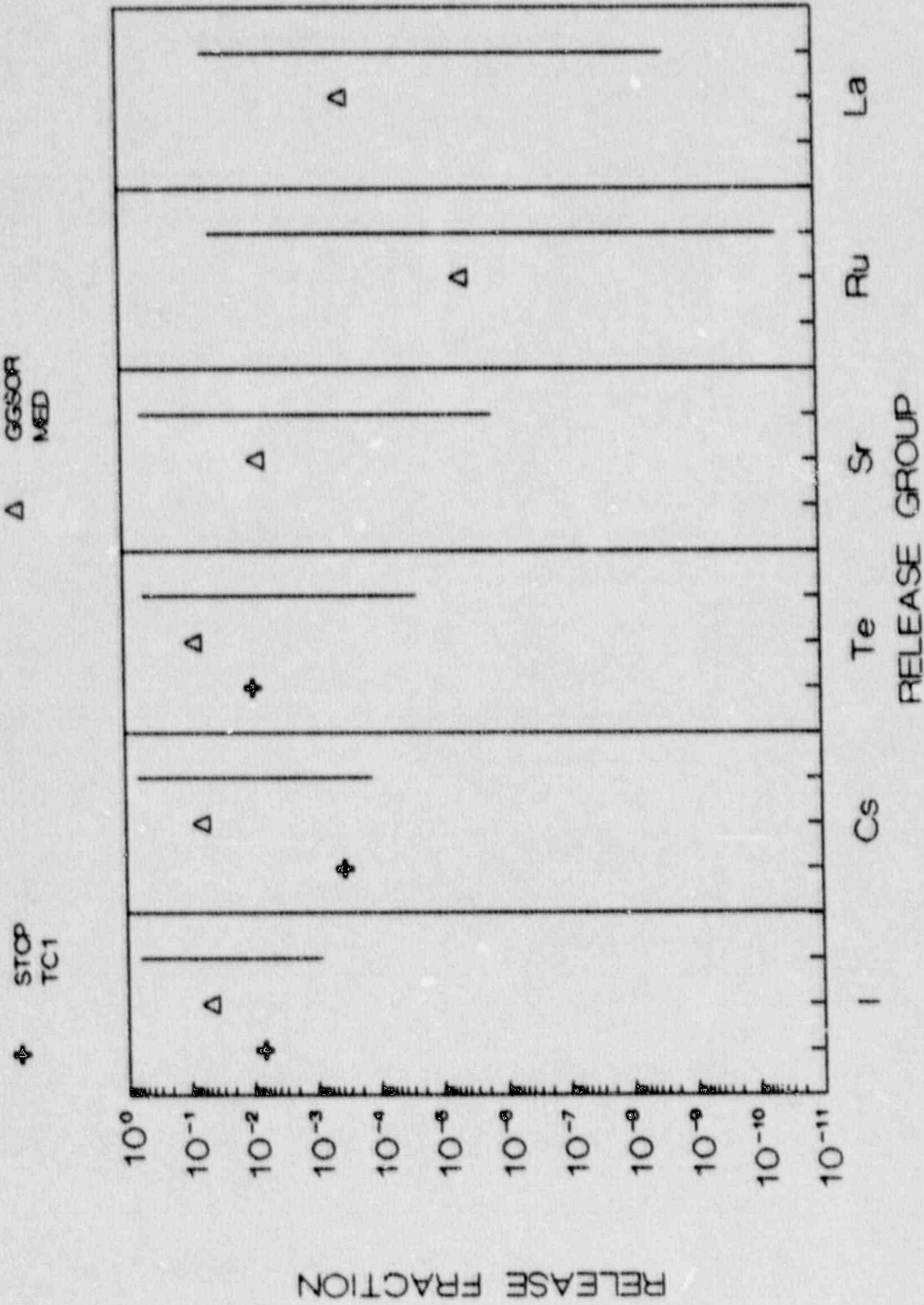


FIGURE C-7
 COMPARISON OF GGSOR
 WITH STOP RESULTS FOR TPI

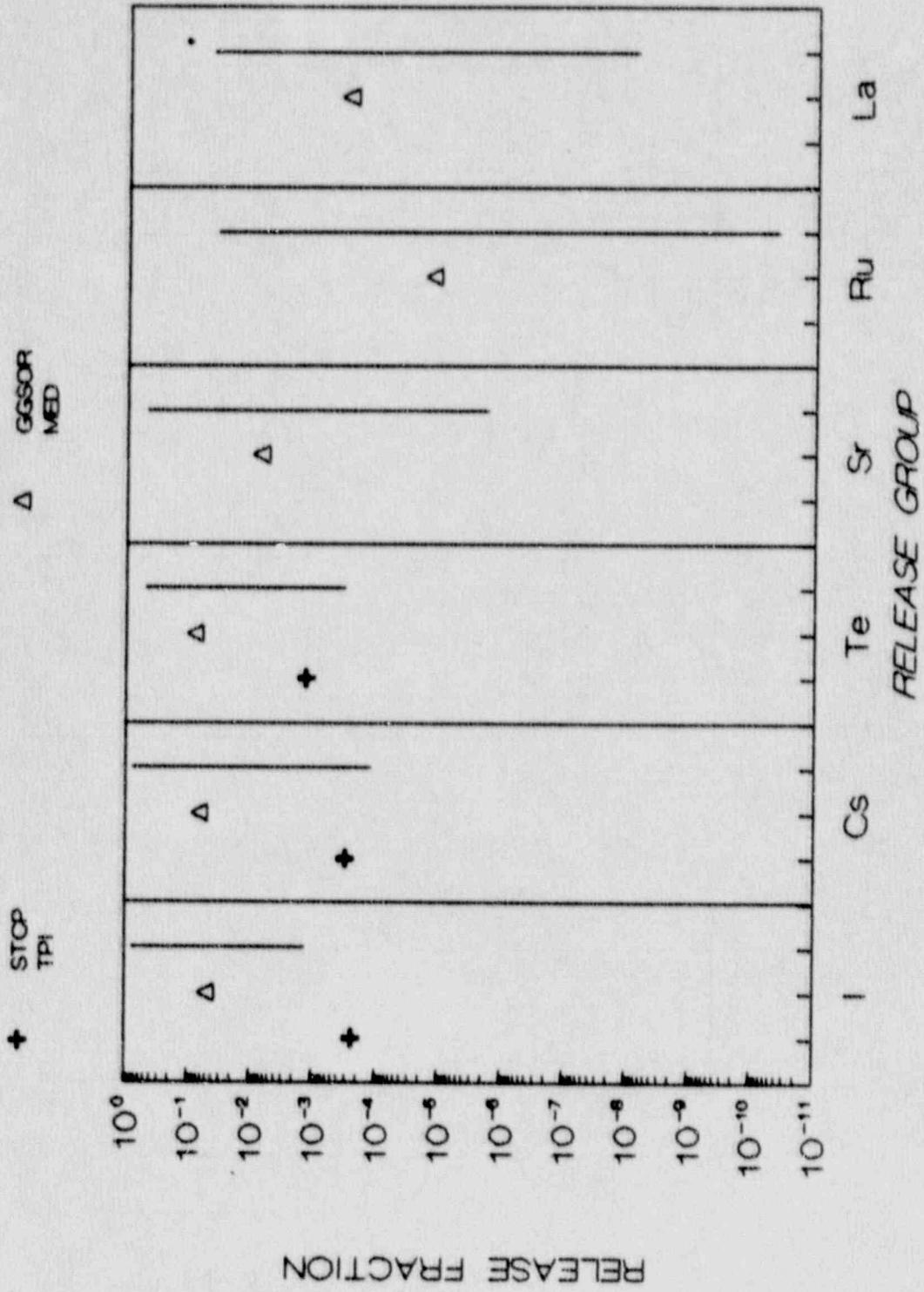
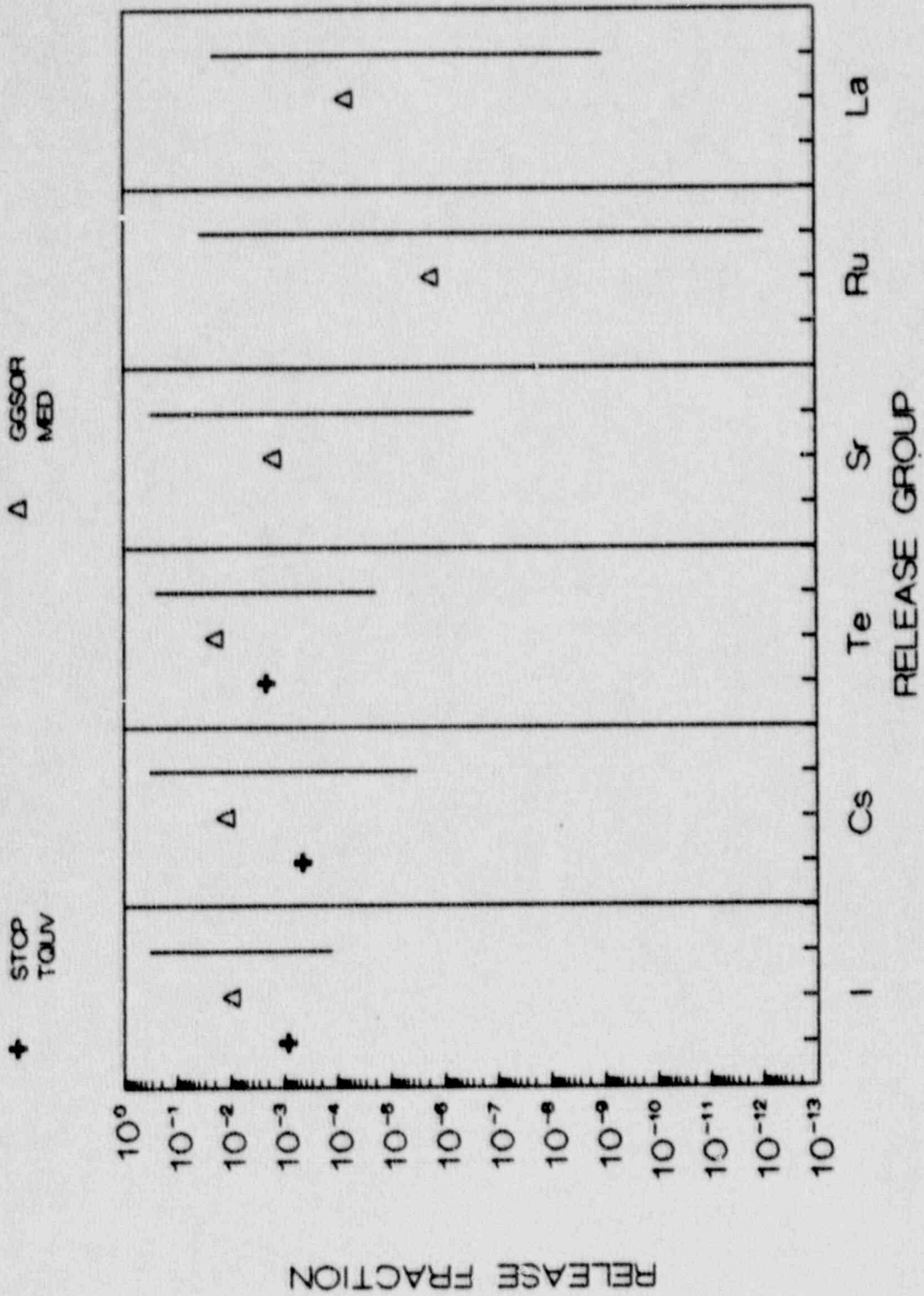


FIGURE C-8
 COMPARISON OF GGSOR
 WITH STOP RESULTS FOR TQUV



APPENDIX D

COMPARISON OF ZISOR AND STCP RESULTS

APPENDIX D

COMPARISON OF ZISOR AND STCP RESULTS

This appendix presents the comparison between ZISOR predictions and the available STCP calculations for the Zion plant. Figures D-1 through D-8 compare the STCP results with ZISOR central and median estimates, as well as showing the range of ZISOR estimates considering uncertainties. The central estimates are based on parameters derived from available STCP calculations. The ZISOR median and uncertainty estimates include input from the expert review panels and take into account uncertainties in the models as well as a variety of phenomena not included in the STCP. The specific issues addressed in the uncertainty quantification included:

- In-vessel fission product release from the fuel,
- Release of fission products from the primary system,
- Decontamination factors for interfacing systems loss-of-coolant-accidents with a submerged path,
- Release of fission products from the containment prior to vessel breach,
- Fission product release from the fuel during concrete attack,
- Release of fission products from containment after vessel breach,
- Containment spray decontamination factors,
- Late iodine release from containment,
- Revolatilization of fission products initially deposited in the primary system,
- Fission product release due to direct containment heating,
- Fission product release through steam generator tube ruptures, and
- Decontamination factors due to water in the reactor cavity.

Figure D-1 shows the comparison for S2DCR-delta, an accident initiated by a small break in the primary system and accompanied by the failure of the emergency core cooling system, the containment sprays operate initially but fail on switchover to recirculation, the containment coolers fail at vessel breach, and containment failure takes place by long term overpressurization. The ZISOR results for iodine and cesium are well above the STCP calculation. The differences appear to be associated with the previously noted differences in the timing of the release of these species. STCP predicts essentially

complete release of these species during the in-vessel phase of the accident; in this scenario the sprays and coolers would attenuate such early releases. ZISOR, as well as the other parametric codes, retain a significant fraction of these species for release ex-vessel; in this case all the safety features are failed by that time. The difference in the iodine releases is also influenced by the consideration of late iodine revolatilization in ZISOR.

Figure D-2 shows the comparison for S2DCF-gamma, an accident initiated by a small break in the primary system and accompanied by failure of the emergency core cooling system, both the containment sprays and coolers are failed, with containment failure taking place at vessel breach. The agreement among the results for this case is quite reasonable, with some scatter in the predicted releases of the less volatile species.

Figure D-3 shows the comparison for S2DCF-delta, the same initiating event as the previous, but with containment assumed to fail by late overpressurization. The agreement among the results for this case is quite good.

Figure D-4 presents the results for TMLU-gamma, a transient in which all makeup to the primary and secondary systems is lost, the containment sprays operate, and containment fails at vessel breach due to a large hydrogen burn or other energetic event. The ZISOR iodine and cesium releases are above those of the STCP because of the previously noted differences in the timing of the release of these species.

Figure D-5 gives the comparison for TMLB-epsilon, a station blackout with containment failure by basemat meltthrough. The STCP results for this case were obtained with an early version. With the exception of iodine, these early STCP results lie above the ZISOR estimates. The ZISOR containment attenuation of aerosols appears to be greater than that in this early version of the STCP. In the case of iodine, consideration of late iodine revolatilization by ZISOR leads to the higher predicted release.

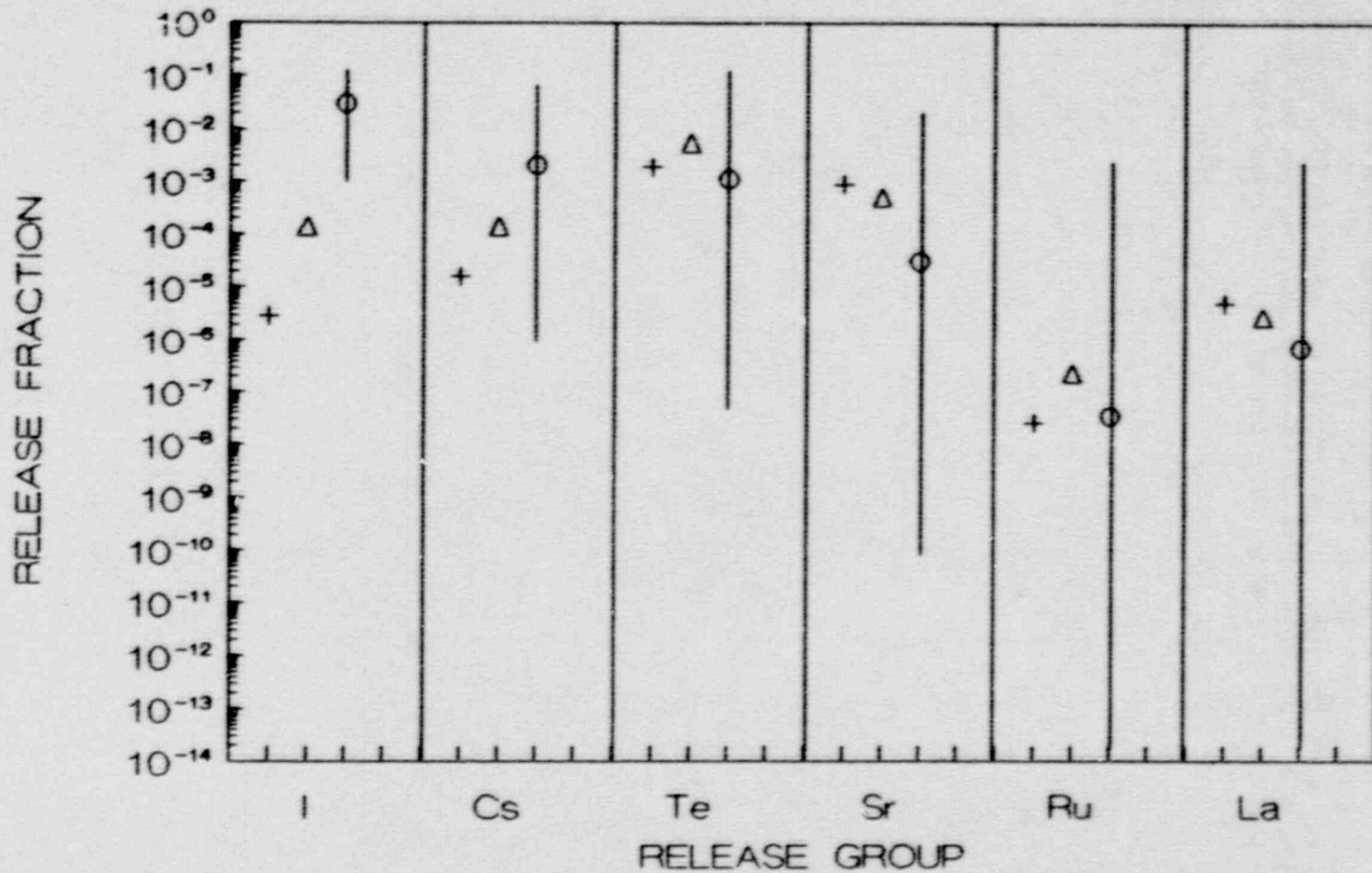
Figure D-6 shows the results for TMLB-leak-before-break, a station blackout in which containment fails by leakage taking place following vessel breach. The STCP results for this case were obtained with an early version, with only three of the species explicitly tracked. The ZISOR estimates for iodine and cesium are well above those of the STCP. The reason here is again the difference in the timing of these releases. In ZISOR a fraction of the releases of iodine and cesium from the fuel take place after vessel breach, when containment leakage has been started. In the STCP essentially all the iodine and cesium are predicted to be released from the fuel early, with some opportunity for attenuation before containment leakage. Also, the STCP calculation gave higher primary system retention than the ZISOR estimates.

Figure D-7 shows the results for TMLB-beta, a station blackout with failure of the containment to isolate. The ZISOR estimates for iodine and cesium are above those of the STCP. Since the containment is leaking from the start of the event in this case, the differences in iodine and cesium releases appear to be related to differences in primary system retention.

Figure D-8 shows the comparison for S2D-epsilon, a small break loss-of-coolant-accident accompanied by failure of the emergency core cooling system, the containment sprays are operating, and containment fails by basement meltthrough. The STCP results for this case are from an early version with only three of the species explicitly tracked. The ZISOR results for iodine release are well above those of the STCP, largely due to the consideration of late iodine volatilization. The cesium and tellurium results are more comparable.

FIGURE D-1
 COMPARISON OF ZISOR WITH STOP
 RESULTS FOR S2DCR-delta

+ STOP S2DCR Δ ZISOR CENTRAL O ZISOR MEDIAN



D-4

FIGURE D-2
 COMPARISON OF ZISOR WITH STOP
 RESULTS FOR S2DCF-gamma

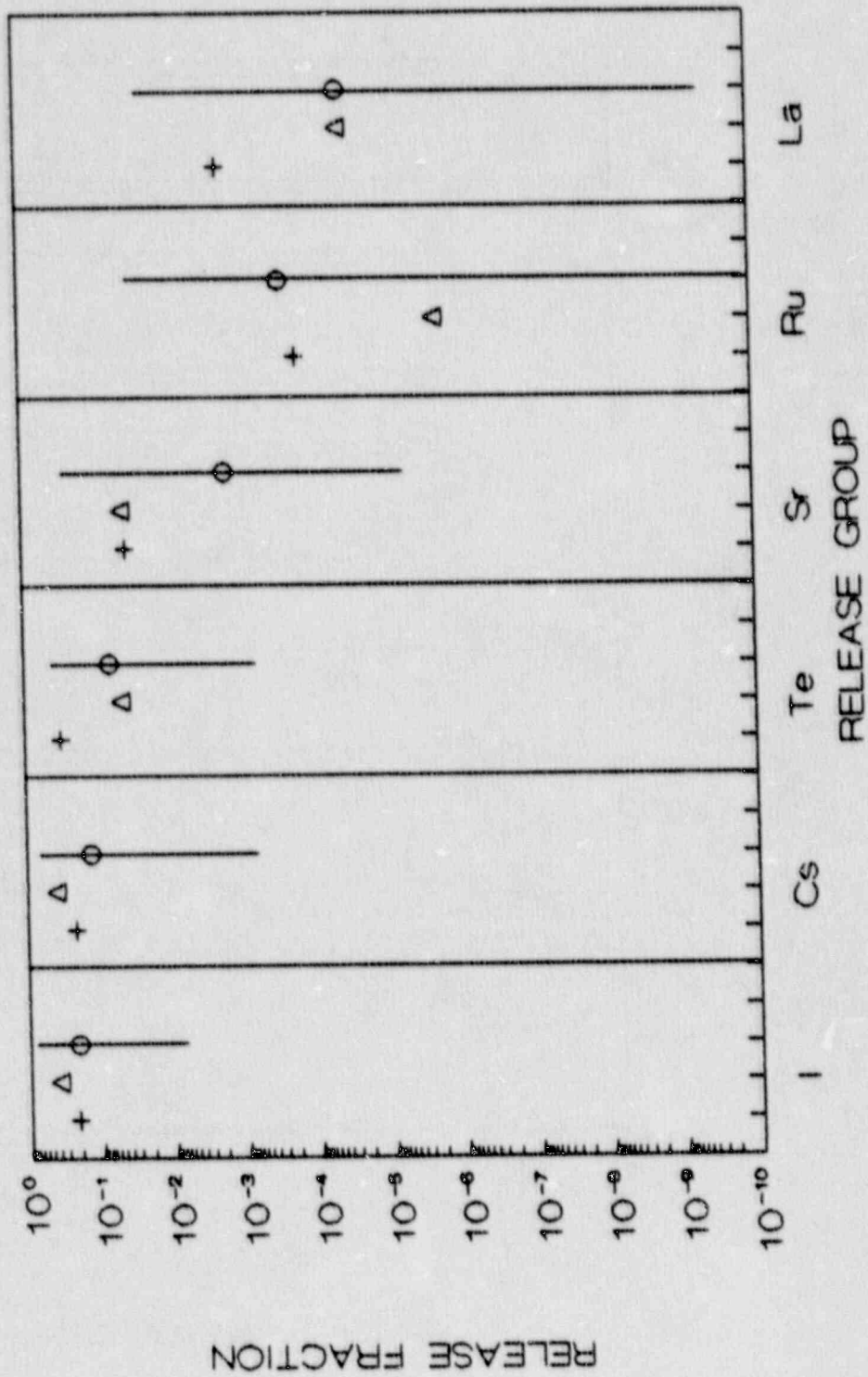


FIGURE D-3
 COMPARISON OF ZISOR WITH STOP
 RESULTS FOR S2DCF-delta

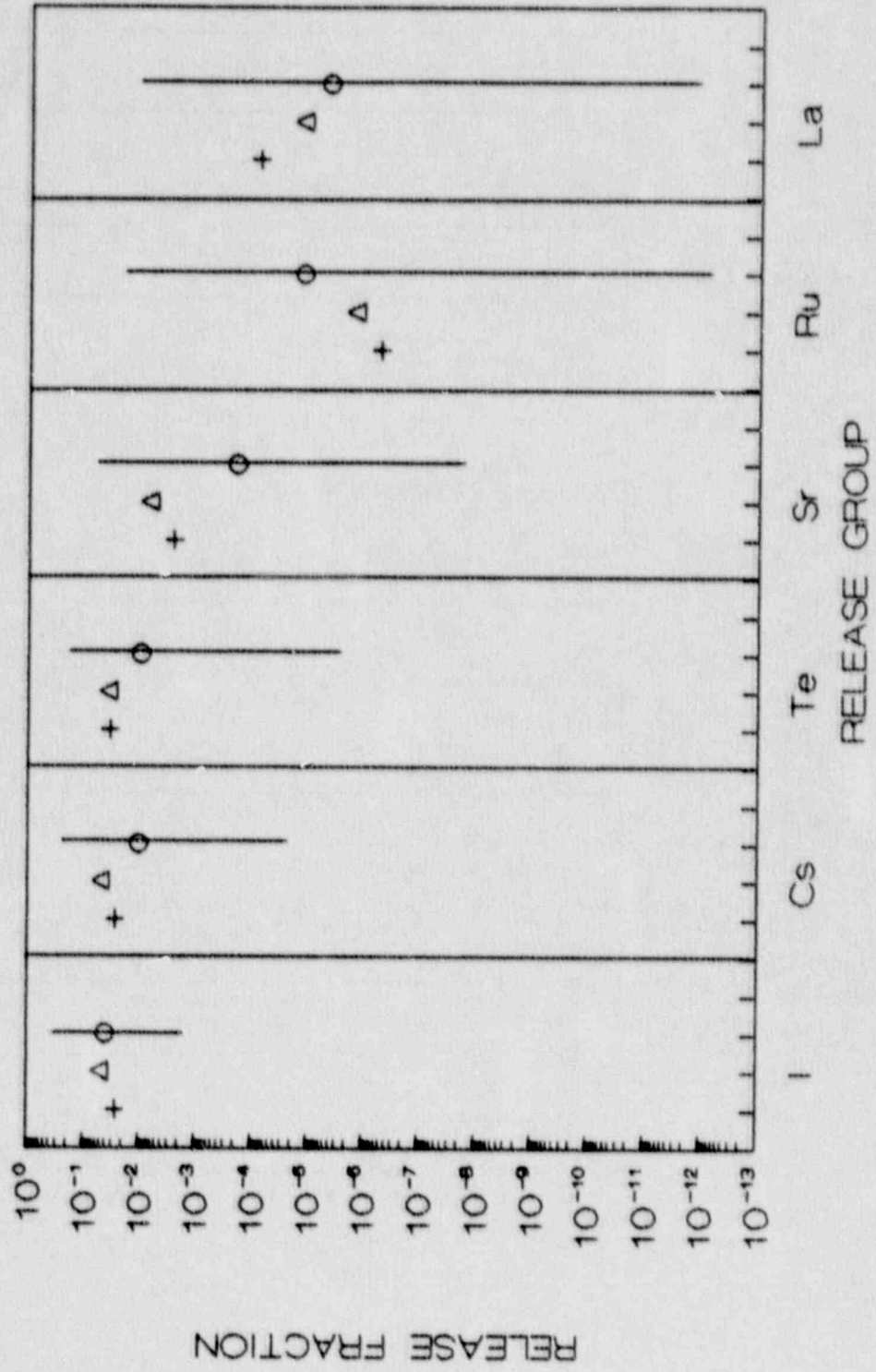
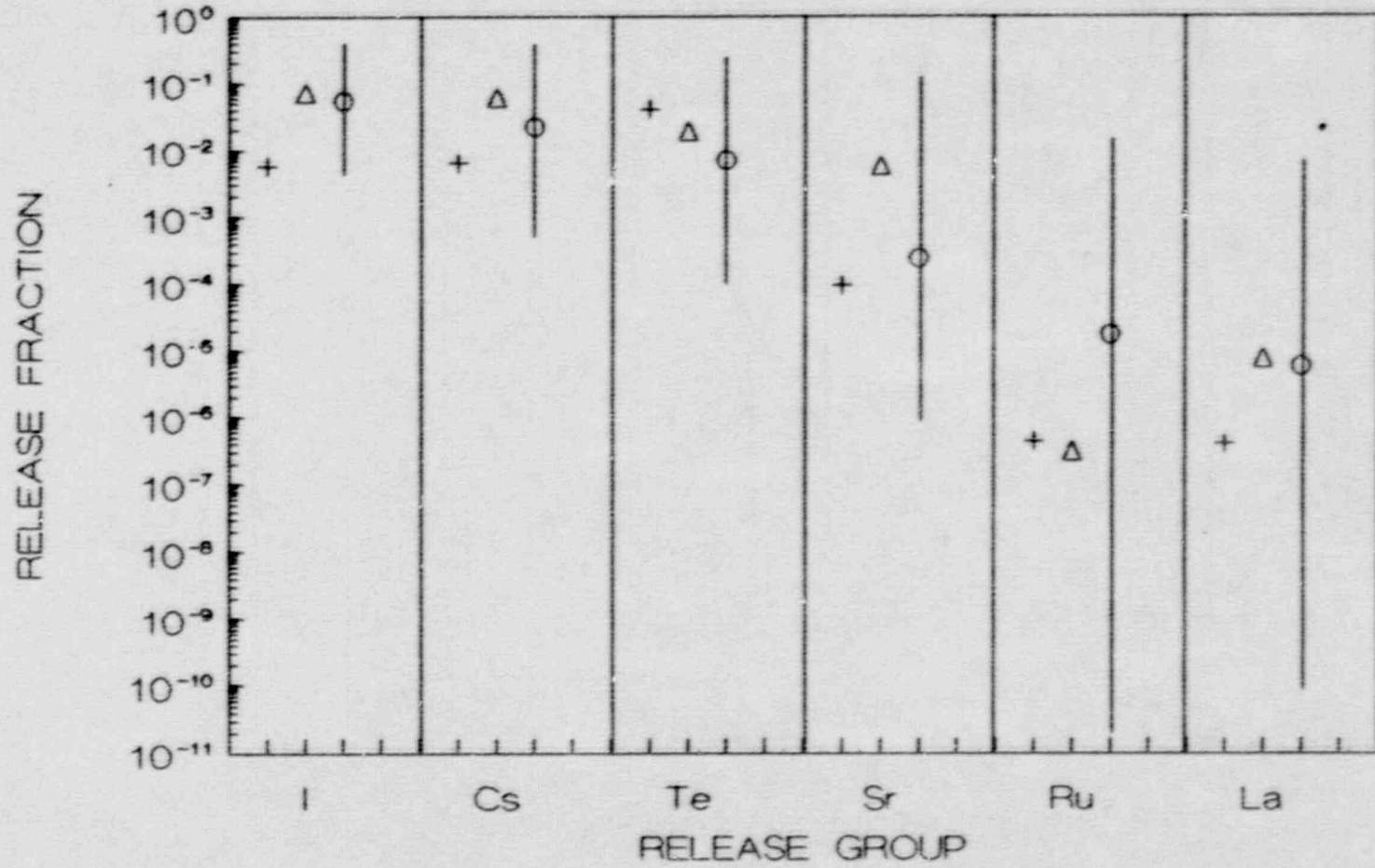


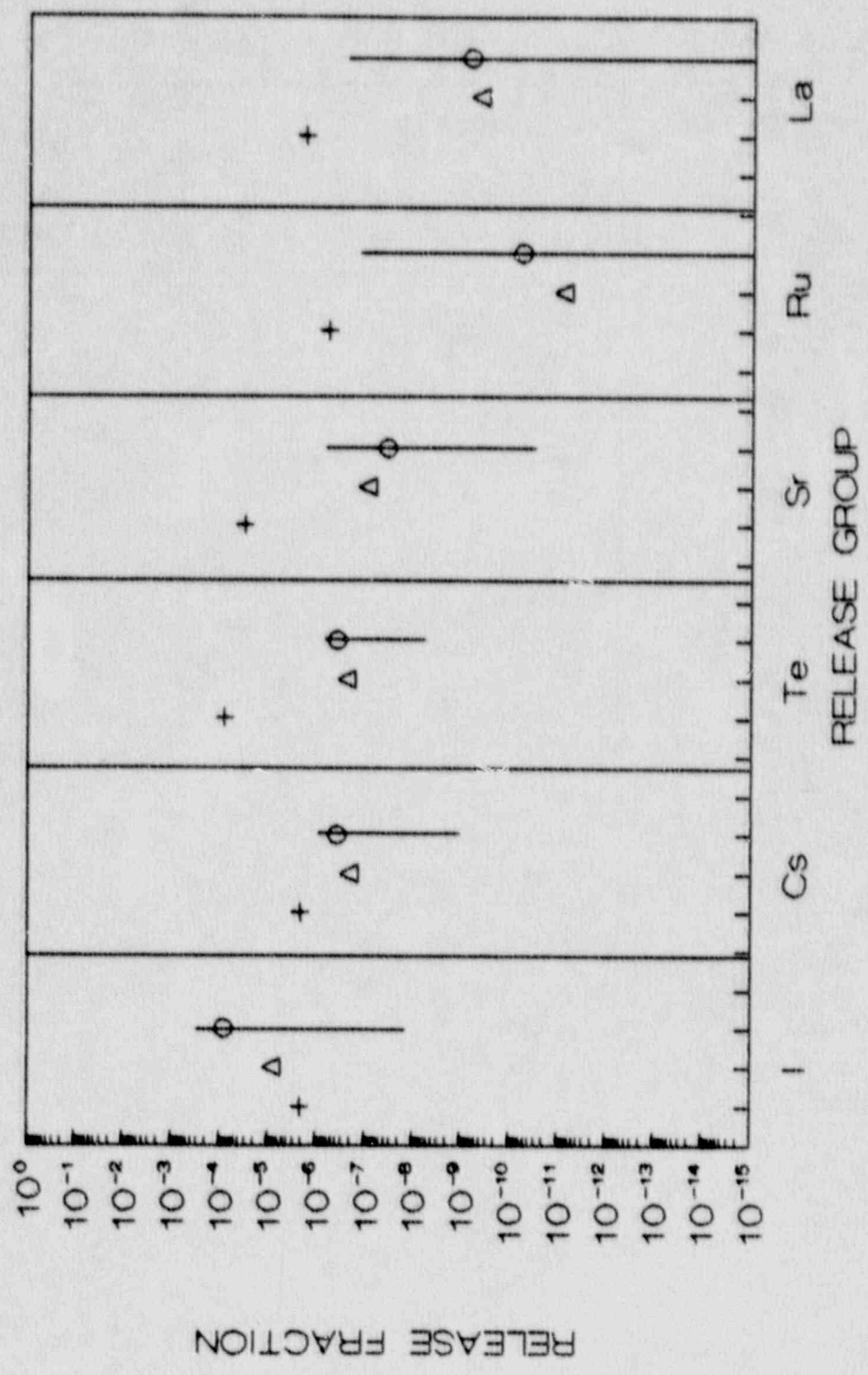
FIGURE D-4
 COMPARISON OF ZISOR WITH STCP
 RESULTS FOR TMLU-gamma

+ STCP TMLU Δ ZISOR CENTRAL ○ ZISOR MEDIAN



D-7

FIGURE D-5
 COMPARISON OF ZISOR WITH STOP
 RESULTS FOR TMLB-epsilon
 + STOP TMLB Δ ZISOR CENTRAL O ZISOR MEDIAN



D-9

FIGURE D-5
COMPARISON OF ZISOR WITH STCP
RESULTS FOR TMLB-leak-before-break

+ STOP TMLB Δ ZISOR CENTRAL ○ ZISOR MEDIAN

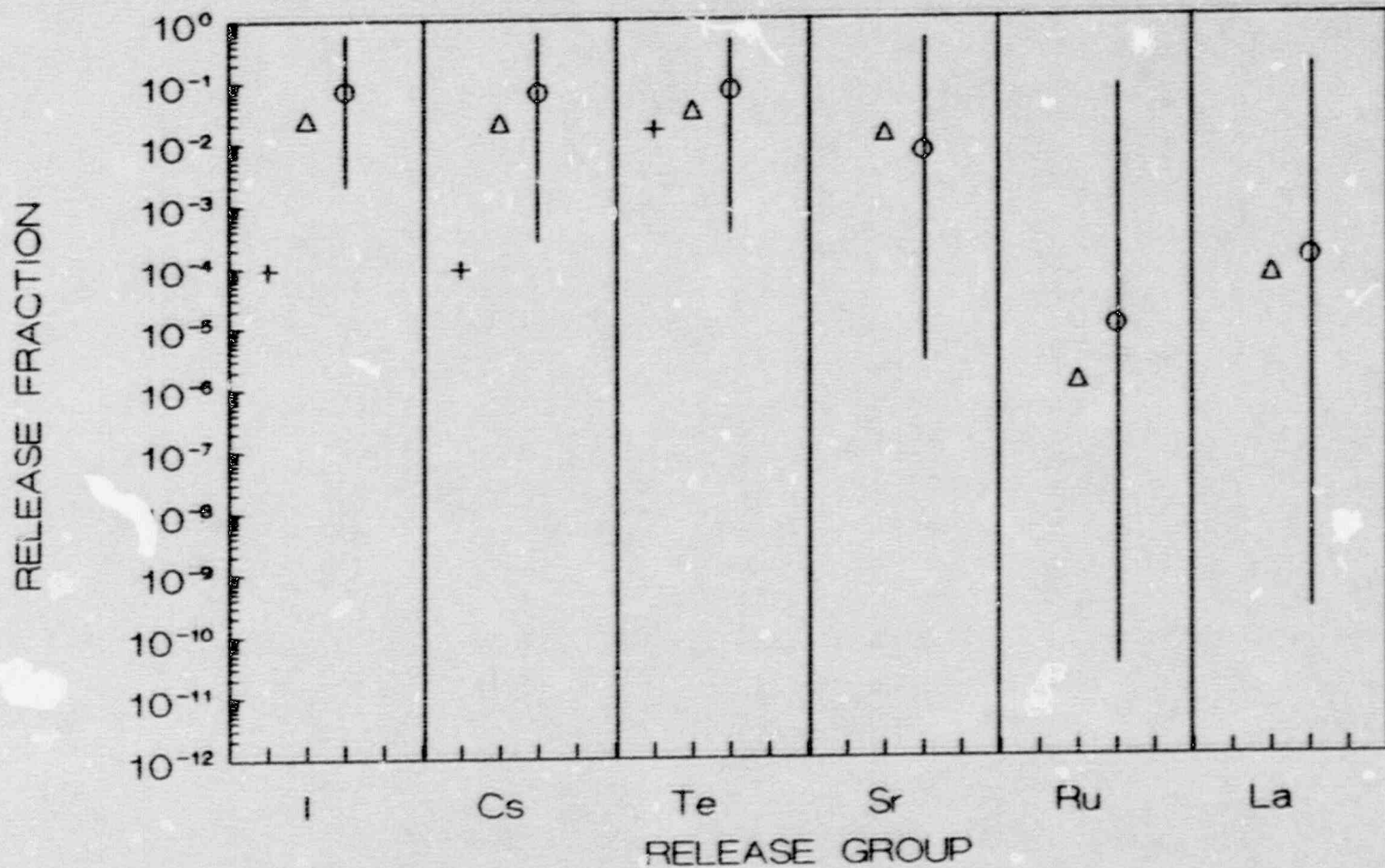


FIGURE D-7
 COMPARISON OF ZISOR WITH STOP
 RESULTS FOR TMLB-beta

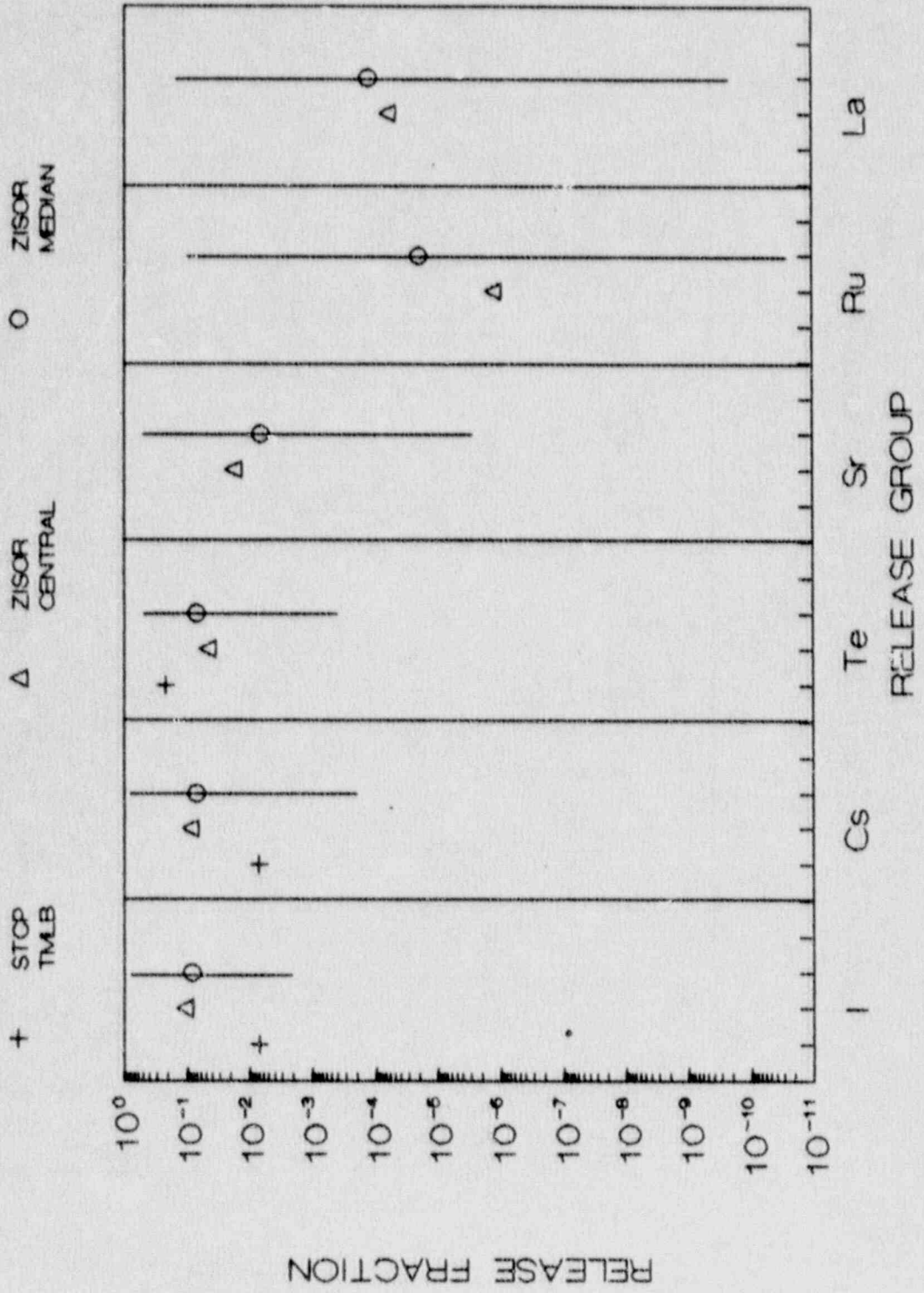
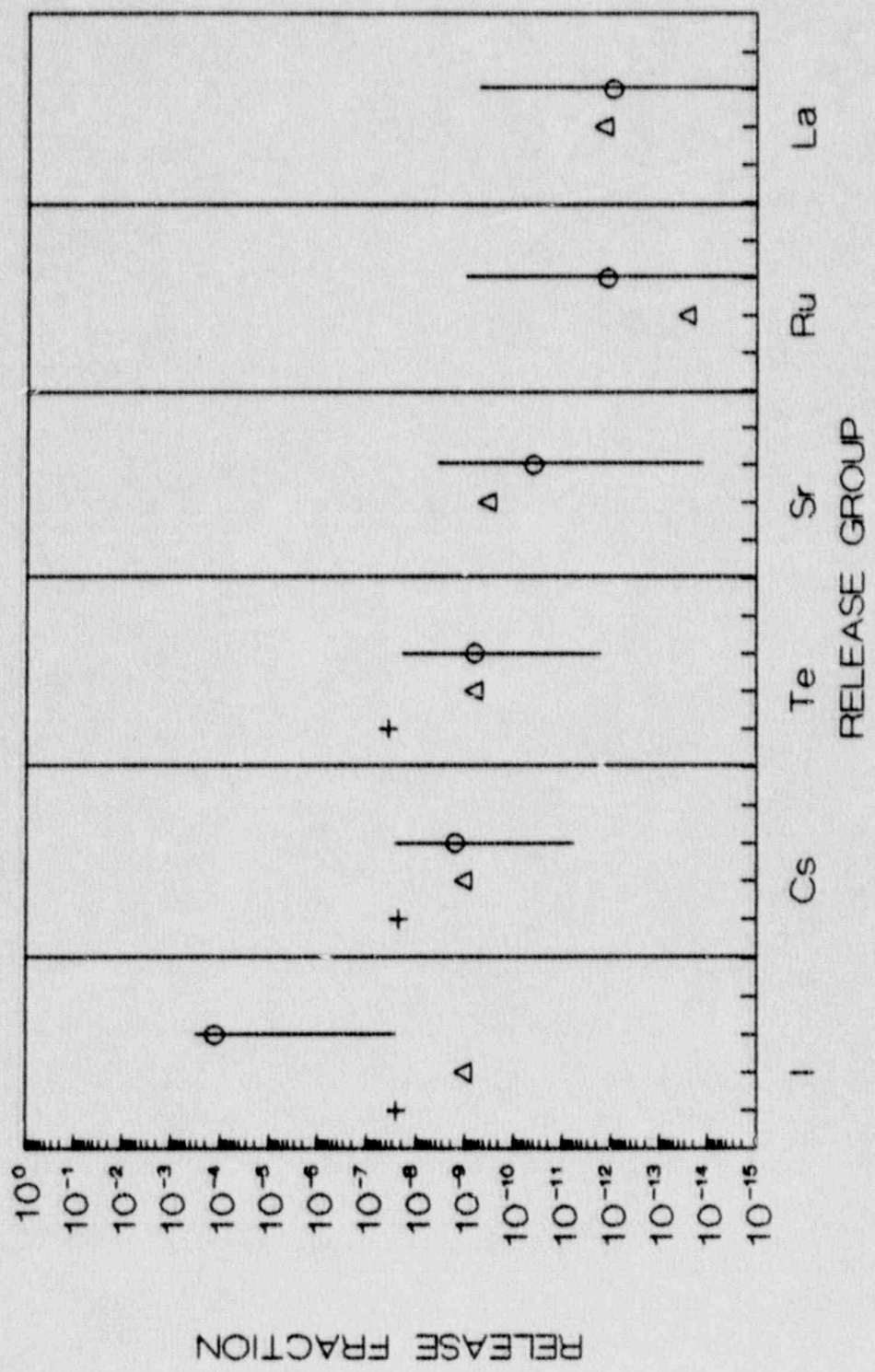


FIGURE D-8
 COMPARISON OF ZISOR WITH STOP
 RESULTS FOR S2D-epsilon



BIBLIOGRAPHIC DATA SHEET

(See instructions on the reverse)

1. REPORT NUMBER
*(Assigned by NRC. Add Vol., Supp., Rev.,
and Addendum Numbers, if any.)*

NUREG/CR-5346
BMI-2171

2. TITLE AND SUBTITLE

Assessment of the XSOR Codes

Final Report

3. DATE REPORT PUBLISHED

MONTH | YEAR
November | 1989

4. FIN OR GRANT NUMBER

D1595

5. AUTHOR(S)

P. Cybulskis

6. TYPE OF REPORT

Technical

7. PERIOD COVERED *(Inclusive Dates)*

8. PERFORMING ORGANIZATION - NAME AND ADDRESS *(If NRC, provide Division, Office or Region, U.S. Nuclear Regulatory Commission, and mailing address; if contractor, provide name and mailing address.)*

Battelle Columbus Division
505 King Avenue
Columbus, OH 43201

9. SPONSORING ORGANIZATION - NAME AND ADDRESS *(If NRC, type "Same as above"; if contractor, provide NRC Division, Office or Region, U.S. Nuclear Regulatory Commission, and mailing address.)*

Division of Systems Research
Office of Nuclear Regulatory Research
U.S. Nuclear Regulatory Commission
Washington, DC 20555

10. SUPPLEMENTARY NOTES

11. ABSTRACT *(200 words or less)*

A major feature of the NUREG-1150 analyses is the quantification of the uncertainties associated with the assessment of reactor accident risks, including the assessment of the uncertainties in the prediction of environmental source terms. The quantification of uncertainties was accomplished by the use of stratified sampling techniques over the ranges of uncertainties of the major variables. Since a separate source term is associated with each combination of variables in the statistical analysis, an extremely large number of source term estimates must be developed. For this purpose simplified methods of analysis, based on a limited number of detailed STCP calculations, were developed by Sandia National Laboratories. These source term estimation algorithms are known as the XSOR codes. These simplified source term methods were used not only as surrogates for the detailed calculations, but also to explore areas not currently addressed by the STCP. This report presents the results of an independent assessment of the ability of the XSOR codes to reproduce the results that would be obtained with the STCP, as well as to evaluate the reasonableness of the results when extended beyond the scope of the available STCP analyses.

12. KEY WORDS/DESCRIPTORS *(List words or phrases that will assist researchers in locating the report.)*

source terms
Source Term Code Package (STCP)
NUREG-1150
Latin Hypercube Sampling (LHS)
XSOR
SORSOR
SEQSOR
PBSOR
GGSOR
ZISOR

13. AVAILABILITY STATEMENT

unlimited

14. SECURITY CLASSIFICATION

(This Page)

unclassified

(This Report)

unclassified

15. NUMBER OF PAGES

16. PRICE

UNITED STATES
NUCLEAR REGULATORY COMMISSION
WASHINGTON, D.C. 20555

OFFICIAL BUSINESS
PENALTY FOR PRIVATE USE, \$300

SPECIAL FOURTH-CLASS RATE
POSTAGE & FEES PAID
USNRC
PERMIT No. G-67

120555139531 1 1AN
US NRC-OADM
DIV FOIA & PUBLICATIONS SVCS
TFS PDR-NUREG
P-223
WASHINGTON DC 20555